JAERI-M
6702

ANNUAL REPORT OF THE OSAKA LABORATORY FOR RADIATION CHEMISTRY JAPAN ATOMIC ENERGY RESEARCH INSTITUTE

(No. 9)

(April 1, 1975 - March 31, 1976)

September 1976

Osaka Laboratory for Radiation Chemistry

日本原子力研究所
Japan Atomic Energy Research Institute

Osaka Laboratory for Radiation Chemistry
Japan Atomic Energy Research Institute
25-1 Mii-minami machi, Neyagawa
Osaka, Japan

JAERI-M 6702

ANNUAL REPORT OF THE OSAKA LABORATORY FOR RADIATION CHEMISTRY JAPAN ATOMIC ENERGY RESEARCH INSTITUTE

(No. 9)

April 1, 1975 - March 31, 1976

(Received August 14, 1976)

This report describes research activities of Osaka Laboratory for Radiation Chemistry, JAERI during one year period from April 1, 1975 through March 31, 1976. The latest report, for 1975, is JAERI-M 6260.

Detailed descriptions of the activities are presented in the following subjects: studies on reactions of carbon monoxide and hydrogen; polymerization under the irradiation of high dose rate electron beams; modification of polymers, degradation, cross-linking, and grafting.

Previous reports in this series are:

Annual Report, JARRP, Vol. 1	1958/1959 *
Annual Report, JARRP, Vol. 2	1960
Annual Report, JARRP, Vol. 3	1961
Annual Report, JARRP, Vol. 4	1962
Annual Report, JARRP, Vol. 5	1963
Annual Report, JARRP, Vol. 6	1964
Annual Report, JARRP, Vol. 7	1965
Annual Report, JARRP, Vol. 8	1966
Annual Report, No. 1, JAERI 5018	1967
Annual Report, No. 2, JAERI 5022	1968
Annual Report, No. 3, JAERI 5026	1969
Annual Report, No. 4, JAERI 5027	1970
Annual Report, No. 5, JAERI 5028	1971
Annual Report, No. 6, JAERI 5029	1972
Annual Report, No. 7, JAERI 5030	1973
Annual Report, No. 8, JAERI-M 6260	1974

* Year of the activities

JAERI－M　6702

昭和50年度日本原子力研究所大阪研究所年報

日本原子力研究所大阪研究所

（1976年8月14日受理）

本報告は、大阪研究所において昭和50年度に行なわれた研究活動を述べたものである。主な研究題目は、一酸化炭素と水素の反応ならびにそれに関連した研究、高線量率電子線照射による重合反応の研究、ポリマーの改質および上記の研究と関連して重合反応、高分子分解、架橋ならびにグラフト重合に関する基礎的研究などである。

日本放射線高分子研究会年報	Vol. 1			1958/1959
日本放射線高分子研究会年報	Vol. 2			1960
日本放射線高分子研究会年報	Vol. 3			1961
日本放射線高分子研究会年報	Vol. 4			1962
日本放射線高分子研究会年報	Vol. 5			1963
日本放射線高分子研究会年報	Vol. 6			1964
日本放射線高分子研究会年報	Vol. 7			1965
日本放射線高分子研究会年報	Vol. 8			1966
日本原子力研究所大阪研における放射線化学の基礎研究	No.1	JAERI	5018	1967
日本原子力研究所大阪研における放射線化学の基礎研究	No.2	JAERI	5022	1968
日本原子力研究所大阪研における放射線化学の基礎研究	No.3	JAERI	5026	1969
日本原子力研究所大阪研における放射線化学の基礎研究	No.4	JAERI	5027	1970
日本原子力研究所大阪研における放射線化学の基礎研究	No.5	JAERI	5028	1971
日本原子力研究所大阪研における放射線化学の基礎研究	No.6	JAERI	5029	1972
日本原子力研究所大阪研における放射線化学の基礎研究	No.7	JAERI	5030	1973
Annual Report, Osaka Lab., JAERI,	No.8	JAERI－M	6260	1974

CONTENTS

I. INTRODUCTION 1

II. RECENT RESEARCH ACTIVITIES

[1] Radiation Effects on the Reaction of Mixtures of Carbon Monoxide and Hydrogen

1. Studies on the Reaction of Gaseous Mixtures 4

2. Radiation Chemical Reactions in the Presence of Iron Catalysts 11

3. ESR Study of γ-Irradiated H_2-CO Mixture Adsorbed on Solid Surfaces 18

4. Optical Emission from Ar-CO Mixture Irradiated by Electrons 19

5. Estimation of the Effective Electron Energies in the Reaction Vessel 21

[2] Radiation-Induced Reaction of Molecules in Adsorbed State

1. Structure and Reaction of Radicals Trapped in the Crystals of Thiophene and 2-Chlorothiophene 25

2. Structure and Reaction of Radicals Produced by γ-Irradiation of Thiophene and Furan Adsorbed on Sillica Gel 26

[3] Radiation-Induced Polymerization of Mixed Multilayers of Octadecyl Acrylate and Elaidic Acid 27

[4] Monomolecular Films of PVA-Polystyrene Block and Graft Copolymers at the Air/Water Interface 31

[5] Polymerization of Vinyl Monomers by High Dose Rate Electron Beams

1. Polymerization of Moderately Dried and Water-Saturated Styrene 34
2. Polymerization of Methyl Methacrylate 39
3. Polymerization of Isobutyl Vinyl Ether 42

[6] Preparation of a Composite Ultrafiltration Membrane from Polystyrene Latex Produced by Radiation-Induced Emulsion Polymerization 45

[7] Preparation of Cross-Linked Hydrogel Membranes by Radiation Technique 48

[8] Modification of Polymers

1. Radiation-Induced Grafting of Acrylic Acid onto Polyvinyl Chloride Fiber. Some Kinetic Features of the Grafting 52
2. Radiation-Induced Grafting of Calcium Acrylate onto Polyvinyl Chloride Fiber 55
3. Radiation-Induced Grafting of Acrylamide onto Polyvinyl Chloride Fiber 57
4. Modification of Polyester Fiber by Radiation-Induced Chlorination and Subsequent Alkali-Treatment 60
5. Fire Retardant Wood Plastic Composite Based on Radiation-Induced Copolymerization of Bis(2-Chloroethyl) Vinyl Phosphonate 62

[9] Electron Beam Curing

1. Electron Beam Curing of PVC Plastisol Based on PVC/Vinyl Monomer Mixtures 66
2. Electron Beam Curing of Chlorinated Polymer/Vinyl Monomer Mixtures by High Dose Rate Electron Beams 69

3. Effect of Dose Rate on Electron Beam Curing of Epoxy Diacrylate 72

4. Comparative Studies on the Curing by Electron Beam and Ultraviolet Irradiation of Epoxyacrylate. Evaluation of Degree of Cross-Linking by DSC Measurement 75

[Appendices]

[1] Dosimetry of Electron Beams from the High Dose Rate Electron Accelerator

1. Calibration of Electron Energy 80

2. Measurements of Energy Dissipation Curves in CTA Films 81

3. Dose Distribution in the Irradiation Zone 82

4. Dosimetry of a Sample Travelling on a Conveyer 84

[2] Measurement of Dose Rate Distribution and Temperature Rise in a Metal Cell Used for the Polymerization of Vinyl Monomers by Electron Beams 87

III. LIST OF PUBLICATIONS

[1] Published Papers 97

[2] Oral Presentations 98

IV. LIST OF SCIENTISTS 101

I. INTRODUCTION

Osaka Laboratory was founded in 1958 as a laboratory of the Japanese Association for Radiation Research on Polymers (JARRP), which was organized and sponsored by some fifty companies interested in radiation chemistry of polymers. The JARRP was merged with the Japan Atomic Energy Research Institute (JAERI) on June 1, 1967, and the laboratory changed its name from Osaka Laboratory, JARRP to Osaka Laboratory for Radiation Chemistry, JAERI. The research activities of Osaka Laboratory have been oriented towards the fundamental research on radiation chemistry.

The results of the research activities of the Laboratory were published from 1958 until 1966 in the Annual Reports of JARRP which consisted essentially of original papers. During the period between 1967 and 1973, the publication had been continued as JAERI Report which also consisted mainly of original papers. From 1974, the Annual Report has been published as JAERI-M Report which contains no original papers, but presents outlines of the current research activities in some detail in English. Readers who wish to have more information are advised to contact with individuals whose names appear under subjects.

The present annual report covers the research activities of the Laboratory between April 1, 1975 and March 31, 1976.

Most of the studies carried out in the Laboratory are continuation from the previous year, emphasis being laid on two projects; one is "Effect of radiation on the reaction of carbon monoxide and hydrogen" and the other, "Radiation-induced polymerization by high dose rate electron beams".

Our new high dose rate electron accelerator (HDRA) was ready for operation on May 31, 1975, and extensive studies were initiated to standardize radiation dosimetry of high dose rate electron beams from the HDRA. Concurrently with these studies, research projects have been carried out using the HDRA and many new results obtained.

Gaseous mixtures of hydrogen and carbon monoxide are irradiated with electron beams at different temperatures and pressures. Several oxygen containing products such as acetaldehyde, methanol, methyl formate, trioxane, and tetraoxane are formed at temperatures even below 30°C. Temperature and pressure dependences of G values of the cyclic ethers suggest that ion clusters of carbon monoxide and hydrogen might be the precursors of the cyclic ethers.

Studies are also carried out with the gaseous mixtures in the presence of catalyst in order to know the possibility of giving selectivity to radiation chemical reactions which form unselectively various products. Instead of various oxygen containing products which are found in the radiation chemical reaction of hydrogen and carbon monoxide in the absence of catalyst, homologues of hydrocarbons are found to be formed selectively by the presence of catalyst which contains iron and copper and is known as Fischer-Tropsch catalyst.

Studies on polymerization of vinyl monomers by electron beam at high dose rate are carried out. In addition to the radical and cationic polymers reported in literatures, new polymers of much higher molecular weight are found to be produced in water-saturated styrene at higher dose rates than 1.2×10^4 rad/sec. In the case of dry methyl methacrylate also new polymers of high molecular weight are formed by the irradiation at high dose rate. Kinetic studies on polymerization of isobutyl vinyl ether by electron irradiation reveal that the radical process also plays an important role in the polymerization as well as the cationic process.

Kinetic study on grafting of acrylamide onto PVC fiber is carried out up to the dose rate of 10^7 rad/sec and reveals that the rate of grafting is proportional to the 0.76th power of the dose rate over a wide dose rate range between 1 and 10^7 rad/sec. The softening temperature of the fiber is much improved without a loss of strength and flame-retardance of the original fiber. Grafting of calcium acrylate onto PVC fiber by a direct method using ^{60}Co γ-ray source and a Van

de Graaff is successful and the softening temperature of the fiber is improved to a great extent by the grafting.

Membranes are prepared by various methods using radiation techniques: hydrogel membranes by radiation-induced cross-linking of water swollen film of polymers; complex membranes from fine polystyrene latex produced by radiation-induced emulsion polymerization; and skeltonized polymer multilayers by radiation-induced polymerization of mixed multilayers.

Radiation-induced curing of mixtures of chlorinated polymers prepared from polymeric hydrocarbons such as polyethylene, polypropylene, and rubber with vinyl monomers coated on steel panel is studied at high dose rate region. By addition of a cross-linking agent, dose required for the complete curing is greatly reduced. The performance test on the coating of steel panel thus prepared gives excellent results.

Comparative studies of electron beam and ultraviolet curing of epoxy acrylate with differential scanning calorimetry and other techniques reveal that cross-linking in the curing is largely affected by the curing temperature.

Administrative changes were made in the Laboratory at the end of March. Prof. Dr. I. Sakurada, who had directed the research activities of the Laboratory as head since 1957, retired, but we are fortunate in maintaining his continued service of conducting research in the Laboratory.

Dr. M. Gotoda was appointed head on April 1, 1976.

June 30, 1976

Dr. Masao Gotoda, Head
Osaka Laboratory for Radiation Chemistry
Japan Atomic Energy Research Institute

II. RECENT RESEARCH ACTIVITIES

[1] Radiation Effects on the Reaction of Mixtures of Carbon Monoxide and Hydrogen

1. Studies on the Reaction of Gaseous Mixtures

It was reported last year[1)] that several oxygen-containing products such as methanol, acetaldehyde, formaldehyde, acetic acid and trioxane are formed by electron irradiation of gaseous mixtures of carbon monoxide and hydrogen at room temperature. These products were found to show complicated variations in their yields with the composition of the reactant gases, indicative of intricate mechanism for the formation of the individual products.

Studies are carried out in order to get informations on the mechanism for the product formation. The experiments are performed on the effects of the pressure and temperature of the reactant gases, energy of incident electrons, and dose rate absorbed by the gases.

The reaction vessel and experimental procedures are the same as described previously except where otherwise noted. Irradiations are performed using either a Van de Graaff electron accelerator (VdG) or a high dose rate electron accelerator (HDRA). Dose rates absorbed by the reactant gases are determined by measuring nitrogen yield in the radiolysis of nitrous oxide, assuming that the energy absorption is proportional to the relative stopping power of the gases concerned. Quantitative analyses of the products are made by a mass spectrometer as in the previous study. A gaschromatograph is also used to help identifications.

The effect of the total pressure of CO and H_2 on the yields of the products is studied in a pressure range from 200 to 900 Torr at fixed CO content of 15 mol %. Electron beams from the Van de Graaff are irradiated through a titanium window of the reaction vessel for 1,000 seconds. Dose rate

estimated is 2.70×10^{-5} eV/molecule·sec for the mixed gases at the total pressure of 630 Torr.

Fig. 1 shows the G values of the main products as a function of the total pressure. Total G value of methyl formate and acetic acid which are indistinguishable in the analysis by a mass spectrometer is included in the figure. It may be seen from Fig. 1 that the G value of methanol and total G value of methyl formate and acetic acid remain nearly constant through the pressure range studied here. The G values of other minor products which are not shown in Fig. 1

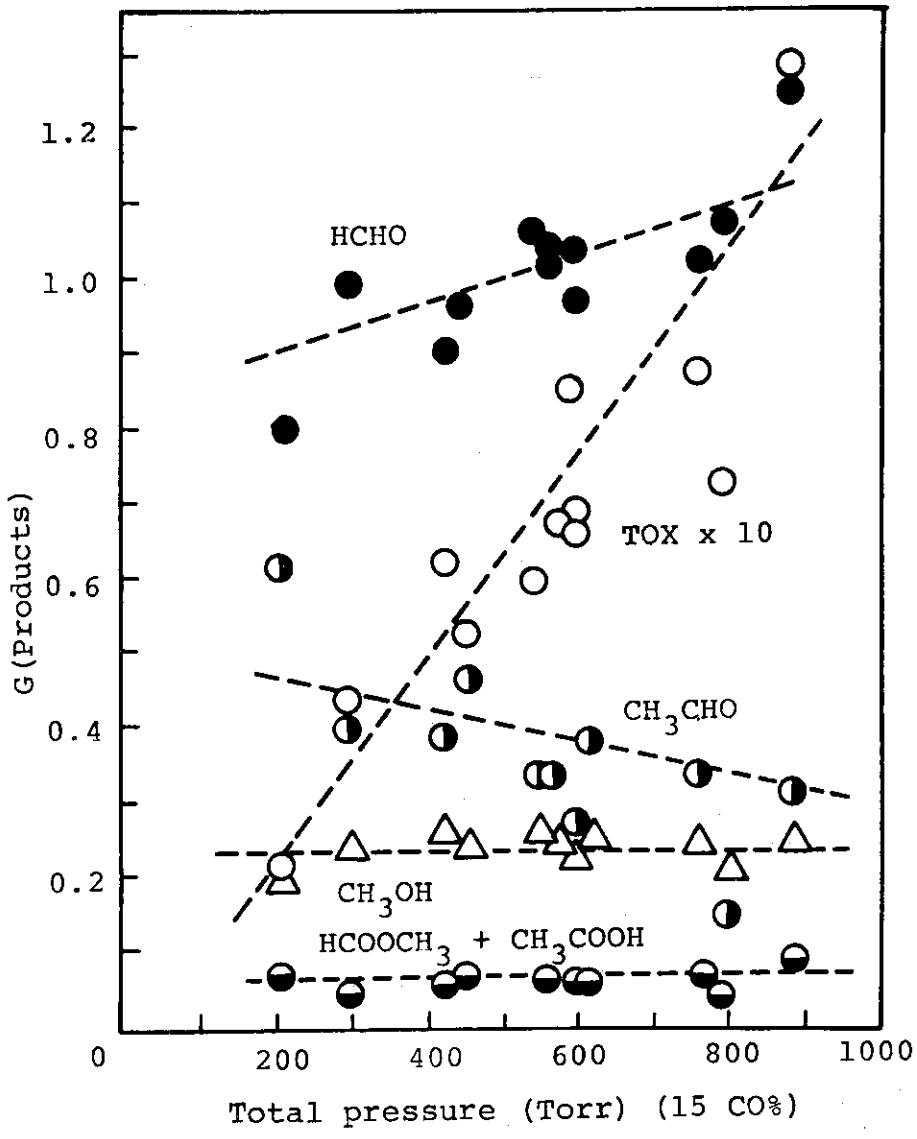

Fig. 1. G values of the main products as a function of total pressure of $CO-H_2$ mixtures.

are also independent of the pressure. The G value of acetaldehyde decreases slightly with the total pressure, the reason for which is not accounted for at present.

In contrast, the G value of trioxane increases markedly and that of formaldehyde increases slightly with the total pressure. The positive dependence of the G value of trioxane on the pressure suggests that the precursor of trioxane becomes abundant in the system with the total pressure under our experimental conditions.

The effects of electron energy and dose rate are studied using the HDRA. Reactant gases at the total pressure of 630 Torr and CO content of 15 mol % are irradiated in the reaction vessel with electron beams at room temperature. The electron

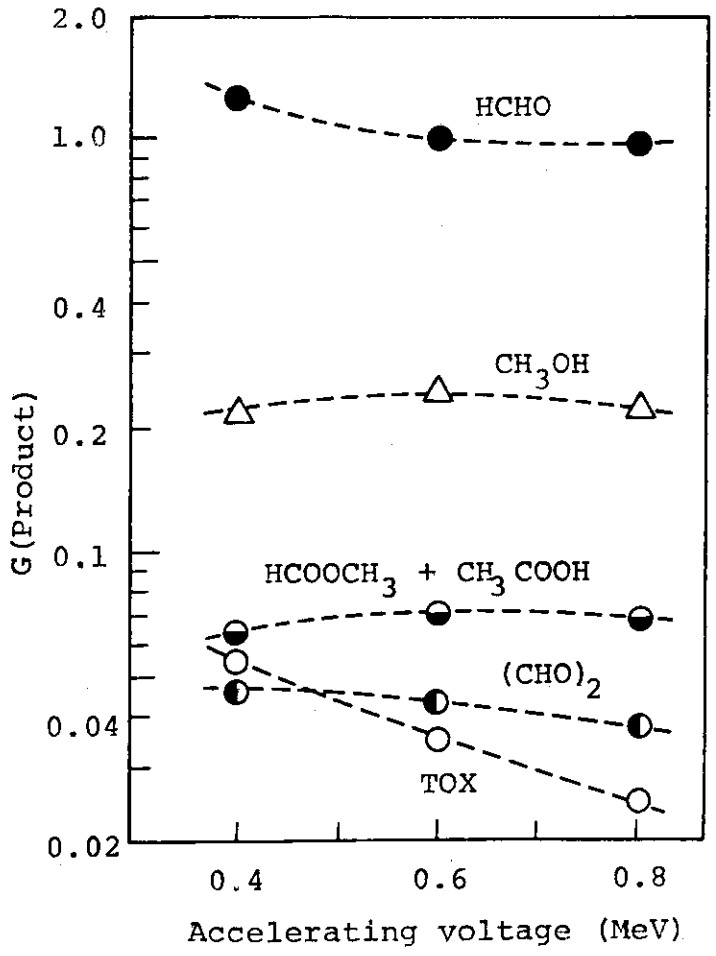

Fig. 2. Effect of electron energy on the G values.
CO content, 15 mole %; total pressure, 630 Torr;
beam current, 5 ma; irradiation time, 20 sec.

energy (accelerating voltage) is varied from 0.4 to 0.8 MeV while keeping the beam current at 5 ma.

It is found that the G values of formaldehyde, methanol, glyoxal, and formic acid, and the total G value of methyl formate and acetic acid are independent of the electron energy as shown in Fig. 2. The G value of trioxane, on the other hand, decreases remarkably with the electron energy.

The effect of dose rate on the G values of the products is examined in a relatively wide range from 4.65×10^{-5} to 1.31×10^{-3} eV/molecule·sec which is attained by varying electron beam current from 0.25 to 7.0 ma. Irradiations are performed at the accelerating voltage of 0.4 or 0.8 MeV. The total dose is kept constant at 2.76×10^{21} eV for irradiations at 0.4 MeV or 3.44×10^{21} eV for irradiations at 0.8 MeV.

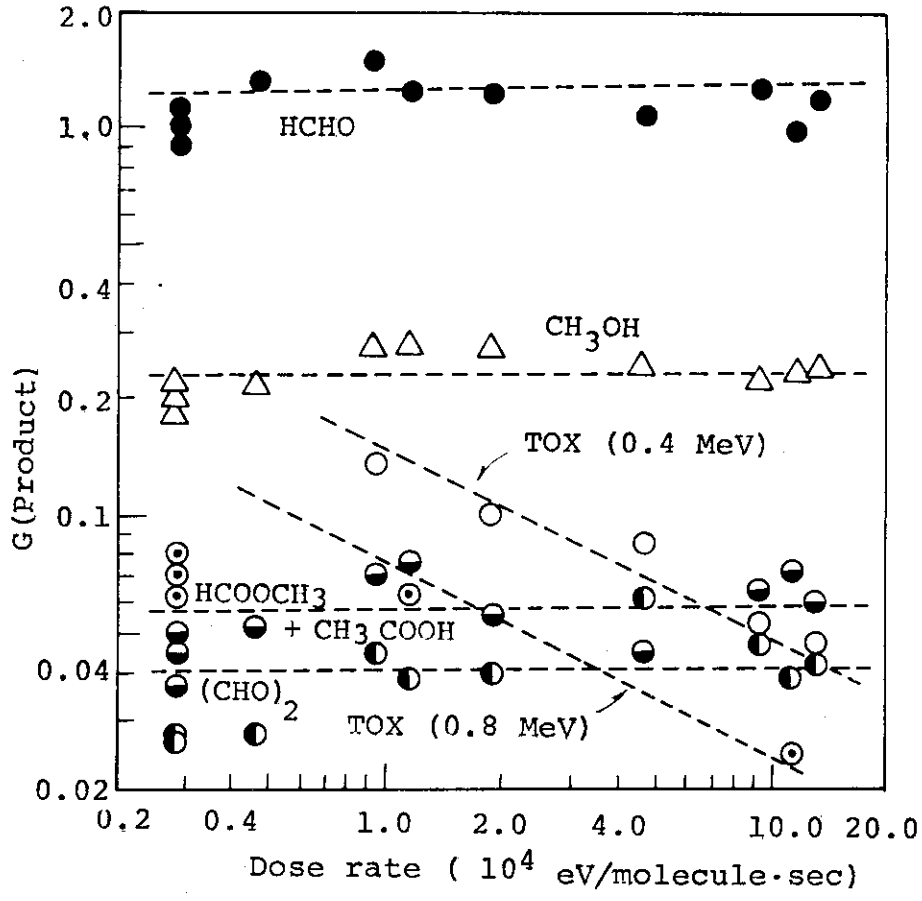

Fig. 3. Effect of dose rate on the G values.
CO content, 15 mole %; total pressure, 630 Torr;
electron energy, 0.4 MeV and 0.8 MeV; dose,
2.76×10^{21} eV and 3.44×10^{21} eV.

Fig. 3 shows the dose rate dependence of the G values of the main products. The two sets of values obtained by irradiations at the two different accelerating voltages are denoted using same symbols for each product except trioxane. Included in Fig. 3 are the data obtained using the VdG (dose rate: 2.70×10^{-5} eV/molecule·sec). It is seen from Fig. 3 that the dose rate has no effect on the G values of formaldehyde, glyoxal and formic acid, and the total G value of methyl formate and acetic acid.

The G value of trioxane is, however, inversely proportional to the square root of the dose rate at both the accelerating voltages, which would suggest that trioxane is formed bimolecularly. On the other hand, the observed decrease in the G (trioxane) with the dose rate, and also with the electron energy as described above, may possibly arise from temperature rise of the reactant gases by the increase of the total input energy. In fact, the G value of trioxane is found to decrease with temperature as described below.

In order to perform irradiation experiments at a low temperature, the reaction vessel is enclosed by cooling jacket aside from the titanium window, and crushed dry ice is filled in the space between the reaction vessel and cooling jacket after charging the reactant gases. In high temperature irradiations, the cooling jacket is removed and the reaction vessel is heated by a mantle-heater. The temperature of the gases is determined by measurement of the pressure change by cooling or heating, assuming that the gases obey the ideal gas law. Electron beam irradiation at three different temperatures is performed by the HDRA at 0.4 MeV and 0.5 ma.

The results when the irradiations are carried out at the total pressure of 630 Torr are depicted in Fig. 4 which shows a plot of the logarithms of the G values versus the reciprocal of absolute temperature of the reactant gases. Tetraoxane, cyclic tetramer of formaldehyde, is further identified in the products obtained by the low temperature irradiation. It is apparent from the figure that the G values of trioxane and

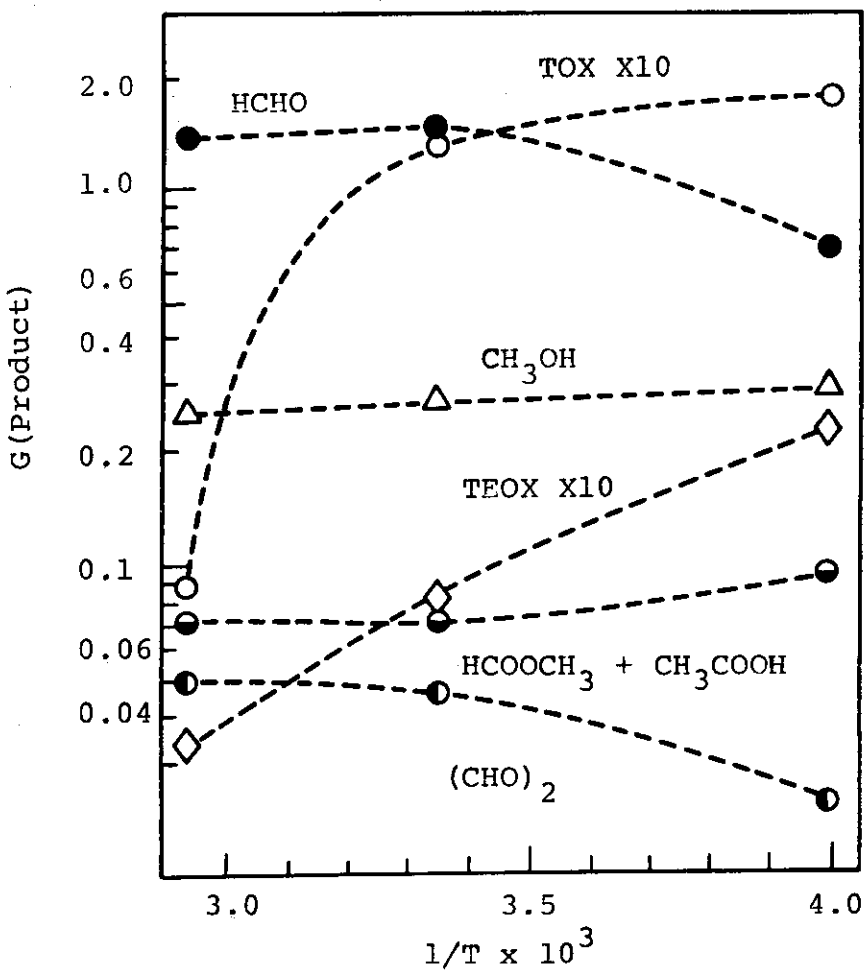

Fig. 4. Effect of temperature on the G values.
CO content, 15 mole %; total pressure, 630 Torr;
electron energy, 0.4 MeV; beam current, 0.5 ma;
irradiation time, 200 sec.

tetraoxane decrease markedly while those of the other products increase slightly with the temperature. Similar results are obtained when the experiments are carried out at the total pressure of 900 Torr, and on CO-D_2 mixtures.

In summary, the G values of trioxane and tetraoxane increase with the total pressure of the reactant gases, and decrease with the energy of incident electrons, dose rate and temperature. The G values of the other products, on the other hand, show little or no dependences on the variables studied here.

The findings in the present study seem to exclude the possibility that trioxane and tetraoxane are formed by successive reactions of some primary stable products and reactant gases. Recently, ion equilibria involving cluster ions are studied for such reactions as

$$CO^+(CO)_{n-1} + 2\ CO = CO^+(CO)_n + CO \qquad (1)$$

and

$$H_3^+(H_2)_{n-1} + 2\ H_2 = H_3^+(H_2)_n + H_2 \qquad (2)$$

by mass spectrometers [2, 3]. By using the equilibrium constants[3] reported for the reaction 2, it is possible to calculate the equilibrium abundances of the various H_n^+ ion clusters as a function of H_2 pressure at constant temperature, and as a function of temperature at constant pressure. Our calculation indicates that the abundances of $H_3^+(H_2)_3$ and $H_3^+(H_2)_4$ show pressure and temperature dependences similar to those found for the G values of trioxane and tetraoxane in the pressure and temperature ranges employed in the present study. This fact leads us to propose that ion clusters such as $CO^+(CO)_n(H_2)_m$ are the most probable candidates as precursors of the trioxane and tetraoxane formation.

By analogy to the reactions 1 and 2, the cluster ions $CO^+(CO)_n(H_2)_m$ are assumed to be formed through the reaction

$$CO^+(CO)_{n-1}(H_2)_{m-1} + CO + H_2 + M = CO^+(CO)_n(H_2)_m + M \qquad (3)$$

where M denotes a third body, and dissociate to produce stable molecules such as trioxane and tetraoxane. (T. Sugiura, S. Sugimoto, M. Nishii)

1) JAERI-M, 6260, 4 (1975).
2) R. C. Horton, J. L. Franklin and B. Mazzeo, J. Chem. Phys., 62, 1739 (1975).
3) H. Hiraoka and P. Kebale, J. Chem. Phys., 62, 2267; 63, 746 (1975).

2. Radiation Chemical Reaction in the Presence of Iron Catalyst

Extensive studies in this laboratory reveal that various types of oxygen containing compounds such as aldehydes and cycloethers are produced by electron beam irradiation of gaseous mixture of hydrogen and carbon monoxide[1]. The same mixture, however, gives only homologues of hydrocarbons under the presence of Fischer-Tropsch catalyst without irradiation[2,3]. The present investigation is carried out in an attempt to see whether or not the radiation-induced reaction unselectively resulting in various products is modified by the presence of a solid catalyst to give selectivity to the reaction, so that the effect of radiation is focused on a limited number of reactions thus enhancing yield of a specific product.

There are a number of studies on the radiation effects on catalysts or catalytic reactions. The radiation effects ever reported[4,5], however, are small, possibly because these studies were carried out using radiations of rather lower dose rate, by which the radiation effects cannot compete effectively with the catalytic effects. Irradiation by electron beams of dose rate employed in the present studies, which is higher by an order of two than those used by the previous investigators, will enlarge the radiation effects on catalytic reactions.

The catalysts used are of a Fischer-Tropsch type containing Fe, Cu, and diatomaceous earth (100 : 25 : 125 in weight) prepared by the method described by Kodama, et al.[3] The reaction vessel made of stainless steel (SUS 27) contains 69 ml catalyst; dimensions of the vessel are 220, 50, and 7 mm, the longest being along the direction of reactant gas flow and the shortest being along that of electron beams which penetrate into the vessel through a titanium window (30 μ thick) equipped at the top.

Irradiations are performed using electron beams (1.5 MeV, 30-100 μa) from a Van de Graaff electron accelerator.

The gas emerged out of the vessel is led to a control room across radiation shield through a 13 m stainless steel tubing (3 mm, i.d.) to be analyzed by a Yanagimoto G-80 gaschromatograph equipped with two sets of columns; 6 m VZ-7 columns with FID and 1.2 m active charcoal columns with TCD. Simultaneous analyses of the reacted gases on these two columns are made for H_2, CO, CO_2, and hydrocarbons from C_1 to C_6 during, before and after the irradiation.

Typical gas chromatograms of the reacted gas during and after the irradiation are shown in Figs. 1 and 2 along with identifications of the peaks made by comparison with gas-chromatograms obtained by Toyoshima[6] as well as with

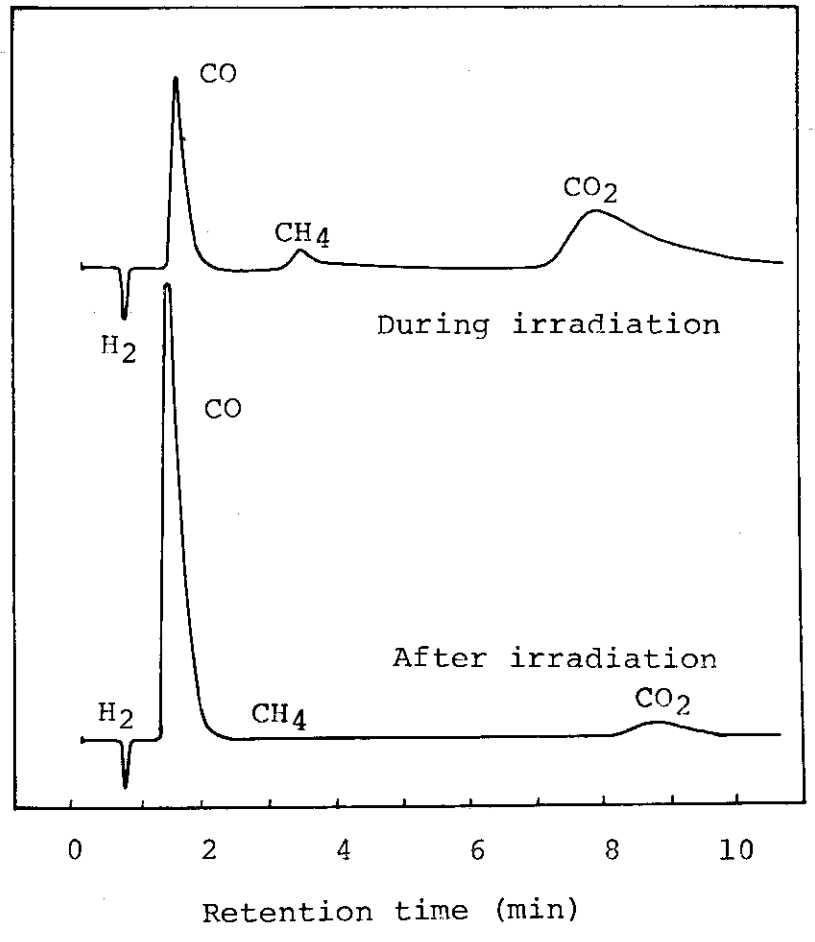

Fig. 1. Typical example of gaschromatograms obtained during and after electron beam irradiation on active charcoal columns with a thermal conductivity detector. Beam current, 50 μa.

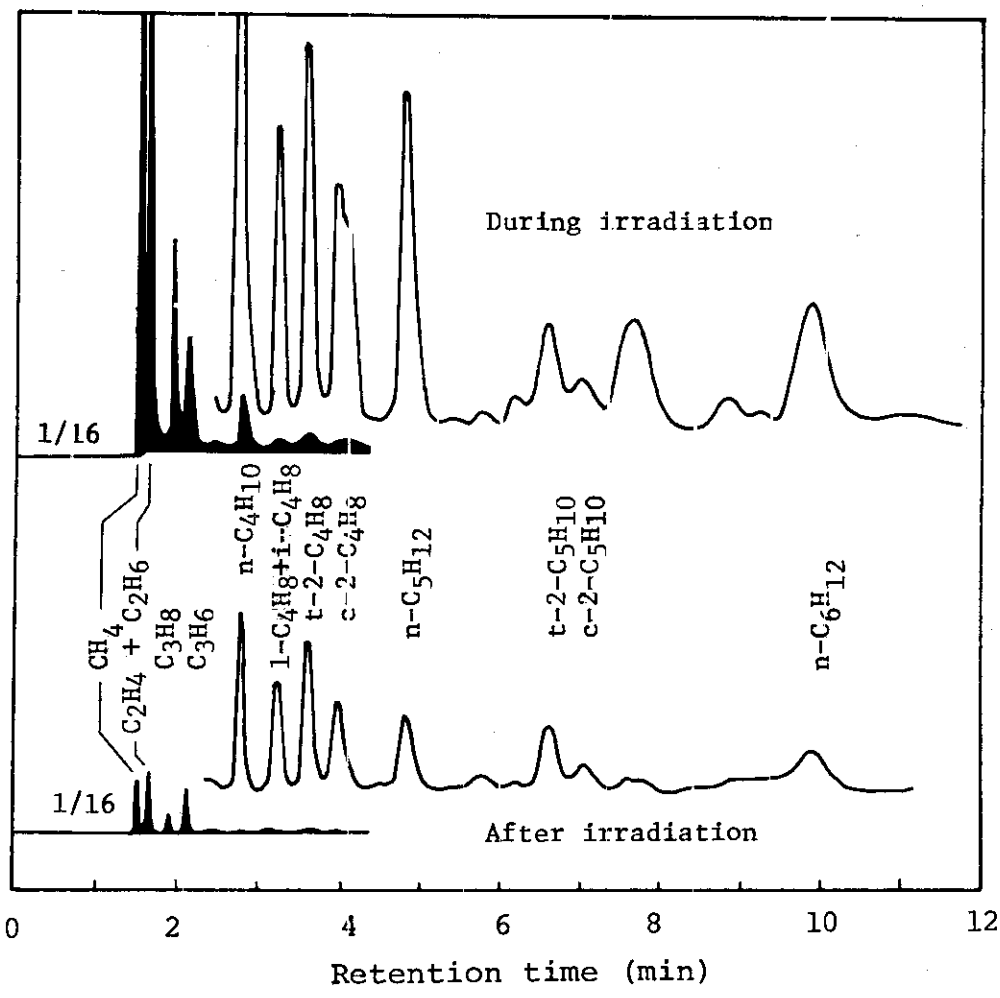

Fig. 2. Typical example of gaschromatograms obtained during and after electron beam irradiation on VZ-7 columns with a flame ionization detector. Beam current, 50 μa.

retention times of standard samples. During the course of the experiment, temperatures of the catalyst and flow rate of gas after removal of condensable products by a liquid cold trap are recorded on an Ohkura multi-channel plotting recorder. An example of the recordings is shown in Fig. 3 along with sampling numbers which are also given in Table 1.

Table 1 summarizes the yields of the products tentatively calculated from the residual gas flow rate and gas analysis with or without irradiation. Carbon dioxide and water obtained in the radiation chemical reaction of gaseous mixtures of hydrogen and carbon monoxide are also found in the products

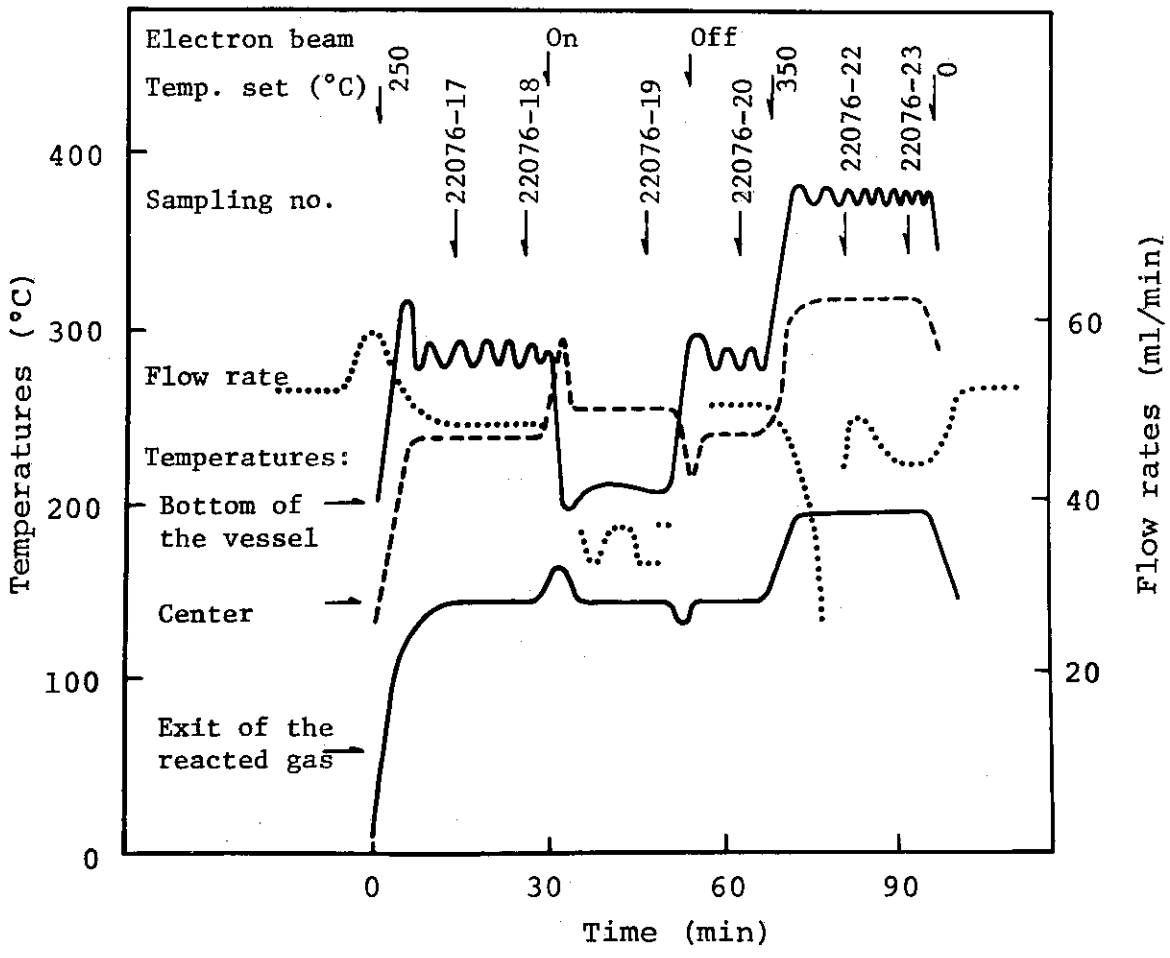

Fig. 3. Recording traces of reaction temperatures and flow rates during experiment.

in the present system. On the other hand, no oxygen-containing organic products such as cycloethers or aldehydes which are the main products in the gaseous mixtures are detected in the present study where catalyst is present.

As obvious from the table, the yield of CO_2 is increased fivefold and yields of hydrocarbons especially of lower members are markedly increased by the irradiation, while by the raise of the reaction temperature this ratio is reduced. This finding excludes the possibility that the irradiation effects found here come exclusively from temperature rise of catalyst caused by the irradiation. The material balance of the reaction is established well within 20%, which is satis-

Table 1. Product Yields of the Reaction of Hydrogen and Carbon Monoxide in the Presence of Fischer-Tropsch Catalyst (Fe:Cu:Diatomaceous earth = 4:1:5) with or without Irradiation

	Run No.	22076-17	22076-19	22076-23
Flow rate of reactant gas (ml/min)		54	54	54
Flow rate of residual gas (ml/min)		49	35.5	44
Gas contraction (%)		9.3	34.3	18.5
Temperature of catalyst (°C)	max	256	276	336
	min	161	157	216
Electron beam current (μa)		0	50	0
Products (gr/m^3 reactant gas)				
	CO_2	100	511.1	301.9
	CH_4	1.1	24.7	8.1
	$C_2H_6 + C_2H_4$	3.1	42.7	17.3
	C_3H_8	1.9	16.0	4.7
	C_3H_6	4.0	7.8	13.5
Gasol	$i\text{-}C_4H_{10}$	0.05	0.5	0.5
	$n\text{-}C_4H_{10}$	1.5	7.2	3.8
	$1\text{-}C_4H_8$	1.4	3.7	5.1
	$trans\text{-}2\text{-}C_4H_8$	2.2	5.1	5.6
	$cis\text{-}2\text{-}C_4H_8$	1.7	4.2	5.1
	?	0.0	0.0	0.3
	$n\text{-}C_5H_{12}$	1.6	7.1	3.6
	$1\text{-}C_5H_{10}$	0.3	0.3	4.6
	?	0.1	0.3	1.2
Benzine	$trans\text{-}2\text{-}C_5H_{10}$	1.8	2.3	18.5
	$cis\text{-}2\text{-}C_5H_{10}$	0.6	0.6	5.2
	?	0.9	4.1	10.4
	?	0.3	0.1	1.2
	?	0.0	0.3	0.3
	$n\text{-}C_6H_{14}$	1.7	5.7	14.2

Table 2. Stoichiometry between the Reactant Gas and Products

Run No.	a=CO/H_2	Flow rate (ml/min)	Beam curr. (μa)	Temperature(°C) Max	Min	x	Composition of the reacted gas (vol %) H_2	CO	CO_2	C_nH_m
22076-18	1.44	54	0	256	161	0.11 (0.1)	39.8 (39.8)	55.2 (55.5)	3.7 (3.7)	1.31 (1.3)
22076-19	1.44	54	0	336	216	0.26 (0.4)	37.3 (33.3)	41.8 (41.7)	14.9 (18.9)	6.72 (6.1)
22076-23	1.44	54	50	276	157	0.34 -	41.0 -	23.8 -	25.7 -	9.45 -
Kodama*	0.96	65	0	275	275	(0.3)	46.9 (48.4)	29.2 (30.8)	18.8 (14.8)	3.4 (8.9)

Calculated values are given in ( ).

*) S. Kodama, et al. J. Chem. Soc. Japan, 44, 663 (1941), Run No.5 in Table 1.

factory when one considers approximation made for analysis and equipments used here.

Hydrogen and carbon monoxide are catalytically converted on iron catalyst to hydrocarbons by:

$$(n + 1)\ H_2 + 2n\ CO \rightarrow C_nH_{2n+2} + n\ CO_2 \qquad (1)$$

$$n\ H_2 + 2n\ CO \rightarrow C_nH_{2n} + n\ CO_2 \qquad (2)$$

Assuming that the reactions (1) and (2) occur in equal weight and average n is 3, the molar ratio in the residual gas for H_2 : CO : CO_2 : total hydrocarbons is calculated to be:

$$(1 - x) : (a - \frac{12}{7}x) : (\frac{6}{7}x) : (\frac{2}{7}x)$$

where x is mole fraction of H_2 consumed in the feed gas (H_2 : CO = 1 : a). The calculated and observed values are compared in Table 2. Excellent agreements between experimental and calculated values for the case of reactions without irradiation at 161-256 and 216-336°C are obtained, but no calculated value which fits to the experimental data obtained with irradiation is found for any x value.

Our efforts to give a selectivity to the radiation chemical reaction by the presence of catalysts are in progress using electron beams of higher dose rate and different types of catalysts at lower temperatures. (M. Hatada, K. Matsuda)

1) T. Sugiura, S. Sugimoto, and M. Nishii, JAERI-M, 6260, 4 (1975).
2) F. Fischer and H. Tropsch, DRP 484337 (1925).
3) S. Kodama, K. Tarama, T. Ohshima, and K. Fujita, J. Chem. Soc. Japan (Ind. Chem. Ed.), 44, 663 (1941).
4) E. J. Gibson, R. W. Clarke, T. A. Doering, and D. Pope, Int. Conf. on the Peaceful Use of Atomic Energy, 29, 312 (1958).
5) H. Pichler and B. Firnhaber, Brennstoff-Chem., 44, 33 (1963).
6) I. Toyoshima, Private communication.

3. ESR Study of γ-Irradiated $CO-H_2$ Mixture Adsorbed on Solid Surfaces

Radical intermediates play important roles in radiation-induced reactions. The present study is carried out in an attempt to detect radicals produced by γ-irradiation of $CO-H_2$ mixture adsorbed on silica-supported metals, in particular Fe/Cu which are the main components of a Fischer-Tropsch catalyst.

Silica gel is dried under vacuum at 500°C for 6-10 hrs. Silica-supported Fe (1.5% in wt.), Fe/Cu (Fe, 1.5%; Cu, 0.6%), and Mn (0.08-7.9%) are prepared by immersing the dried silica gel in aqueous solutions of the corresponding nitrates and drying the products in an oven at 110°C. They are then reduced under an H_2 pressure of ca. 150 Torr at 400°C. The powders are γ-irradiated in the presence of 100 Torr of CO or H_2, or 200 Torr of the $CO-H_2$ mixture (1 : 1) at 77°K. ESR spectra are obtained before and after γ-irradiation at 77°K and various temperatures up to room temperature.

The silica-supported Fe and Fe/Cu show ESR spectra due to Fe^{3+} and Cu^{2+}, respectively, after drying at 110°C. The spectra decrease in intensity with the time of the drying, and no signals are detected after H_2-reduction. The silica-supported Mn after the reduction, on the other hand, reveals a broad spectrum which prevents a detailed examination of the radicals produced from the adsorbed gases or surface complexes such as metal carbonyls.

γ-Irradiation of the silica-supported Fe/Cu in the presence of the $CO-H_2$ mixture produces four kinds of radicals. Among these, one is assigned to CO_2^- on the basis of the g-values and ^{13}C hyperfine splittings. The CO_2^- is also observed to form by admitting CO gas to the previously irradiated silica at 77°K, confirming that the radical is formed by a secondary reaction between adsorbed CO and O^- formed in the irradiated gel.

The second radical is HCO which may be formed apparently by a reaction between adsorbed CO and H atom. The H atom

participating in the reaction originates not from adsorbed H_2 but from the silica since the HCO radical is also observed for the adsorbed sample containing CO only. In contrast to the CO_2^-, addition of CO to the pre-irradiated silica results in no spectrum ascribable to the HCO, suggesting that some excited state of either adsorbed CO or H atom may be responsible for the formation of the HCO radical.

Adsorbed H_2 yields H atom by γ-irradiation, and it may compete with adsorbed CO against the reaction with O^- in the gel since the concentration of the CO_2^- is lower than that for the sample containing CO only.

The fourth radical reveals a single line at $g = 2.050$ which increases in intensity on warming the sample from 77°K. The fact that the spectrum is observed also for the adsorbed samples of CO on the silica-supported Fe/Cu, Fe, and Mn but not for those on silica gel containing no metals implies that the signal arises from a species involving the metal atom. (S. Nagai)

4. Optical Emission from Ar-CO Mixture Irradiated by Electrons

As a part of series of studies on excited states by high energy electron irradiation of a single gas, optical emission from Ar-CO mixture system is studied.

In Fig. 1 emission spectra of the mixture with varying CO pressure are shown. The spectrum (a) is obtained with 200 Torr of Ar in the absence of CO irradiated by 15 μa of collimated electron beams of 1.5 MeV energy. A broad continuum centered at about 2200 A is recombination spectrum involving the formation of argon dimer and the peaks between 3000 and 4800 A are the emission from N_2 ($C \rightarrow B$) of N_2 contaminated as a trace impurity in Ar. Emissions from pure CO are shown in Fig. 1 (e). Two peaks D and F are due to CO^+.

The effects of the addition of CO gas to Ar are shown in spectra (b)-(d). In spite of the decrease in intensities of the emission from N_2 ($C \rightarrow B$) with addition of CO, emissions

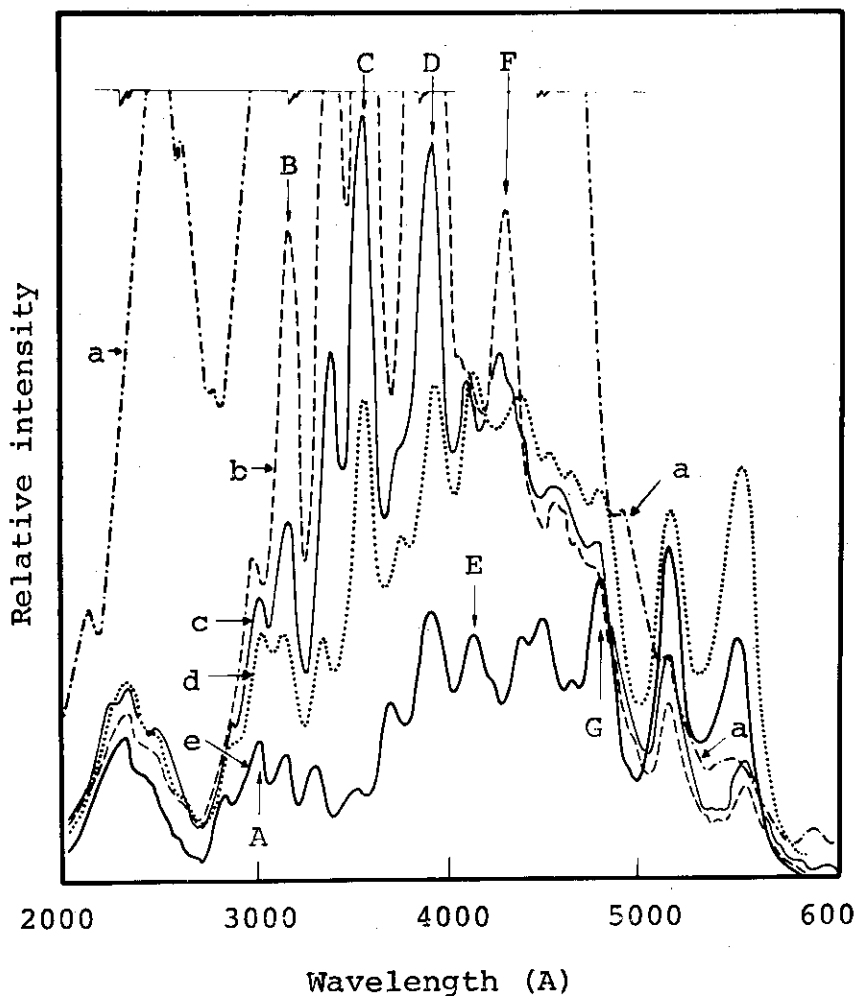

Fig. 1. Emission spectra from Ar, CO, and their mixtures.
a, Ar (200 Torr); b, Ar (200 Torr) + CO (50 Torr);
c, Ar (200 Torr) + CO (75 Torr); d, Ar (200 Torr)
+ CO (200 Torr); e, CO (200 Torr).
Emission peaks are assigned as; A, CO (b→a)(0,0); B, N_2 (C→B)(0,0); C, N_2 (C→B)(0,1); D, CO^+ (B→A)(0,0); E, CO (B→A)(1,0); F, CO^+ (A→X)(2,0); G, CO (B→A)(0,1).

from CO do not change its intensities greatly. The emission from CO^+ (B → A) is pronounced remarkably in the case of mixture with Ar. Intensity of this emission is about two orders of magnitude higher than the case of pure CO. These results indicate that the sensitization of CO and CO^+ emission is possibly due to the energy transfer from long-

lived super-excited states of Ar atom at ca. 21-25 eV which was reported recently by several investigators. (Y. Nakai, K. Matsuda)

5. Estimation of the Effective Electron Energies in the Reaction Vessel

Electrons which penetrate into a vessel containing gases through titanium windows have a broad spectrum due to scattering by the titanium windows and back scattering at the wall of the vessel. Thus, the effective energy of electrons in the vessel is different from that of the incident electrons of 300 keV ∿ 800 keV. In this work, estimation is made on the effective energy of electrons in the vessel containing hydrogen or carbon monoxide, which are of main concern in our laboratory, by comparing the stopping power ratio of the component gases with that calculated by Berger, et al[1], as a function of electron energy.

The stopping power ratio of hydrogen and carbon monoxide is given by,

$$\frac{S(H_2)}{S(CO)} = \frac{I(H_2)}{I(CO)} \cdot \frac{W(H_2)}{W(CO)} \qquad (1)$$

where I and W denote ionization yield and W-value, respectively. Using this relation, the stopping power ratios are obtained from the known W-values for hydrogen, 36.3 eV[2], and carbon monoxide, 32.2 eV[3], and ionization yield measurements which are carried out using the ionization chamber specially designed and made for the present purpose.

Fig. 1 shows the curves of the ionization current vs. applied voltage between the electrodes for hydrogen (646 Torr) and carbon monoxide (646 Torr) obtained with incident electrons of different energies. The ionization current approaches asymptotically to "saturation current" for the given incident energy.

In Fig. 2, the stopping power ratio, $S(H_2)/S(CO)$ calculated from Eq. (1) using the saturation current is plotted

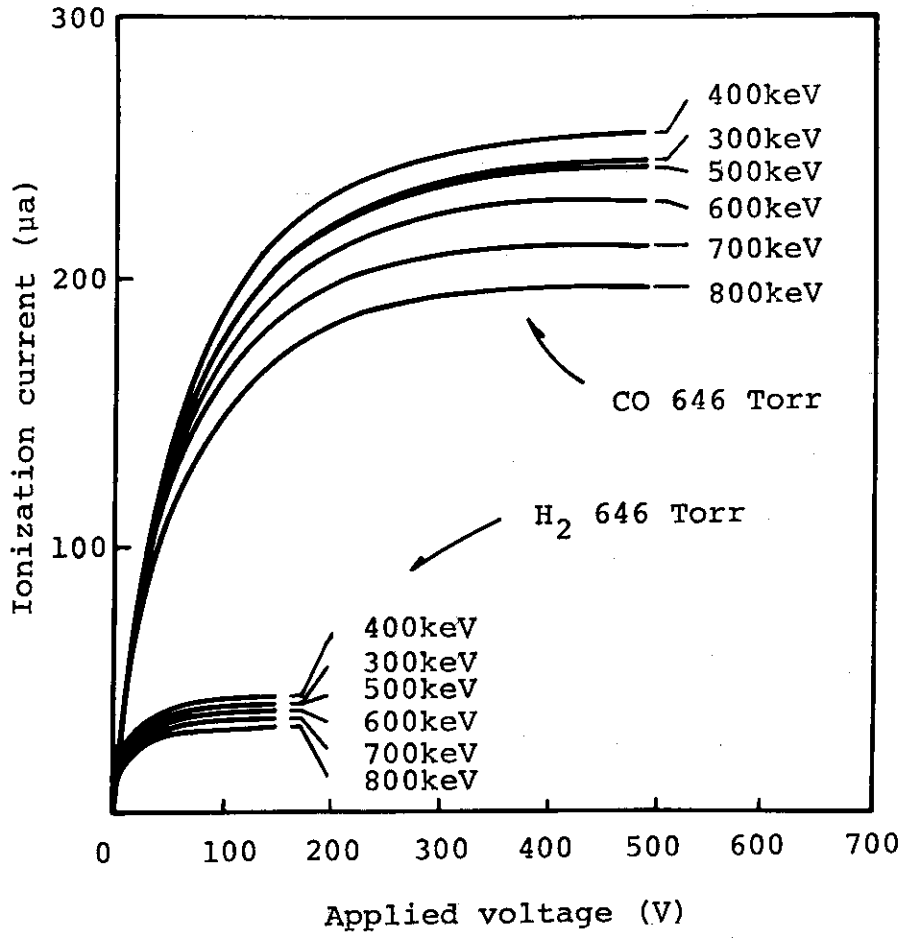

Fig. 1. Ionization current as a function of voltage applied between the electrodes. Electron beam current, 15 μa; distance from the irradiation window to the cell, 4 cm; and gap between the electrodes, 2 cm.

against the incident electron energy along with the curve calculated by Berger et al[1]. The fact that the experimental curve comes above the predicted curve indicates that the average energy of electrons in the vessel is far lower than that of the incident electron energy. The effective energy of electrons in the vessel is estimated as the energy at which the calculated stopping power ratio agrees with the experimental value, and is given in the Table 1.

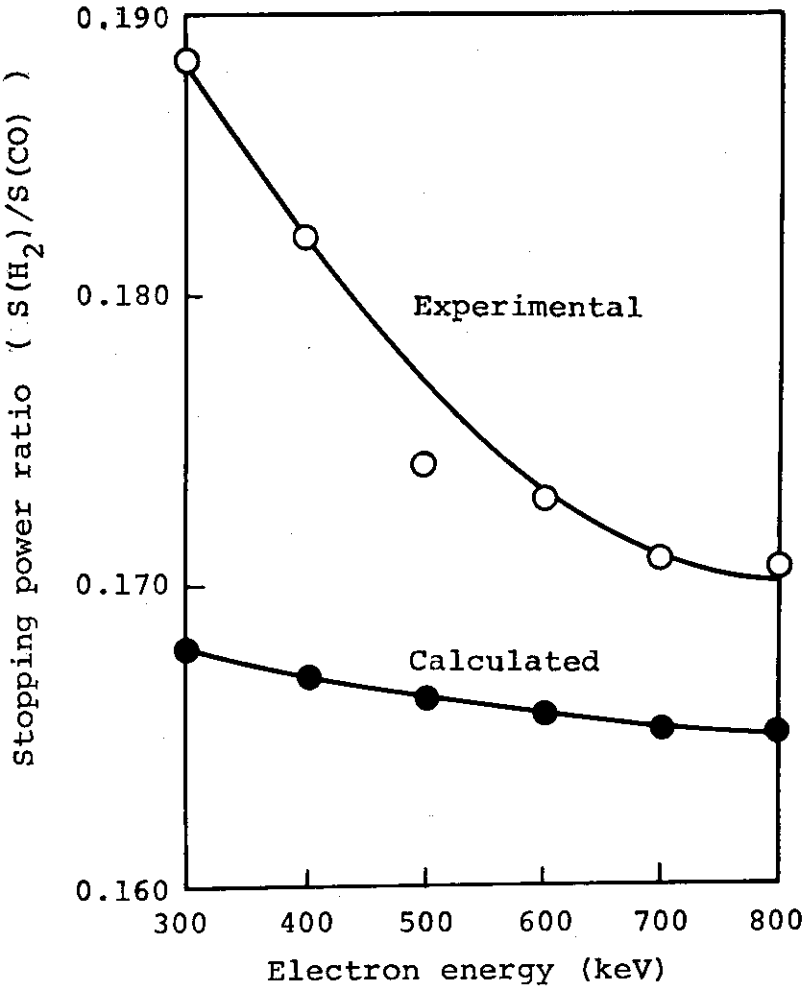

Fig. 2. Stopping power ratio $S(H_2)/S(CO)$ as a function of incident electron energy.

Table 1.

Incident electron energy (keV)	300	400	500	600	700	800
Effective energy of electrons in the vessel (keV)	10	15	45	75	100	100

As is noticed in the table, at incident energy of 800 keV, effective energy of electrons (E_{eff}) in the vessel is one-eighth of the incident electron energy, while at 300 keV, the E_{eff} is only one-thirtieth of the incident electron energy. The reason for this is that the scattering of electrons at the windows and in air path becomes larger as the incident electron energy decreases. (Y. Nakai, K. Matsuda, T. Takagaki)

1) M. J. Berger and S. M. Seltzer, NASA Report, SP-3012 (1964).
2) G. G. Meisels, J. Chem. Phys., 41, 51 (1964).
3) W. P. Jesse and J. Sadauskis, Phys. Rev., 107, 776 (1957).

[2] Radiation-Induced Reaction of Molecules in Adsorbed States

1. Structure and Reaction of Radicals Trapped in the Crystals of Thiophene and 2-Chlorothiophene

Radiolysis studies of liquid thiophene indicate that bithienyls and polymers are formed in high yields[1]. Little is known, however, about the intermediates and mechanisms for the products formation. The present ESR study[2] is carried out on radiation-induced radicals in the crystals of thiophene and 2-chlorothiophene.

Single crystals of thiophene and 2-chlorothiophene are grown at -110°C in Suprasil tubes using a technique described previously[3]. Irradiation is performed by ^{60}Co γ-rays in the dark at 77°K. ESR spectra are obtained not only for the single crystals but also for the polycrystals for comparison.

Analyses of the ESR spectra indicate that cation radicals of thiophene and allyl-type radicals produced by H atom addition to thiophene are formed at 77°K and the latter radicals undergo addition reaction to thiophene at temperatures higher than 193°K to form similar radicals in dimeric form.

γ-Irradiated single crystals of 2-chlorothiophene show an anisotropic spectrum with primary quartet splittings due to chlorine nuclei. On the basis of spin densities calculated by the CNDO method, the spectrum is assigned to the anion radical of 2-chlorothiophene which appears to be a δ^* radical, the unpaired electron being mainly confined to the anti-bonding orbital on the chlorine, Cl-C carbon, and sulfur atoms. (S. Nagai, T. Gillbro)

1) S. Berk and H. Gisser, Radiat. Res., 56, 71 (1973).
2) A part of this study was made at the Swedish Research Council's Laboratory.
3) T. Dahlgren, T. Gillbro, G. Nilsson and A. Lund, J. Phys. Sci. Instr., 4, 61 (1971).

2. Structure and Reaction of Radicals Produced by γ-Irradiation of Thiophene and Furan Adsorbed on Silica Gel

ESR study is carried out on radicals produced by γ-irradiation of thiophene and furan adsorbed on silica gel. The principal purpose of the present study is to get detailed informations on the cation radicals of thiophene which have been suggested to form in irradiated thiophene crystals. Silica gel seems to be a suitable matrix for our purpose since it has been established that cation radicals of adsorbed molecules are formed in high yields by irradiation of aromatic hydrocarbons on silica gel. Adsorbed furan is also studied to help identifications.

The ESR spectrum for adsorbed thiophene after γ-irradiation at 77°K is highly dependent on thiophene content in the samples. The samples with low thiophene content show predominantly a triplet of triplets spectrum which can be ascribed to the monomer cation of thiophene. On raising the temperature, the triplet of triplets changes to a composite spectrum consisting of two distinct components. Of these, one is the same as that observed at 77°K for the samples with higher thiophene content, and is tentatively assigned to the dimer cation of thiophene. The other component shows hyperfine splitting values characteristic of allyl-type radicals containing one β-proton, which suggests that the radical responsible for the spectrum is in a dimeric form. Since the spectrum appears at the expense of the signal due to the thiophene cation, the allyl-type radical would contain a cationic end in contrast to the same allyl-type radical formed in the irradiated thiophene crystals.

The samples with high thiophene content, on the other hand, give results similar to those obtained for the irradiated crystals.

For adsorbed furan, the results are identical with those described above for adsorbed thiophene. The findings in the present study provide an evidence of cationic process occurred in irradiated thiophene and furan. (S. Nagai, T. Gillbro)

[3] Radiation-Induced Polymerization of Mixed Multilayers of Octadecyl Acrylate and Elaidic Acid

It is known that a skeltonized fatty acid soap multilayer is formed when a mixed multilayer of the fatty acid and its soap is soaked in a solvent which dissolves out the free fatty acid modifying the properties of the multilayer. In the present study, the radiation-induced polymerization of multilayers is extended to mixtures of octadecyl acrylate (ODA) and elaidic acid (EA) in order to see whether the mixed multilayer gives skeltonized multilayer of poly(ODA) when the irradiated mixed multilayer is soaked in a solvent, dissolving out unreacted EA molecules.

The servo system employed in the previous work[1] to keep the surface pressure constant during building-up the multilayers by Langmuir-Blodgett technique is not satisfactory in the present work where slower speed (18 mm/min) of up and down trips of the glass plate is required. Therefore, the surface pressure is maintained at a desired value by slow compression of monolayer using a barrier, the movement of which is interrupted when the surface pressure exceeds a preset value. The multilayer is built-up from a monolayer containing ODA and EA (5 : 2 by weight) on pure water at 17°C up to ca. 100 layers, the type of the deposition being that of Y type.

The methods of electron beam irradiation using a Van de Graaff accelerator and the evaluation of irradiation effect are the same as those employed in the previous work[1].

Surface pressure-area(ΠA) curves of mixed monolayer from which the mixed multilayer is prepared give information on the state of aggregates or patches of molecules in the monolayer. Thus, the difference between a ΠA curve of a two-component monolayer delivered from a mixed solution of ODA and EA and one prepared by spreading one component followed by spreading the other indicates the difference in miscibility of the two components in the monolayers.

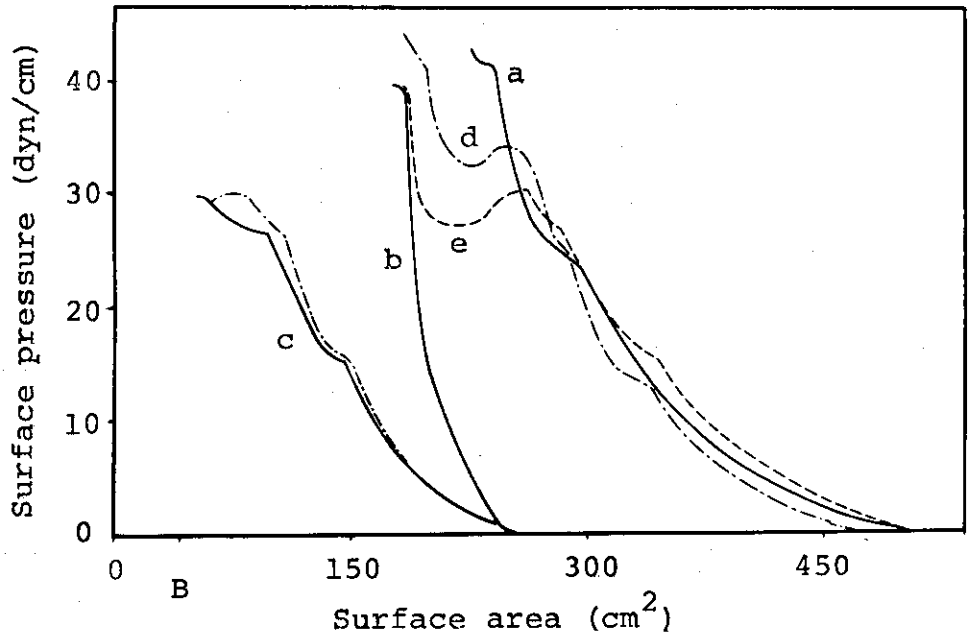

Fig. 1. Surface pressure-area curves. a, mixed monolayer of ODA and EA delivered from a mixed solution (ODA : EA = 5 : 2 by weight)(0.07 mg); b, ODA monolayer (0.05 mg); c, EA monolayer (0.02 mg); d, monolayer of ODA (0.05 mg) and EA (0.02 mg) delivered successively; and e, superposition of b and c. B denotes position of the barrier at minimum surface area.

Fig. 1 shows ΠA curves of the monolayers. Curve (a) is the ΠA curve of the monolayer spread from the mixed solution of ODA and EA. The curves (b) and (c) are the ΠA curves of monolayers of ODA and EA, respectively. Curve (d) is obtained for the monolayer spread by successive depositions of ODA and of EA. Curve (e) is the one predicted as a superposition of curves (b) and (c). Larger deviation of curve (a) of the mixed multilayer from the calculated curve (e) than that between (d) and (e) indicates that the patches of one component are small enough to exhibit the interaction of one to the other.

The patches are, however, still large enough to give

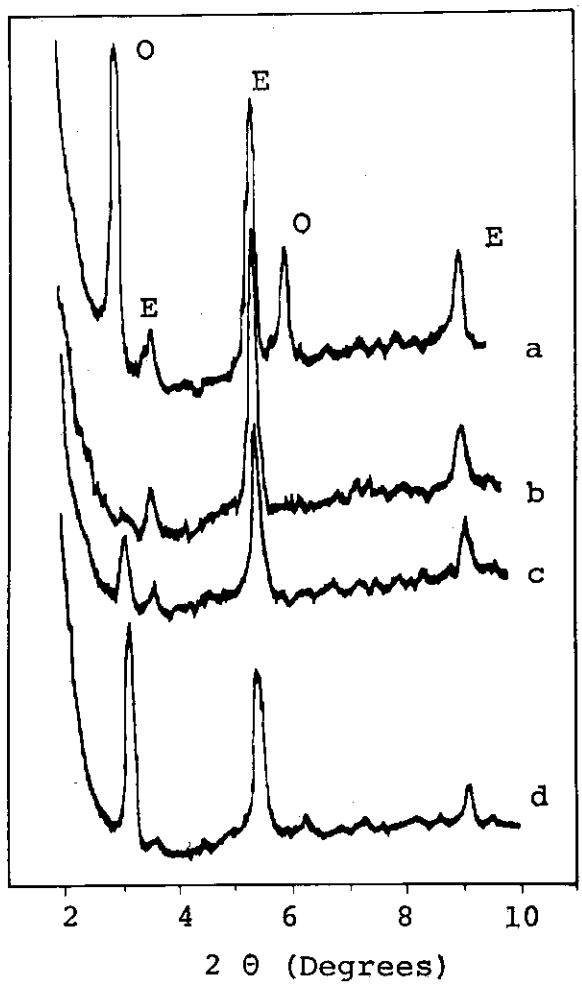

Fig. 2. Change in X-ray diffraction curves of mixed multilayer of ODA and EA upon irradiation. a, before irradiation; b, 1; c, 3; and d, 35 Mrad; O denotes reflections due to ODA and E denotes those due to EA.

reflections in the X-ray diffraction diagram of the mixed ODA-EA multilayer (Fig. 2a), which shows the presence of reflections due to both the components. The spacing of ODA (29.9 A) is not affected by the presence of EA indicating that the mixture does not form solid solutions.

Infrared spectrum of the mixed multilayer appears as a superposition of those of the two components. The absorptions due to vinyl groups of ODA disappear on irradiation, confirming that the polymerization of ODA takes place, while the absorption due to trans vinylene group of EA changes little.

The disappearance of the vinyl group in the mixed multilayer with increasing dose is almost the same as that observed for ODA multilayer which is simultaneously irradiated for a reference purpose. Since EA molecules homogeneously mixed with ODA would result in retardation of the rate of polymerization of ODA, this result again indicates that EA molecules are present as small patches in the mixed multilayer.

The intensities of reflections due to ODA decrease on irradiation in nitrogen atmosphere, and new reflections due to poly(ODA) appear when the irradiation continues further as was found in the polymerization of pure ODA multilayer[1], while the reflections due to EA remain unchanged (Fig. 2 b - d).

The reflections due to EA disappear when the irradiated mixed multilayer (dose, 35 Mrad) is immersed in n-hexane suggesting that EA molecules are dissolved out and porous skeltonized polymer multilayer is formed. (M. Hatada, M. Nishii)

1) M. Hatada, M. Nishii, and K. Hirota, JAERI, 5030, 26 (1975).

[4] Monomolecular Films of PVA-Polystyrene Block and Graft Copolymers at the Air/Water Interface

Surface pressure-area isotherms were determined for graft and block copolymers at air/aqueous medium interfaces in an attempt to investigate amphiphilic properties of the copolymers. The copolymers employed in the present work are a graft copolymer from poly(vinyl acetate) (PVAc) carrying one grafted polystyrene (PS) branch, a graft copolymer from poly(vinyl alcohol) (PVA) carrying one grafted PS branch (this was obtained by hydrolysis of the PVAc-PS graft copolymer), and a PVA-PS diblock copolymer. The graft copolymers are products of radiation-induced grafting, while the block copolymer was synthesized by condensation coupling between PS with one acyl chloride end-group and PVAc with one amino end-group. The molecular weights of component chains are given in Table 1, together with the conditions of surface pressure measurement.

Table 1. Characteristics of Polymer Samples and Conditions of Surface Pressure Measurement

Polymer	$\bar{M}_n \times 10^4$		Surface pressure measurement		
	PS	PVAc(PVA)	Solvent	Substrate	Temp. (°C)
PVAc homopolymer	——	29.5	water	0.2 N NaOH	20
PVA homopolymer	——	5.90	phenol	Water, 20% Na_2SO_4	25
PVAc-g-PS	14.0	23.6	benzene	0.2 N NaOH	20
PVA-g-PS	14.0	12.1	phenol	Water, 20% Na_2SO_4	25
PVA-b-PS	9.38	3.87	phenol	Water, 20% Na_2SO_4	25

The surface pressure of PVAc-PS graft copolymer at 20°C at the air/0.2 N NaOH interface reduced with hydrolysis time, reaching a minimum after 150 min. However, the critical area at which the surface pressure increased steeply with decreasing area, remained constant, regardless of hydrolysis time. It is clear that the steep rise of surface pressure should be ascribed to onset of the interaction among PS sequences. When the monomolecular films of PVA-PS graft copolymer were spread over the air/water interface, the surface pressure originating from the PVA chain could not be observed practically, but merely that of PS sequence appeared. On the other hand, the monomolecular films of PVA-PS graft copolymer on the 20% Na_2SO_4 substrate, in which PVA is insoluble, exhibited the surface pressure of both sequences. The result is shown in Fig. 1. Similar surface pressure-area isotherms were observed for the block copolymers, which suggests that there is no essential difference in molecular orientation at the interfaces between the PVA-PS graft copolymer and the PVA-PS diblock copolymer. Comparison of the findings with those of the corresponding homopolymers, leads to the conclusion that

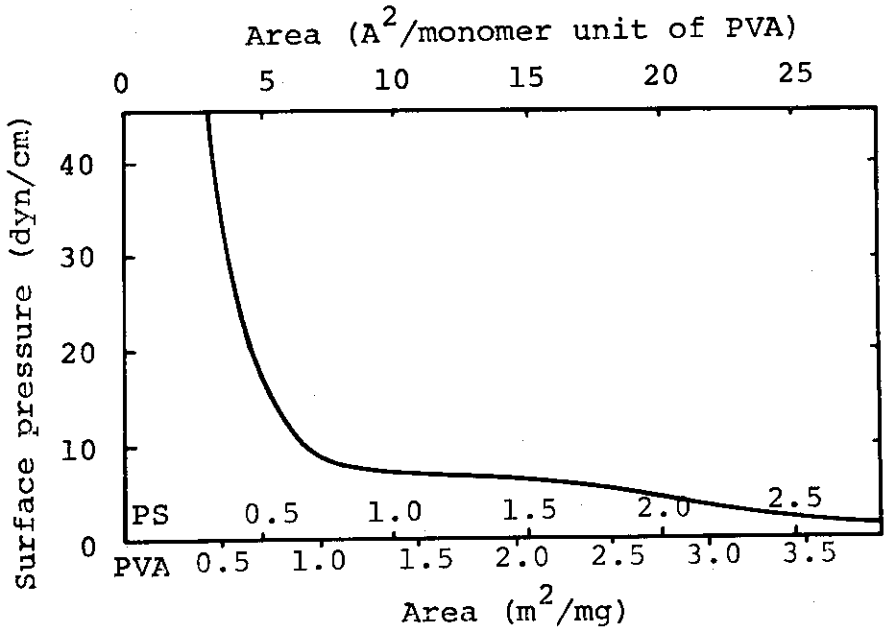

Fig. 1. Surface pressure-area isotherms for PVA-PS graft copolymer at air/20% Na_2SO_4 aqueous solution interface.

the PS sequence of PVA-PS graft and block copolymers has a spherical form on the substrate, while the PVA sequence is "dissolved" in the water medium at the air/water interface and "expanded" as a monomolecular film at the air/20% Na_2SO_4 interface. The PVAc sequence of the PVAc-PS graft copolymer seems to be hydrolyzed to PVA by 0.2 N NaOH substrate, resulting in a "dissolved" sequence. (Y. Ikada, H. Iwata, S. Nagaoka, M. Hatada)

[5] Polymerization of Vinyl Monomers by High Dose Rate Electron Beams

1. Polymerization of Moderately Dried and Water-Saturated Styrene

Studies of radiation-induced polymerization of moderately dried (water content, ca. 3 X 10^{-3} mole/l) and water-saturated (water content, ca. 3 X 10^{-2} mole/l) styrene are extended to a dose rate of 10^7 rad/sec, which is about two orders of magnitude over the highest dose rate adopted in this laboratory for the polymerization of styrene[1].

Fig. 1 shows an example of molecular weight distribution curve of polymer obtained by polymerization at a very high dose rate; in this case the dose rate is 8.4 X 10^6 rad/sec and the conversion 7.43%. The curve has one main peak which is due to polymer by cationic mechanism and two small peaks for oligomers. There is neither a peak nor a shoulder which indicates the presence of polymer by radical mechanism. It may be, therefore, concluded that only a small amount of radical polymer is contained even if it is present. This

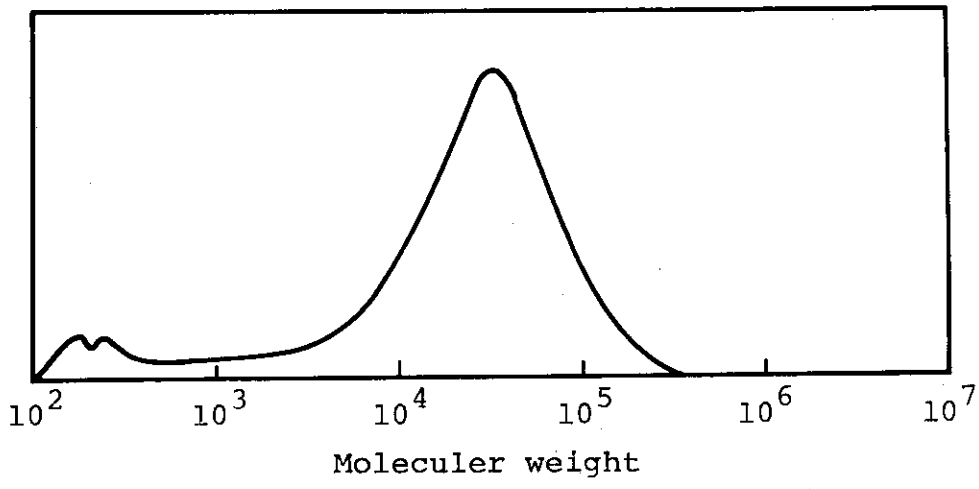

Fig. 1. Molecular weight distribution curve of polystyrene by GPC. Moderately dried styrene; dose rate, 8.4 X 10^6 rad/sec; conversion, 7.43%.

conclusion is just as was expected as a simple extrapolation of the experiments at lower dose rates.

Fig. 2 shows the dose rate dependence of the rate of polymerization of the moderately dried styrene in a very wide range of dose rate, i.e. from 10 to 10^7 rad/sec. At lower dose rates γ-rays of ^{60}Co, at the intermediate dose rates electron beams of a Van de Graaff Accelerator, and at higher dose rates those of the new high dose rate accelerator are employed for the polymerization. All points may be plotted by a slightly concave curve; the initial inclination of the curve is very near to the square root rule for the dependence of polymerization rate on dose rate, and radical mechanism

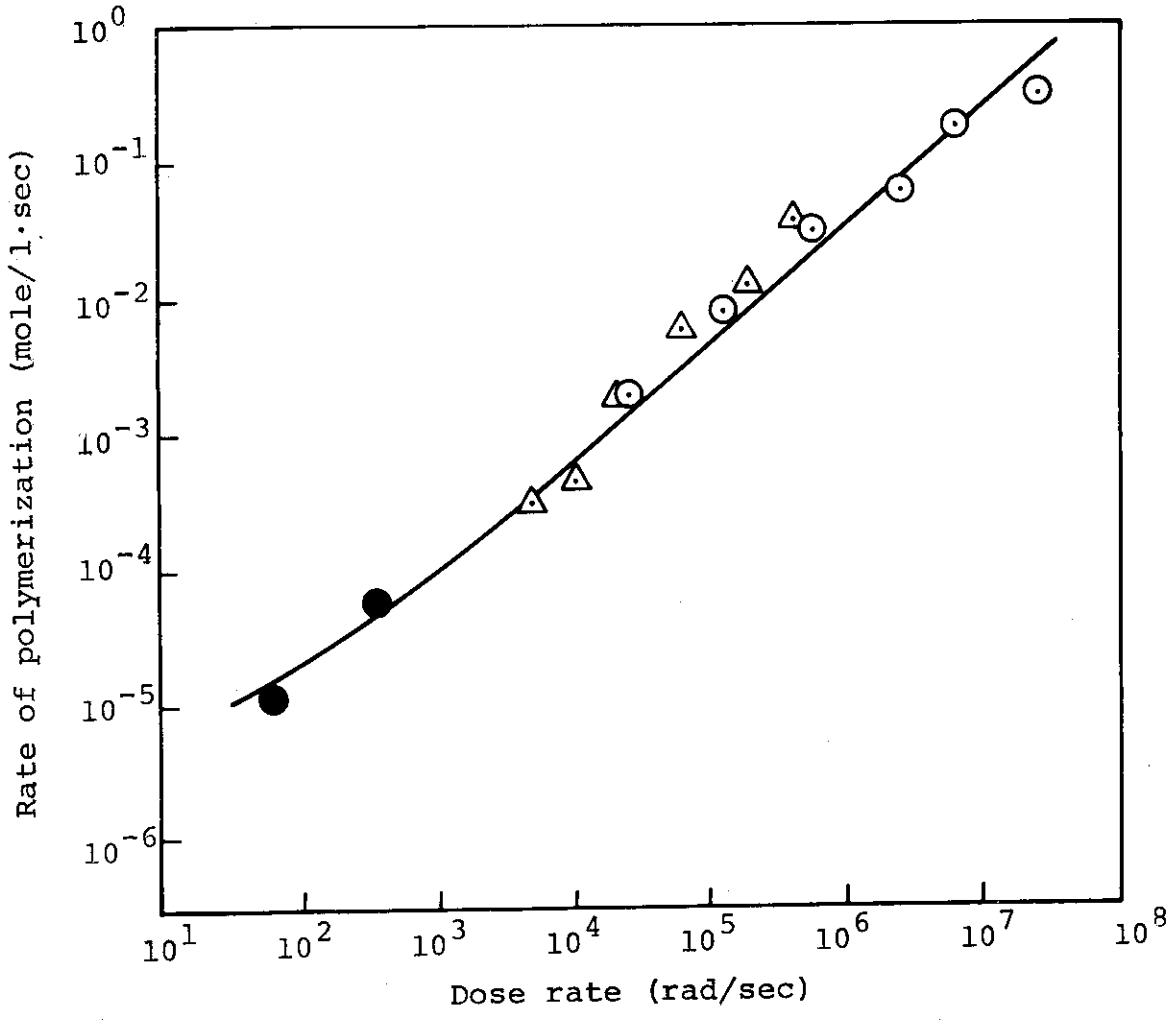

Fig. 2. Effect of dose rate on the rate of polymerization of moderately dried styrene. (○) HDRA; (△) VdG; (●) ^{60}Co.

dominates in this region; on the other hand the final inclination is about 0.9 and cationic polymerization is dominant here.

In contrast to moderately dried styrene, polymerization of water-saturated styrene at high dose rates can not be regarded as a simple extension of polymerization at lower dose rates, though the experimental results of the polymerization rates show similar dependence on the dose rate (Fig. 3) as in the case of polymerization of moderately dried styrene. At a dose rate of 1.2×10^4 rad/sec a new peak of GPC curve for the molecular weight distribution appears as is shown in Fig. 4. It is located at very high molecular

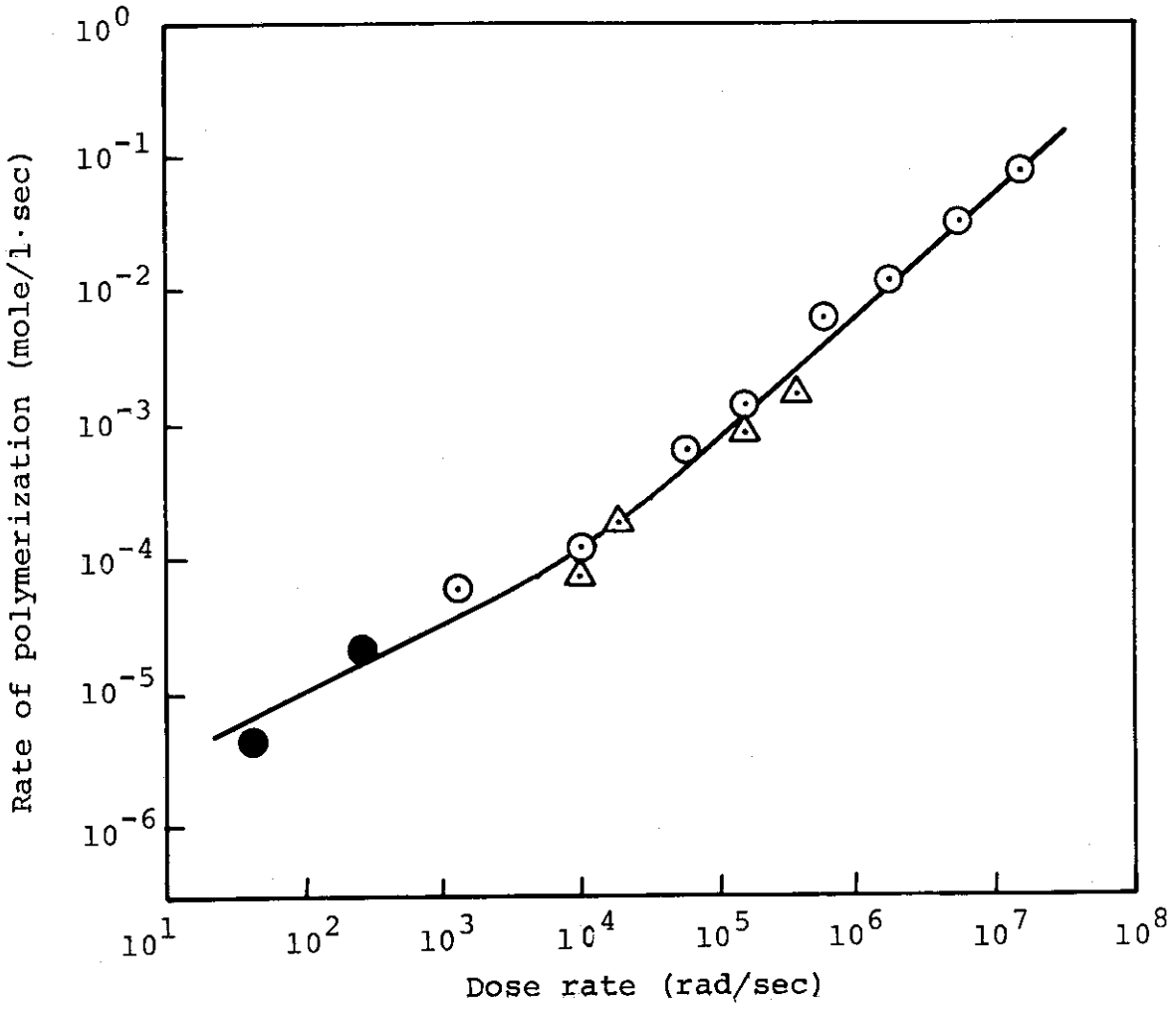

Fig. 3. Effect of dose rate on the rate of polymerization of water-saturated styrene. (○) HDRA; (△) VdG; (●) ^{60}Co.

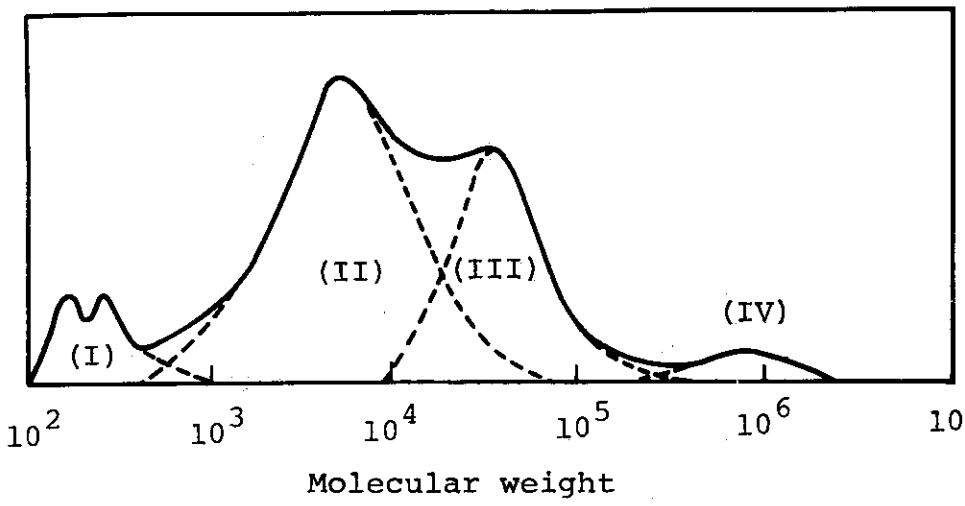

Fig. 4. Molecular weight distribution curve of polystyrene by GPC. Water-saturated styrene; dose rate, 1.2×10^4 rad/sec; conversion, 3.08%.

weight region of about 10^6, and we call this region by Nr. IV. Region Nr. I, II and III correspond to oligomer, radical polymer and cationic polymer, respectively. It is interesting that polymer molecules of very high molecular weight are formed not in dried but in water-saturated styrene. Fraction IV is not observed at 1.2×10^3 rad/sec, appears at 1.2×10^4 rad/sec and increases with increasing dose rate. The highest content of IV was about 20% of the total polymer in the initial stage of polymerization at 1.8×10^7 rad/sec, becomes 3% at 1.2×10^4 rad/sec and 0% at 1.2×10^3 rad/sec.

It is interesting that not only water but also other additives such as ammonia, acetic acid, benzophenone, and nitrogen give rise to the formation of polymer IV. When DPPH is added to moderately dried styrene in an amount of 2.5×10^{-2} mole/l, it is observed that the amount of polymer IV is about 40% of the total polymer. It is noteworthy that the position of the peak IV is practically independent of the kind of the additive. For the present it is difficult to predict the nature of the active species responsible for the formation of polymer IV; it seems, however, to be likely that a pair of styrene cation and counter anion contribute to the

formation of the polymer.

Solution polymerization of styrene in binary mixtures of styrene with carbon tetrachloride, 1,2-dichloroethane, dichlorobenzene, and nitrobenzene is carried out at a dose rate of 1 X 10^7 rad/sec and total dose of irradiation of 1 X 10^8 rad (uncorrected for the density change of the mixture). As a typical example, polymerization in styrene-dichloroethane is shown in Fig. 5. At the beginning of the curve where the solvent content is low the rate of polymerization is a little lower than that of styrene, and after passing a flat minimum it increases abruptly to show a sharp maximum at a composition of 90 mole % dichloroethane. The polymerization rate at the maximum is ten times greater than that of pure styrene. The conversion calculated by a con-

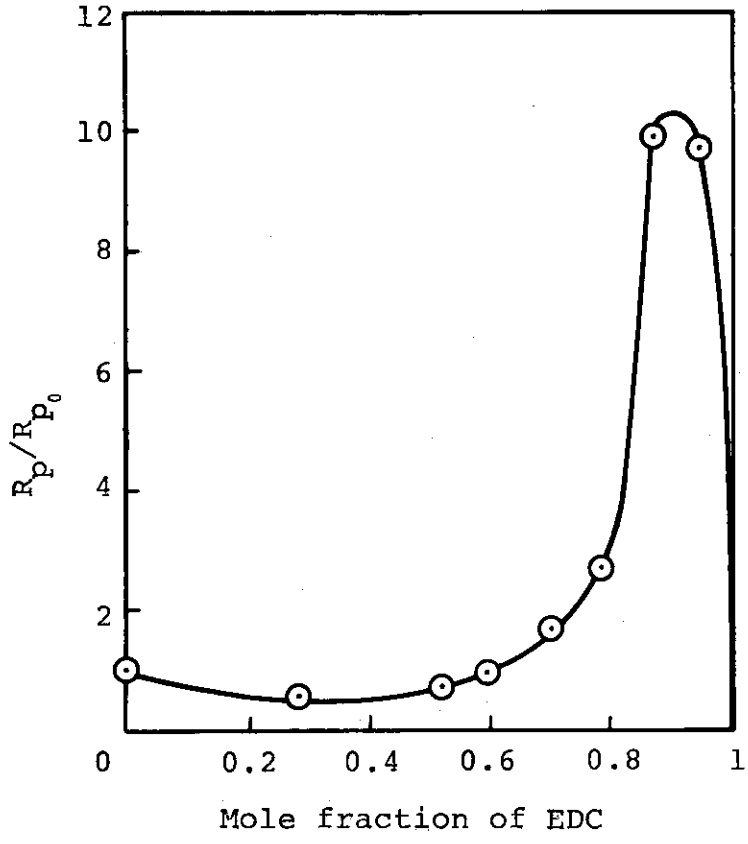

Fig. 5. Polymerization of styrene in binary mixtures with 1,2-dichloroethane at 1 X 10^7 rad/sec. The ordinate means the ratio of the polymerization rate for binary mixture (R_p) to that for pure styrene (R_{p_0}).

ventional way from the polymer weight at the maximum exceeds 100% and amounts to 130%, which means that some solvent molecules are chemically bound to polymers. All other solvents show essentially similar behavior though the height of the maximum is different from one solvent to another and is, for example, in the case of nitrobenzene only 1.5 times greater than pure styrene at a solvent content of 85 mole %.

It is interesting that in some cases, i.e. in the cases of binary mixtures with carbon tetrachloride, dichloroethane, and nitrobenzene, peak IV is observed in their GPC curves at the same position as in the case of water-saturated styrene. It seems that we are only in the beginning of study in the polymerization of styrene at high dose rates. (I. Sakurada, T. Okada, Ka. Hayashi, J. Takezaki)

1) JAERI-M, 6260, 31 (1975).

2. Polymerization of Methyl Methacrylate

It was reported last year[1] that molecular weight distribution curves of polymethyl methacrylates obtained by radiation-induced polymerization are unimodal at dose rates lower than 1.1×10^3 rad/sec, while the curve of polymer prepared at 7.0×10^4 rad/sec has a weak shoulder at higher molecular weight side of the peak, and that of polymer prepared at 2.4×10^5 rad/sec has two distinct peaks. One peak is large and the other small; the former is apparently the same peak as in other curves and the latter is new and observed only in the polymerization at higher dose rates.

More detailed experiments about the new peak are carried out. Fig. 1 shows a GPC curve of the polymer obtained by electron beam irradiation at 2.1×10^5 rad/sec; the conversion is 10% and the amount of the higher molecular weight fraction is about 10% of the total polymer; the molecular weight at the peak of this fraction is about 2×10^5, while that at the larger peak is about 2×10^3. The percent of the higher molecular weight polymer fraction increases with increasing dose rate; decreases, however, with increasing

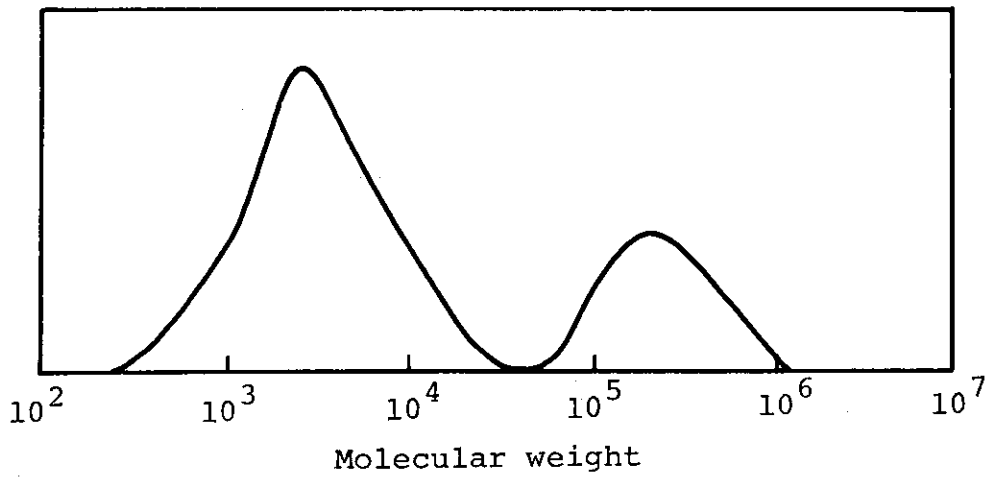

Fig. 1. Molecular weight distribution curve of PMMA by GPC. Dose rate, 2.1 X 10^5 rad/sec; conversion, 10%.

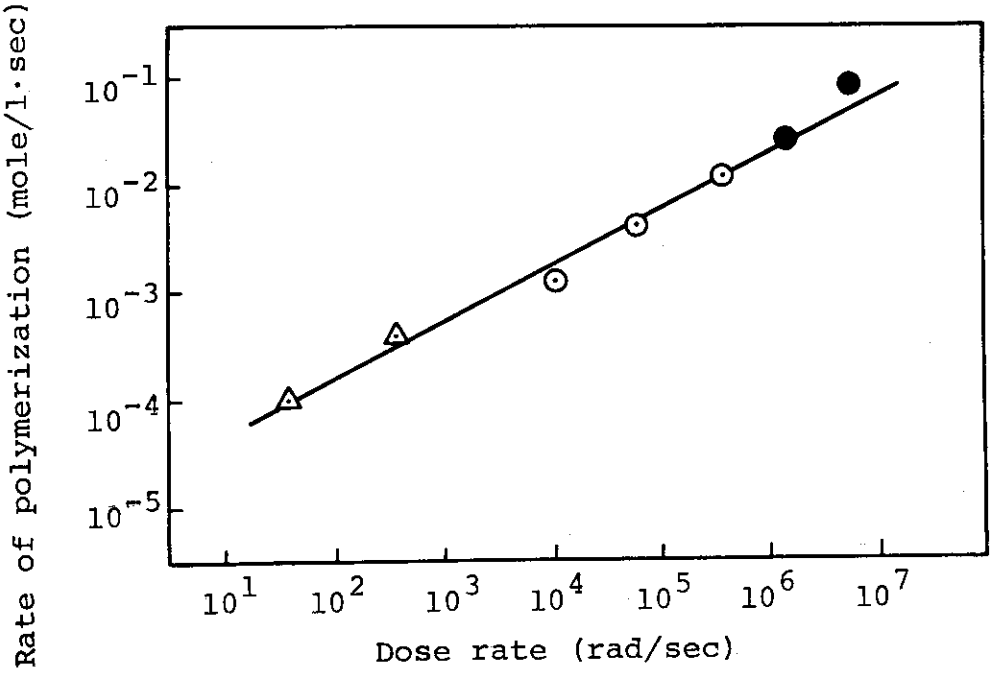

Fig. 2. Effect of dose rate on the rate of polymerization of MMA. (Δ) ^{60}Co; (o) VdG; (●) HDRA.

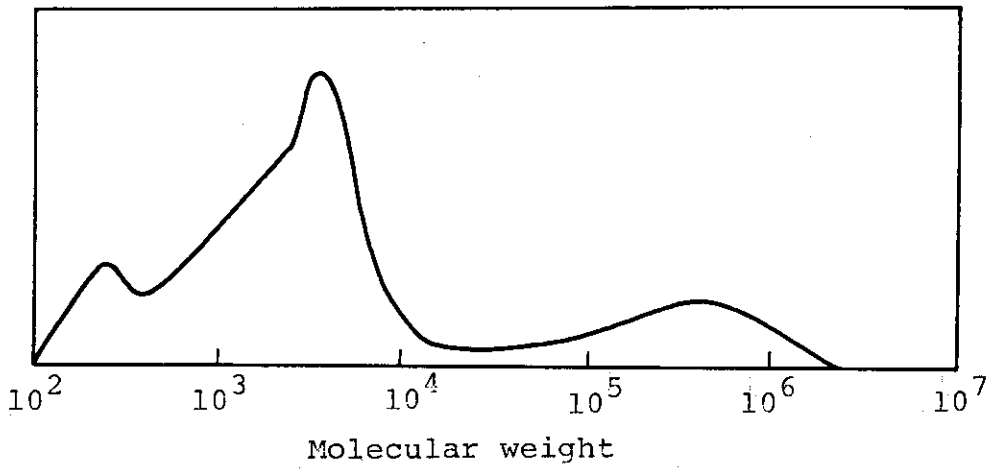

Fig. 3. Molecular weight distribution curve of PMMA by GPC. Dose rate, 1.2 X 10^6 rad/sec; conversion, 1.47%.

time of reaction, i.e. with increasing total dose of radiation, perhaps due to radiation-induced decomposition of the polymer. Though the square root relationship of the rate of polymerization holds up to ca. 10^7 rad/sec (Fig. 2), it is difficult for the present, to know the kinetic feature for the formation of the higher molecular weight polymers.

Effect of additives on the new peak is also studied. Addition of H_2O, N_2O, and CH_3COOH has no remarkable effect on the new peak while by an addition of DPPH it disappears without giving effect to the main peak, which is due to radical polymerization. Polymerization mechanism which gives rise to the new peak has to be studied.

It is noteworthy that at a still higher dose rate than that of the appearance of the peak for the higher molecular weight polymer, the third peak corresponding to molecular weight of oligomers appears as is shown in Fig. 3. The mechanism of the formation of the oligomers is also a question at present. (I. Sakurada, T. Okada, Ka. Hayashi, J. Takezaki)

1) JAERI-M, 6260, 34 (1975).

3. Polymerization of Isobutyl Vinyl Ether

Isobutyl vinyl ether (IBVE) is dried with calcium hydride before distillation, then degassed and sealed in a cell which is illustrated in Fig. 1 in Appendix II. Irradiation is carried out with 1.5 MeV electron beams from a Van de Graaff Accelerator and the temperature of the sample is maintained during the irradiation at 25°C by circulating liquid of constant temperature through a jacket of the cell. The details of dosimetry and temperature measurement under irradiation are described in Appendix II.

First the polymerization with γ-rays is studied in the dose rate range of 8.2-280 rad/sec. The conversion increases linearly with irradiation time after an induction period, and R_p is proportional to 0.48th power of the dose rate, though the R_p itself is 1/4 of that of styrene by radical mechanism. The number-average molecular weight, $\bar{M}_n$ determined

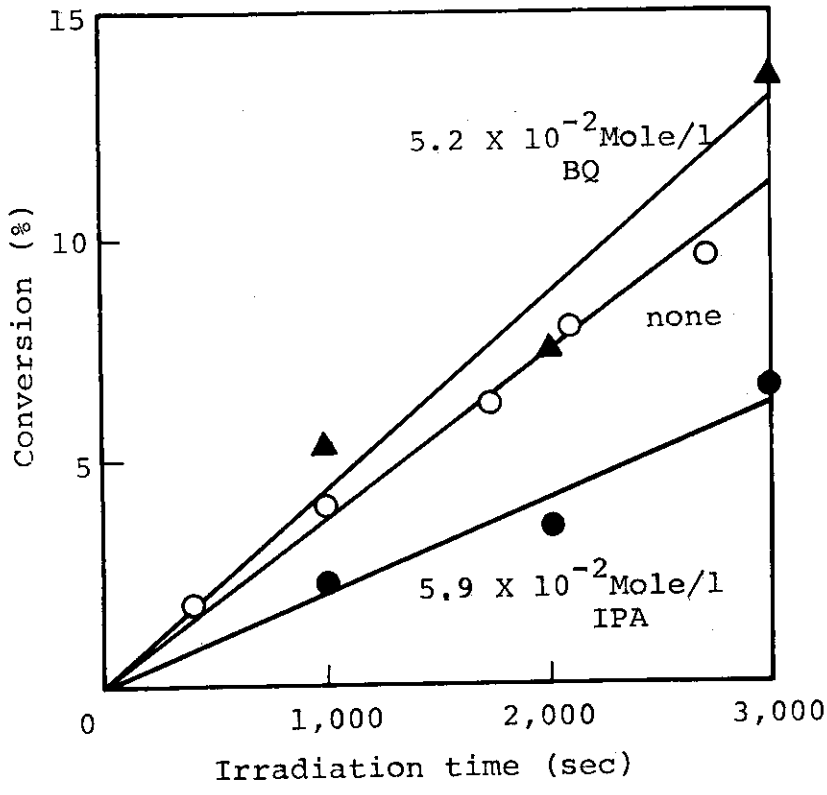

Fig. 1. Polymerization of IBVE at 25°C.
Dose rate, 8.8 X 10^3 rad/sec.

by vapour pressure osmometry decreases with increasing dose rate, from 4,600 at 8.2 rad/sec to 2,500 at 280 rad/sec. An addition of benzoquinone (BQ) greatly reduces not only R_p but also $\bar{M}_n$, while isopropylamine (IPA) does not give a significant change in R_p. All of these kinetic features indicate radical polymerization of IBVE, which is confirmed by the fact that IBVE polymer of ca. 2,000 in molecular weight is obtained by the initiation with azobisisobutyronitrile at 60°C.

Results with electron beam irradiation at the dose rate range of $8.8 \times 10^3 - 2.2 \times 10^5$ rad/sec are shown in Fig. 1. The conversion increases linearly with irradiation time and R_p is proportional to 0.75th power of the dose rate. $\bar{M}_n$ of the polymers is so low, 900-1,100, and independent of the dose rate. Addition of IPA reduces R_p substantially but that of BQ does not reduce R_p. The dose rate dependences of R_p and $\bar{M}_n$ are shown in Fig. 2. In the figure, we can see that when IPA is added R_p's fall on the linear extrapolation of the R_p in γ-ray region. This indicates that radical and cationic polymerization are taking place as in the case of styrene. Molecular weight distributions of the

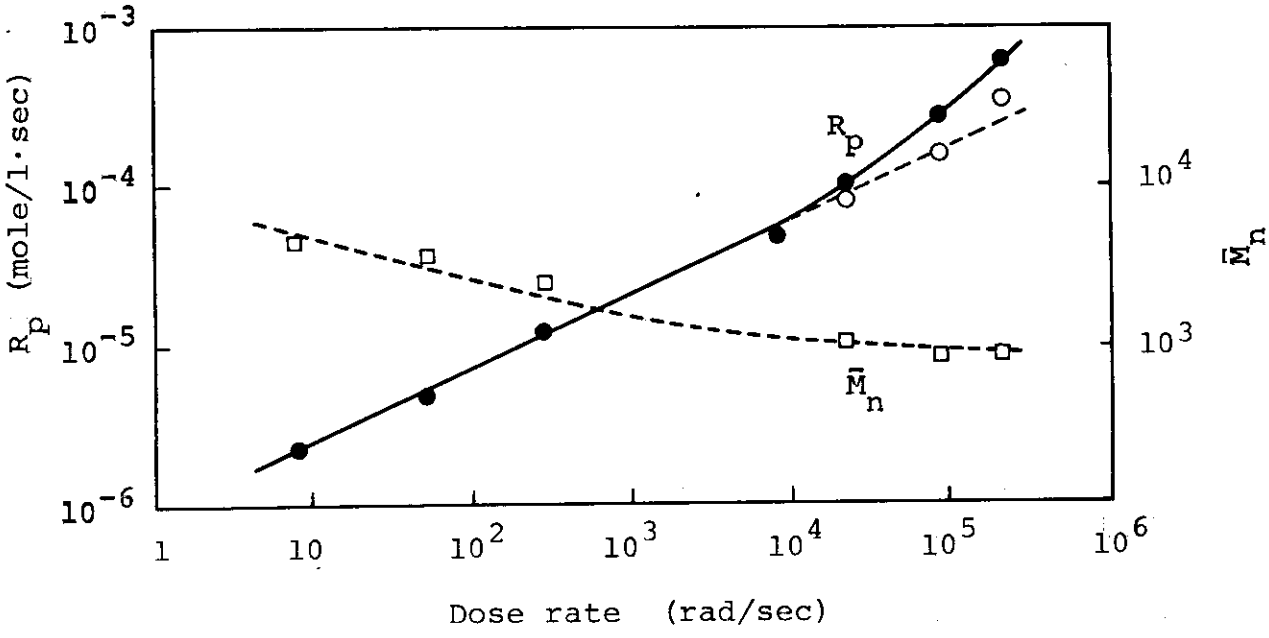

Fig. 2. Dose rate dependences of R_p and $\bar{M}_n$.
●, R_p; o, R_p in the presence of IPA; □, $\bar{M}_n$.

polymers by gel-permeation chromatograph are single-peaked and addition of IPA gives a greater molecular weight to some degree depending on dose rate and IPA concentration.
(I. Sakurada, T. Okada, Ka. Hayashi, J. Takezaki)

[6] Preparation of a Composite Ultrafiltration Membrane from Polystyrene Latex Produced by Radiation-Induced Emulsion Polymerization

Composite ultrafiltration membrane is prepared by forming thin layer of polystyrene latex on one side of porous thin substrate films.

Latex obtained by electron-induced emulsion polymerization is composed of fine polystyrene particles having diameters of 20-30 nm. By drying the latex at room temperature transparent pale yellow and brittle thin film is obtained, the broken surface of which appears to be smooth without noticeable defect under observation of high magnification by a scanning electron microscope. Since the temperature at which the film is perpared is far lower than the glass transition point of polystyrene (100°C), there should be a number of small holes which are not recognized by the microscopic observation. The size of holes may be assumed to be 4.5 nm, close to that of void space of the closest hexagonal packing of the particles, which is 16% of the particle diameter.

The polystyrene latex is prepared from deaerated aqueous mixture containing 20% monomer and 1% sodium dodecyl sulphate as an emulsifier. The mixture is irradiated under stirring for an hour with 1.7 MeV electron beams from a Van de Graaff accelerator at a dose rate of 2.8 krad/sec. Average particle diameter of the latex thus produced is estimated to be ca. 28 nm from its spectral turbidity.

Since thin layer of polystyrene latex is not mechanically strong enough for handling, composite membrane is prepared by forming thin layer of polystyrene latex on porous substrate membrane for support. Two types of porous substrate films made of polypropylene are tested: Guragard 2400 and Guragard 2400W (supplied by Japan Plastics Co.), the latter being prepared from the former by pretreating the film with a surface active agent of an ester type. The films are of

25 μm thick having pores of 100 X 220 nm with porosity of 35%. The minimum pressure required to initiate permeation of water through the film of 2400 type is 42 kg/cm^2.

Since the composite membrane with 2400 type film is not suitable for permeation experiments, the experiments are carried out on the composite membrane with 2400W which shows appropriate water penetration. Water-flux and solute retention of the composite membrane at 15 kg/cm^2 are measured for Rhodamine-B (MW 480), Gramicidine-S (1,140), Dextran (61,500 and 215,000), and deoxyribonucleic acid (2,500,000).

The composite membrane (W), obtained by use of the polystyrene latex of 20% solid, showed water flux for pure water scattered in a range from 2 to 18 ml/hr for an effective area of 10.8 cm^2. By repeated coating of dilute latex of 5% solid, the water flux is lowered gradually with increasing cycle of coat-dry-wash operation, and reaches a constant value of about 2 ml/hr in a few cycle. Best results in the solute retention are shown in Fig. 1, in which the

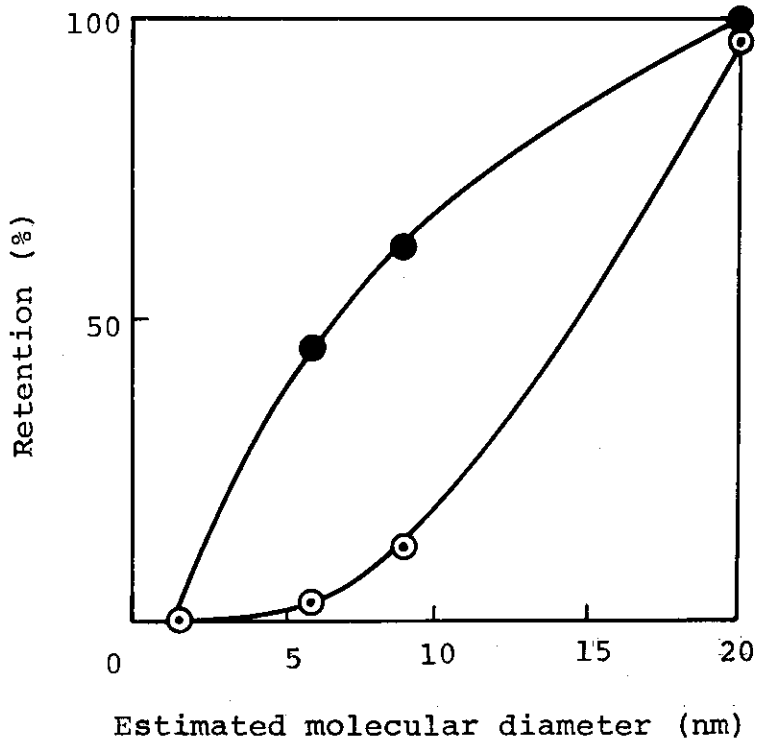

Fig. 1. Solute retentions for the original film (o) and the composite membrane (●).

abscissa means diameter of a solute molecule which is estimated from its molecular weight assuming sphere molecular shape having density of 1.0 g/cm^3. Improvement in the rejection property was not so good as expected, and the hole diameter seems to be larger than the expected value of 4.5 nm.

Infrared spectra of the composite membranes (W) indicate that a considerable amount of sodium dodecyl sulfate is settled in the membrane and thickness of the polystyrene layer is smaller than 1,000 nm. Measurement of sorption isotherms of water vapor for the composite membranes shows that their water sorption capacity is reduced to some extent as compared with that of the original film. (H. Kamiyama)

[7] Preparation of Cross-Linked Hydrogel Membranes by Radiation Technique

As a continuation of the study on preparation of hydrogel membranes, moderately concentrated, aqueous solutions of poly(ethylene oxide) (PEO), polyacrylamide (PAAm), polyvinylpyrrolidone (PVP), and methyl cellulose (MC) were cast on a glass plate and irradiated with electron beams to yield cross-linked hydrogels. Irradiation was carried out in the similar way as to the aqueous solution of poly(vinyl alcohol) (PVA). In all cases, no attempt was made to expel air from the polymer-water mixture to be irradiated, since water-insoluble hydrogels were readily formed by placing a glass plate or a polyethylene film on the mixture. The hydrogel membranes thus obtained were stored in plenty of water at room temperature and subjected to measurement of the degree of swelling (DS) in water, defined as gram of water in the swollen membrane per gram of the dried polymer.

The degree of polymerization (DP) of the polymer samples is tabulated in Table 1 together with the gelation

Table 1. Gelation Dose of Aqueous Polymer Solutions Irradiated with Electron Beams

Polymer		DP	Polymer conc. (wt%)	Gelation dose (Mrad)
Poly(vinyl Alcohol),	PVA	2,000	10	1
Polyacrylamide,	PAAm	10,000	10	1
Polyvinylpyrrolidone,	PVP	6,000	16	2
Poly(ethylene Oxide),	PEO	10,000	10	3
" , ,	"	500	40	8
Methyl cellulose,	MC	100	10	10

dose of the aqueous solutions irradiated at the given concentrations.

The DS of the hydrogels prepared on irradiation of the cast solutions is plotted against the radiation dose in Fig. 1. It is seen that PVA yields highly cross-linked gels on irradiation with relatively low doses, while the irradiation

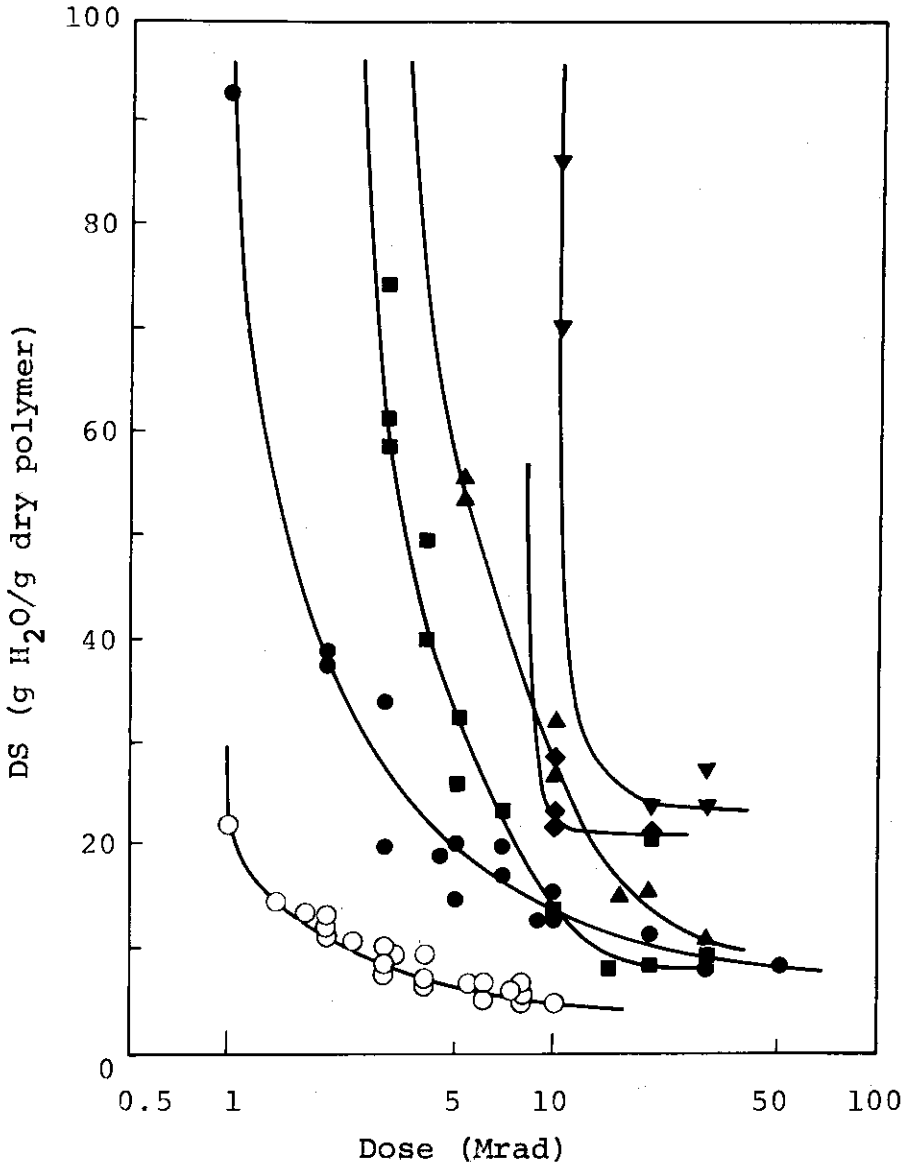

Fig. 1. Degree of swelling (DS) of hydrogels obtained on irradiation of cast solutions. Dose rate, 0.1 Mrad/sec; (o) PVA; (●) PAAm; (■) PVP; (▲) PEO(10,000); (▼) PEO(500); (◆) MC.

of the other polymers, especially MC and PEO having low DP, results in formation of hydrogels of high DS even though irradiated with high doses. However, as can be seen from Fig. 2, highly cross-linked hydrogels could be prepared from PAAm, PVP, and PEO (DP = 10,000), when the hydrogels formed on irradiation of the cast solutions were peeled off from the glass plate and then placed again on the glass plate with plenty of water, followed by irradiation. On the other hand

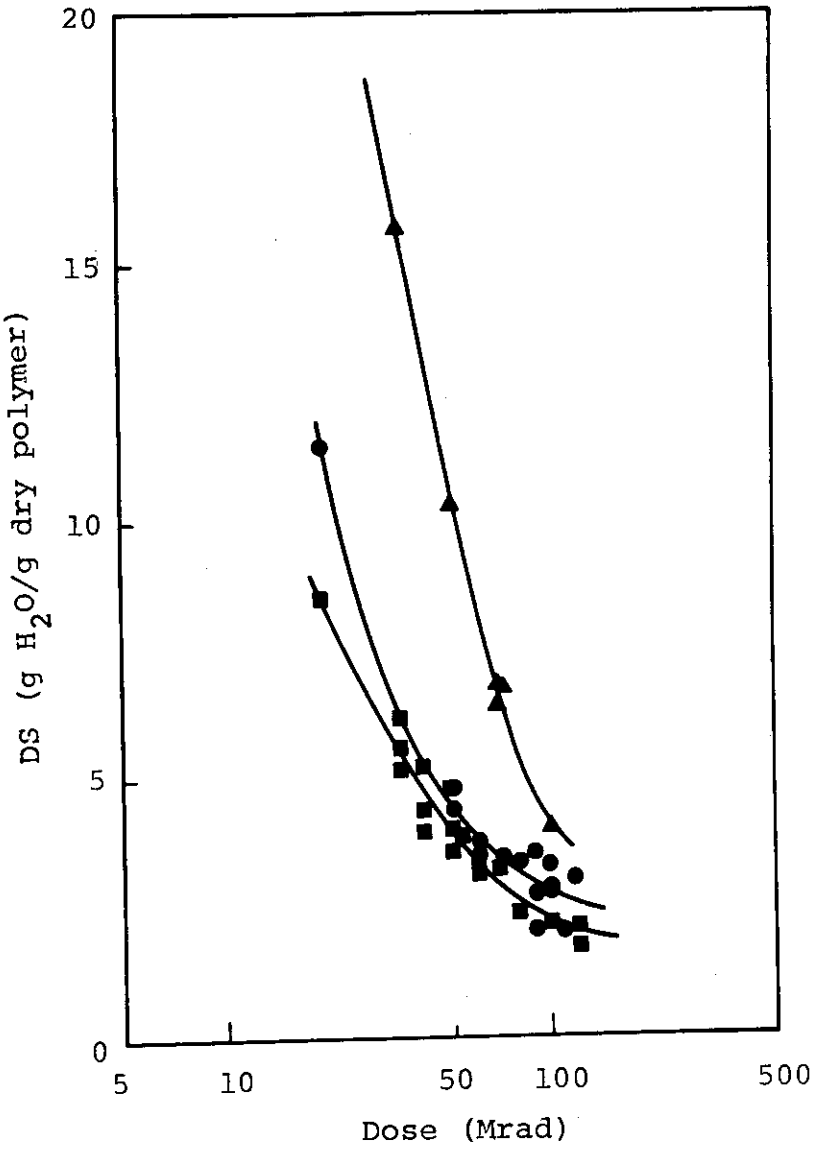

Fig. 2. Degree of swelling (DS) of hydrogels obtained on irradiation of water-swollen films. Dose rate, 0.1 Mrad/sec; (●) PAAm; (■) PVP; (▲) PEO(10,000).

it was not successful to get moderately cross-linked hydrogel membranes from MC and PEO (DP = 500) even by such repeated irradiations.

Neither coloration nor significant spectral change in the ultraviolet and infrared region was observed of the hydrogels prepared with such high doses as 100 Mrads.

The hydrogels obtained were fragile, but tolerable for measurements of permeability of water. Comparison of the water permeability in the hydrogels at the same volume fraction of water revealed that the PVA hydrogel gave the lower permeability and the hydrogel from PAAm the highest. (Y. Ikada, T. Mita, F. Horii, I. Sakurada, M. Hatada)

[8] Modification of Polymers

1. Radiation-Induced Grafting of Acrylic Acid onto Polyvinyl Chloride Fiber. Some Kinetic Features of the Grafting

It has already been reported that the grafting of acrylic acid (AA) onto polyvinyl chloride (PVC) fiber was smoothly conducted by irradiation of γ-rays in a monomor mixture containing ethylene dichloride as a swelling agent and a small amount of Mohr's salt as an inhibitor of polymerization outside of the fiber. The graft fiber exhibited high heat-shrinkage temperature and improved hygroscopicity without serious loss of flame-retardance of the original fiber. Studies were extended in order to elucidate some kinetic features of the grafting.

At first, influence of the concentration of ethylene dichloride in the monomer mixture on the rate of grafting was investigated. The amount of ethylene dichloride added to aqueous solution of AA of various concentrations is varied while the concentration of Mohr's salt, the dose rate, and the irradiation temperature are maintained at constant values of 2×10^{-3} mole/l, 2.3×10^{5} rad/sec, and 23°C, respectively. For a given concentration of AA, the rate of grafting increases steadily with addition of ethylene dichloride; a sharp rise in the rate of grafting is observed when ethylene dichloride is added to the monomer solution in an amount, where phase separation occurs. For example, for 50% aqueous solution of AA, phase separation occurs when 13.4 volume parts of ethylene dichloride are added to 100 volume parts of the monomer solutions. The percents graft of 85 and 126% are obtained by the irradiation of 5 minutes for the solutions containing 13 and 15 parts of ethylene dichloride; the percent graft, however, is only 33 when 10 volume parts of ethylene dichloride are added to the solution.

To suppress the homopolymerization outside of the fiber various metal salts are incorporated in the monomer mixture,

and it was found that Mohr's salt or copper sulfate at a concentration of 10^{-2} to 10^{-3} mole/l in the solution is suitable for the purpose. In the following experiments the monomer mixture consisting of AA, water, and ethylene dichloride (50 : 40 : 10, by volume) containing Mohr's salt (4×10^{-3} mole/l) is employed. Percent graft-irradiation time curves obtained at various dose rates from 8.5×10^{3} to 1.4×10^{5} rad/hr are shown in Fig. 1.

With increasing dose rate the rate of grafting increases. Initial rate of grafting is found to be proportional to the 0.76th power of the dose rate. Simple kinetic analysis suggests that the value of 1.0 is expected for the dose rate exponent of homopolymerization in which chains terminate primarily by the metal cations and bimolecular termination between polymer radicals is negligible. The exponent of 0.76 obtained for the grafting is indicative of a mixed form of termination by ferrous ion and by bimolecular reaction

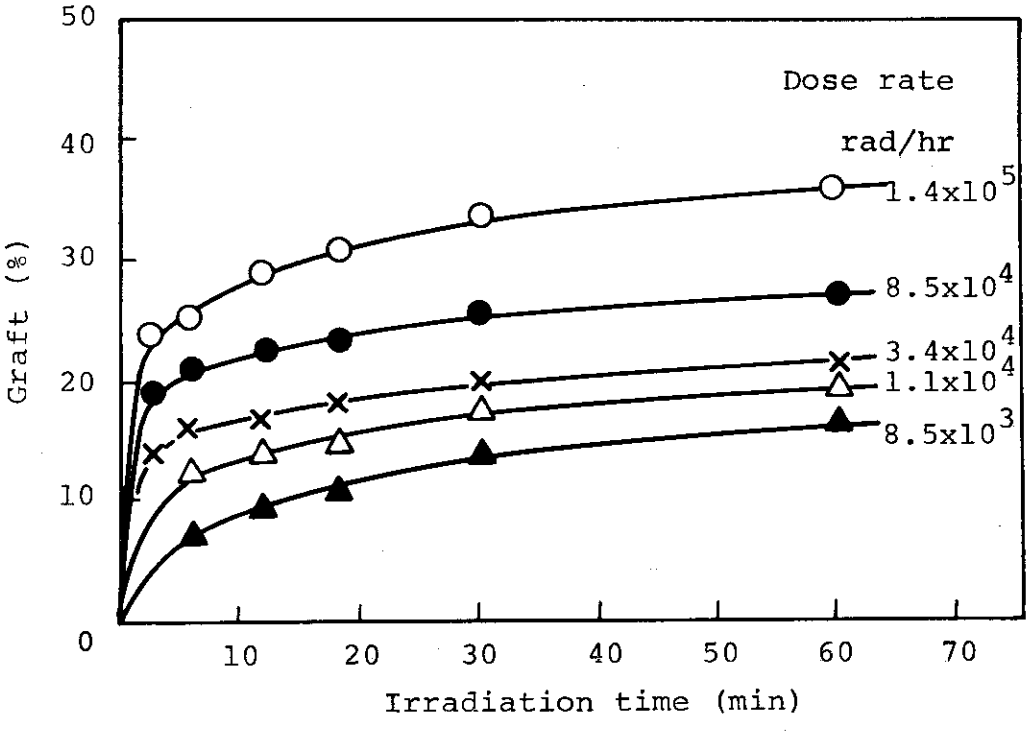

Fig. 1. Grafting of AA onto PVC fiber at 25°C at different dose rates. Monomer mixture, AA : H_2O : EDC = 50 : 40 : 10; $[Fe^{++}] = 4 \times 10^{-3}$ mole/l.

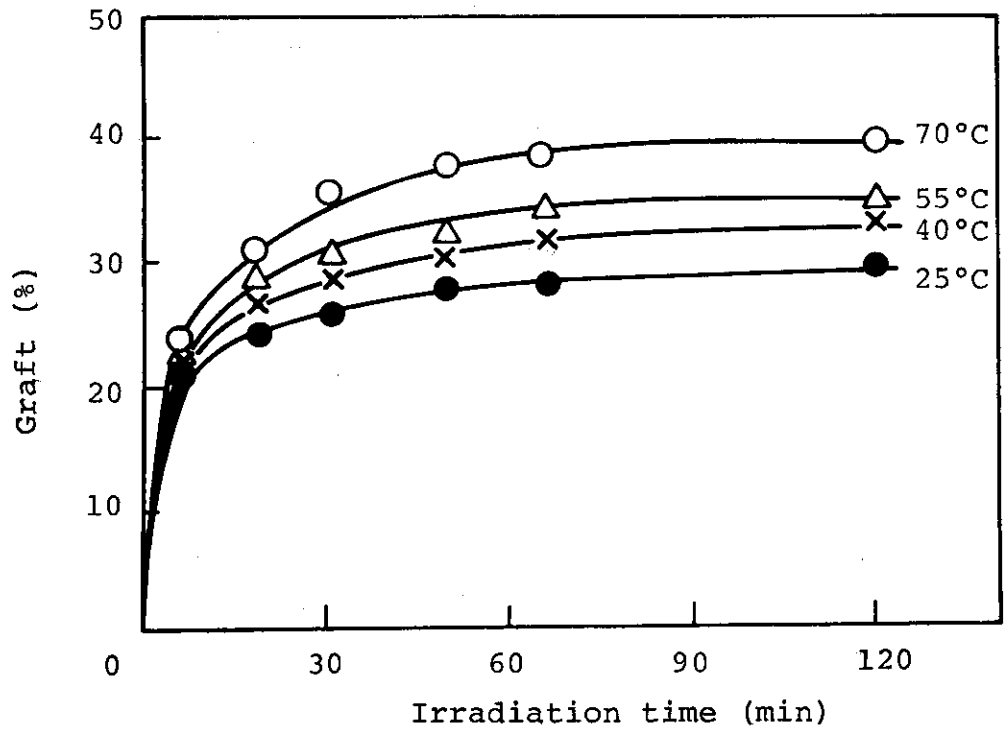

Fig. 2. Grafting of AA onto PVC fibers at 8.5 X 10^4 rad/hr at different temperatures. Monomer mixture, AA : H_2O : EDC = 50 : 40 : 10; $[Fe^{++}]$ = 4 X 10^{-3} mole/l.

between growing chains. Nearly the same dose rate exponent was found in the grafting of AA onto polyester fiber in aqueous solution of AA containing Mohr's salt.

As shown in Fig. 1 there is a tendency that percent graft approaches with time of irradiation to a certain levelling-off value which is dependent on the dose rate.

The grafting experiments are also carried out at various temperatures: 25, 40, 55, and 70°C. Fig. 2 shows the grafting curves at different temperatures while other parameters are constant. Both the initial rate of grafting and levelling-off value of percent graft increase slightly by raising irradiation temperature. Arrhenius plot of the initial rate of grafting gives apparent overall activation energy of 0.7 kcal/mole. (I. Sakurada, T. Okada, K. Kaji, C. K. Lee)

2. Radiation-Induced Grafting of Calcium Acrylate onto Polyvinyl Chloride Fiber

As an extension of studies to modify properties of polyvinyl chloride (PVC) fiber by radiation-induced grafting of acrylic acid, similar experiments are carried out with calcium acrylate (Ca-acrylate). By use of Ca-acrylate, one can get rid of troubles which may be encoutered during grafting precedure of acrylic acid due to its high vapor pressure and strong odor. The process can be simplified by replacing two steps, i.e., grafting of acrylic acid and cross-linking of the graft fiber with calcium ion, with one step, i.e. direct grafting of Ca-acrylate.

The grafting of PVC fiber can be carried out smoothly in a mixture of Ca-acrylate,methanol,water, and ethylene dichloride with irradiation of γ-rays from a ^{60}Co source. It is also

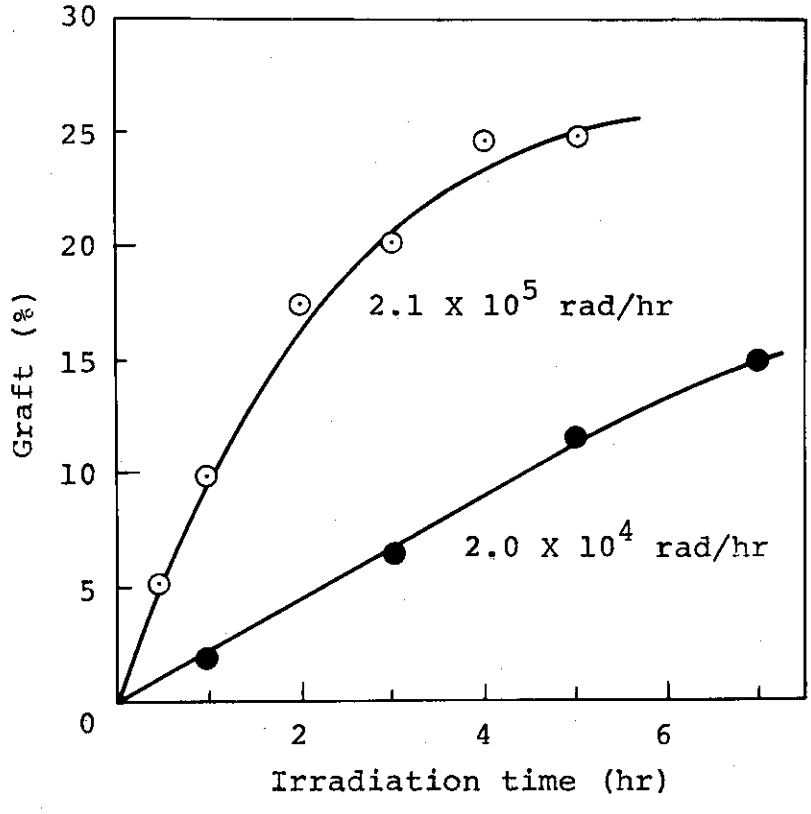

Fig. 1. Grafting of Ca-acrylate onto PVC fiber with γ-rays. Monomer mixture, Ca-acrylate : H_2O : MeOH : EDC = 15 : 39 : 39 : 6 (by weight)

necessary to add $FeCl_2$ to the mixture in order to prevent useless homopolymerization of the monomer outside of the fiber.

Fig. 1 shows the plots of percent graft against irradiation time at 2.1 X 10^5 and 2.0 X 10^4 rad/hr. At the dose rate of 2.1 X 10^5 rad/hr, one hour irradiation is needed to attain 10% graft. It means that the rate of grafting is only one-tenth of that for acrylic acid.

Measurement of tensile properties of the fibers with up to 30% graft shows that strength, elongation, and initial Young's modulus are not decreased by the grafting. Similar results are found for Ca-acrylate graft fiber prepared by the two-step procedure.

Ca-acrylate graft fibers have satisfactorily high heat-shrinkage temperature. In Fig. 2 heat-shrinkage of graft fibers against temperature is given along with that of the original fiber. The fiber of 20% graft gives maximum shrinkage of 30% which is much lower than that of the original fiber, but breaks off at 190°C as the original fiber. The fiber of 34% graft shows shrinkage of less than 20% and retains its fiber form even above 300°C.

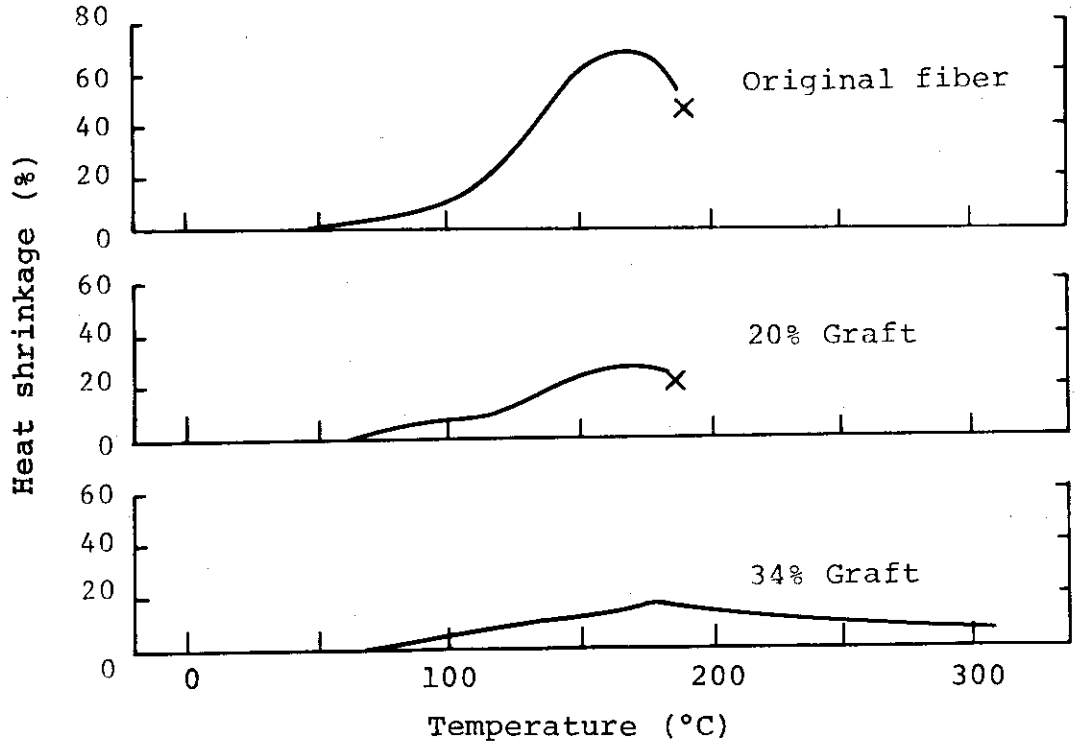

Fig. 2. Heat-shrinkage of Ca-acrylate graft PVC fibers.

When properties of Ca-acrylate graft fibers prepared by one-step and two-step methods are compared, the former shows lower temperature of heat-shrinkage.

No difference of the fiber surface appearance is observed between the two methods as examined by a scanning electron microscope at the magnification of 1,000. (I. Sakurada, T. Okada, K. Kaji)

3. Radiation-Induced Grafting of Acrylamide onto Polyvinyl Chloride

As a continuation of the grafting of acrylic acid onto polyvinyl chloride (PVC), acrylamide (AAm) is taken up in order to avoid troubles which may be encountered during grafting procedures because of high vapor pressure and strong odor of acrylic acid, and the properties of AAm-grafted PVC fiber are studied. PVC fiber dipped in a mixture of AAm, methanol, and ethylene dichloride (EDC) is irradiated with γ-rays from a ^{60}Co source or with electron beams from a Van de Graaff accelerator (VdG) or from a high dose rate electron accelerator (HDRA). After irradiation, PVC fiber is taken out, washed with ethanol and then with water, dried and weighed. The apparent graft percent is calculated by weight increment of PVC before and after the grafting. EDC is necessary for the grafting as a swelling agent, because no grafting takes place at all in a mixture of AAm and MeOH or other common solvent.

In order to prevent formation of homopolymer outside of fiber, effects of addition of various metal salts on the grafting are examined, among which ferrous chloride is the most suitable for the present purpose.

The dose rate dependence on the grafting is studied over an extremely wide range of dose rate: from 1.3 to 3.1 X 10^2 rad/sec using γ-rays from the ^{60}Co source; from 2.6 X 10^3 to 3.5 X 10^5 rad/sec by electron beams from the VdG and from 1.1 X 10^5 to 9.6 X 10^6 rad/sec by electron beams from the HDRA. The results are shown in Fig. 1 where logarithms of

the initial rates of grafting are plotted against logarithms of the dose rates. Obviously, the plots lie on a straight line which indicates the initial rate of grafting is proportional to the 0.76th power of the dose rate covering the whole range of the dose rate studied (1 - 10^7 rad/sec).

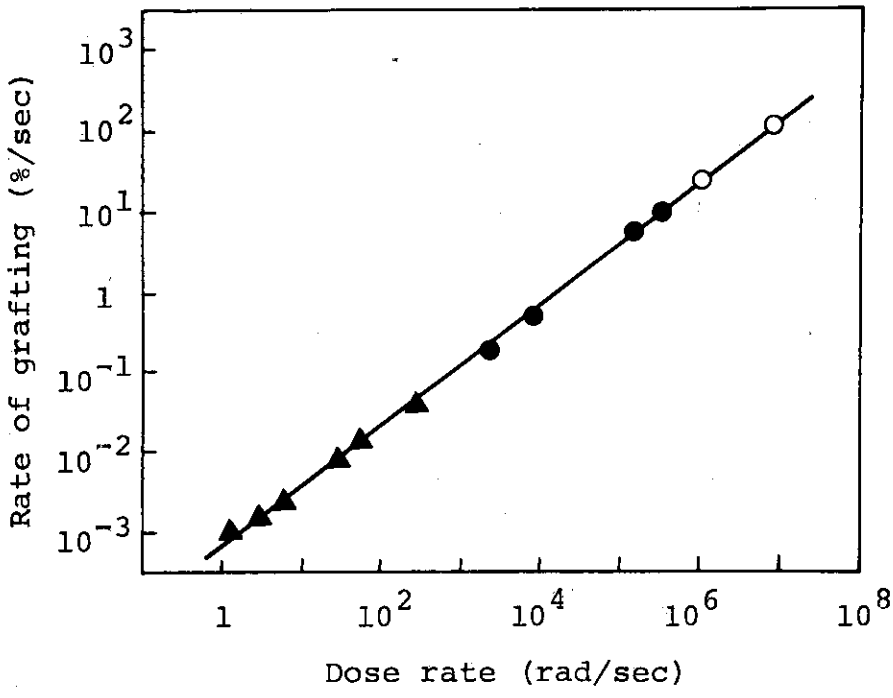

Fig. 1. Grafting of acrylamide onto PVC fiber at different dose rates at 23°C. (o) HDRA; (●) VdG; (▲) ^{60}Co.

The grafting reaction proceeds quickly at a dose rate of 9.6 X 10^6 rad/sec, and 20% grafting is attained in 1 sec irradiation as shown in Fig. 2.

Studies on tensile properties of the grafted fiber using an Instron tensile tester reveal that strength, elongation, and initial Young's modulus are not affected by 56% grafting. Tenacity (in g/d) of fiber is decreased with increasing graft percent. Such a drop of the tenacity is always the case when a fiber is grafted. Original PVC fiber exhibits little hygroscopicity, but the hygroscopicity of the grafted PVC fiber increases with increasing graft percent and at 50% it is almost equal to that of cotton, and further increases when the AAm-grafted PVC is hydrolyzed in aqueous solution

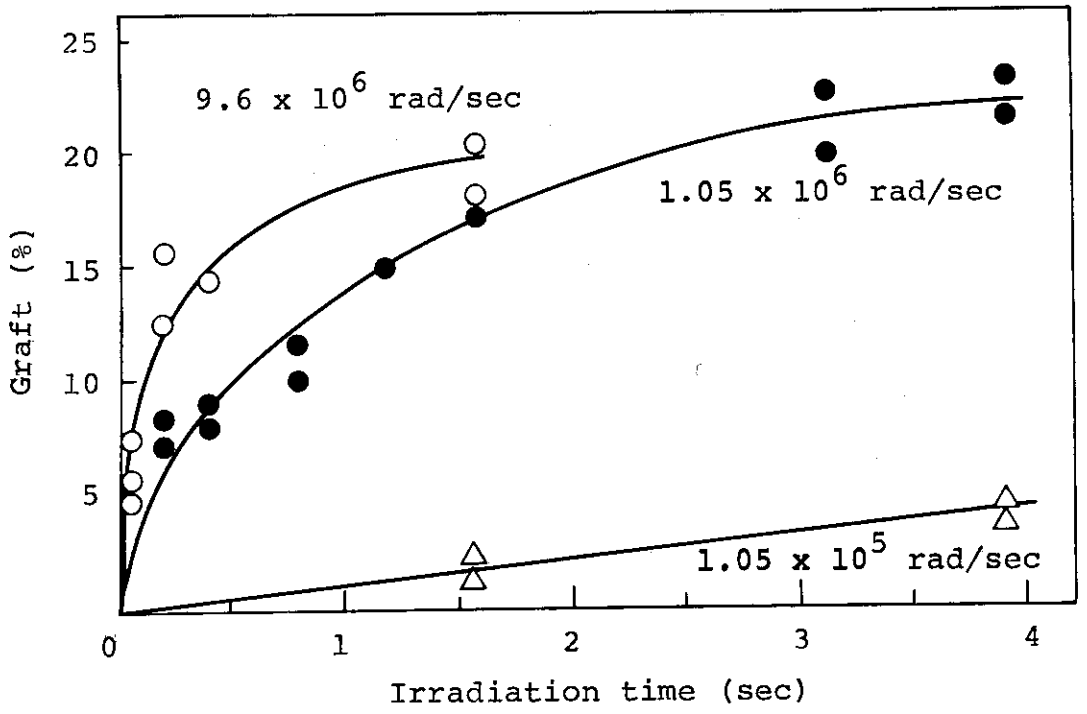

Fig. 2. Grafting of acrylamide onto PVC fiber at different dose rates. Monomer mixture, AAm : MeOH : EDC = 25 : 50 : 25; $[FeCl_2]$ = 10^{-2} mole/l; irradiation by HDRA, 0.8 MeV.

of NaOH. Untreated PVC fiber cannot be dyed with cationic dyes, while the AAm-grafted PVC can be dyed at 10% graft percent.

Original PVC fiber shrinks on heating, giving maximum shrinkage of 70% and is broken at 180-190°C; by grafting with AAm of 40%, the maximum shrinkage is reduced to ca. 20% and fiber form is retained above 300°C. The fiber is, however, elongated by a small load above 200°C. Heat-treatment of the AAm-grafted fiber further decreases the shrinkage and elongation above 200°C. When the hydrolyzed AAm-grafted fiber (40% graft) is cross-linked with calcium ion by the treatment in aqueous solution of calcium acetate, the maximum shrinkage becomes less than 10% and neither elongation nor breaking of the fiber does occur even above 300°C. Fire-retardance test of the AAm-grafted fiber reveals that the fiber of 65% graft has nearly the same self-extinguishing property as that of the original fiber. (I. Sakurada, T. Okada, K. Kaji)

4. Modification of Polyester Fiber by Radiation-Induced Chlorination and Subsequent Alkali-Treatment

As previously reported,chlorinated polyester fabric is prepared by irradiating fabric in chlorine gas of about atmospheric pressure with γ-rays at room temperature. By this procedure fabrics of up to 20% chlorine content are obtained as shown in Fig. 1.

When the chlorinated fabrics are subjected to an alkali-treatment such as heating up to 100°C in aqueous solution of sodium carbonate, it causes, more or less, a weight loss and a decrease in mechanical strength of the fabrics and the extent of damage of the fabrics is dependent on the alkali-treating condition. The chlorinated fabrics after alkali-treatment, however, exhibit improved dye-uptake.

The chlorinated fabric of at least 8% chlorine content can be dyed to deep color with cationic and disperse dyes

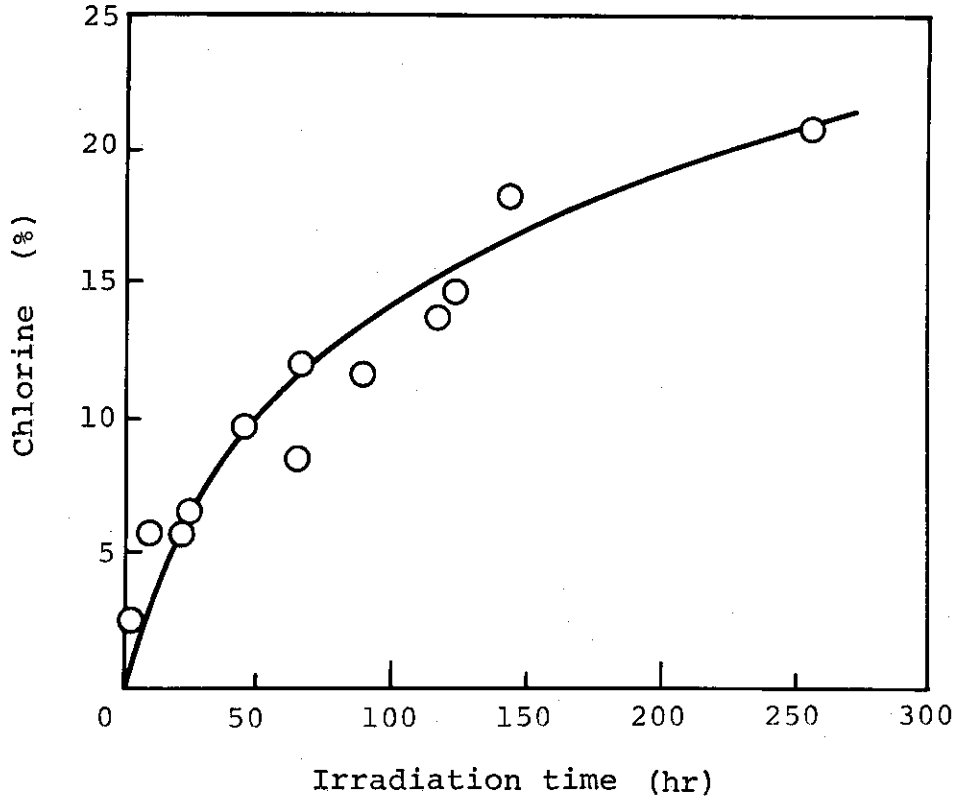

Fig. 1. Chlorination of polyester fabric with γ-ray irradiation in gaseous phase at 23°C. Dose rate, 5.6 X 10^4 rad/hr.

after heat-treatment in 1% aqueous solution of sodium carbonate at 100°C for 4 hr, whereas the fabric before alkali-treatment is dyed only to faint color.

Hygroscopicity is examined by measuring wicking time for the treated fabrics. Wicking time means the time required for a water droplet to be absorbed in the fabric and is a measure of water-absorption rate. As shown in Table 1 wicking time for the original fabric or the fabrics chlorinated to different degrees are longer than 600 sec; hydrophilic fabric requires less time for the wicking. For example, fabric having more than 5% chlorine content absorbs,after the alkali-treatment, water droplet in less than 3 sec.

Table 1. Effect of Alkali-Treatment on the Wicking Time of Chlorinated Polyester Fabrics

Chlorine (%)	Wicking time, sec[a)]	
	Before Alkali-treatment	After Alkali-treatment
0	> 600	405
4.1	> 600	14.9
4.8	> 600	3.1
8.3	> 600	2.9
20.4	> 600	2.7

a) Average value of 3 ∿ 6 samples.

Scanning electron microscopic observation of the fabrics before and after the alkali-treatment reveals that a large number of pores (the size up to 10 μ) are formed by the treatment on the surface of the fabric. Enhancement of the dye-uptake and improvement of hygroscopicity may be at least partially attributed to the formation of pores by the alkali-treatment. (T. Okada, K. Kaji)

5. Fire Retardant Wood Plastic Composite Based on Radiation-Induced Copolymerization of Bis(2-Chloroethyl) Vinyl Phosphonate and Vinyl Monomers

It was reported that the polymerization of mixtures of bis(chloroethyl) vinyl phosphonate (BCVP) and vinyl monomers such as acrylonitrile (AN) and vinyl acetate (VA) impregnated in wood improves dimensional stability of wood[1]. It is, however, generally known that smoke evolution increases with increasing fire retardance. The studies are now carried out to find appropriate amount of polymer loading which is effective to give enough fire-retardance to wood without serious smoke evolution.

Commercially available BCVP, AN, methyl methacrylate (MMA), styrene (St), N-vinyl pyrrolidone (VP), and vinylidene chloride (VDC) are used without further purification. Two types of Japanese beach specimens, A, 50 (axial) x 10 (radial) X 5 (tangential), and B, 5 X 30 X 30 in mm, are impregnated with monomer mixtures under vacuum by the method described in the previous report[1]. The specimens are irradiated with γ-rays from a ^{60}Co source at a dose rate of 0.2 Mrad/hr and the irradiated specimens are dried in vacuum at 50°C to remove unreacted monomer.

The WPC's of type A thus prepared are subjected to burning test which consists of weight decrease measurement of the specimen after 30 second burning in reducing flame of a Bunsen burner[1]. The smoke evolution is determined by the decrease of light transmittance in a smoke chamber which collects smoke evolved from the specimen heated in an electric oven. Simultaneously, the weight decrease rate of the specimen is measured[2].

Dose-conversion curves of BCVP and mixtures of BCVP with one or two other monomers in wood (Fig. 1) reveal that the mixture of BCVP with monomers (except with VP) is less reactive than pure BCVP. The polymerization, however, proceeds more rapidly when 1% AIBN is added to the mixture of BCVP and St (1 : 2) which is the least reactive case.

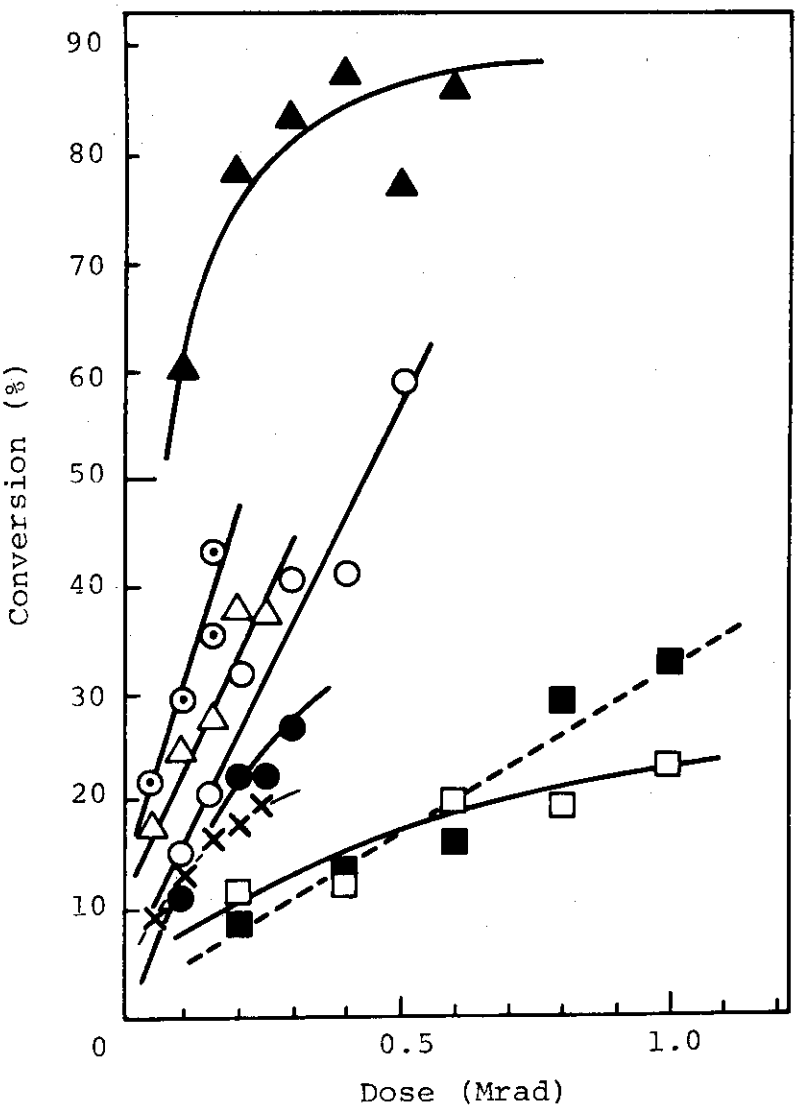

Fig. 1. Dose-conversion curves of BCVP and mixture of BCVP and monomers. (○) BCVP; (▲) BCVP/VP/VDC (1 : 1 : 1); (●) BCVP/VA (1 : 3); (□) BCVP/VDC (1 : 2); (△) BCVP/AN (1 : 2); (x) BCVP/MMA (1 : 2); (■) BCVP/St (1 : 2); (○) BCVP/St (1 : 2) + 1% AIBN.

Mixture of BCVP with VP and VDC is an exceptional case in which steep rise of conversion with dose is observed.

The burning test reveals that fire retardance is improved with increasing polymer loading but 20% polymer loading is found to give good fire retardance to wood. For instance, the weight loss decreases sharply up to 20% polymer loading

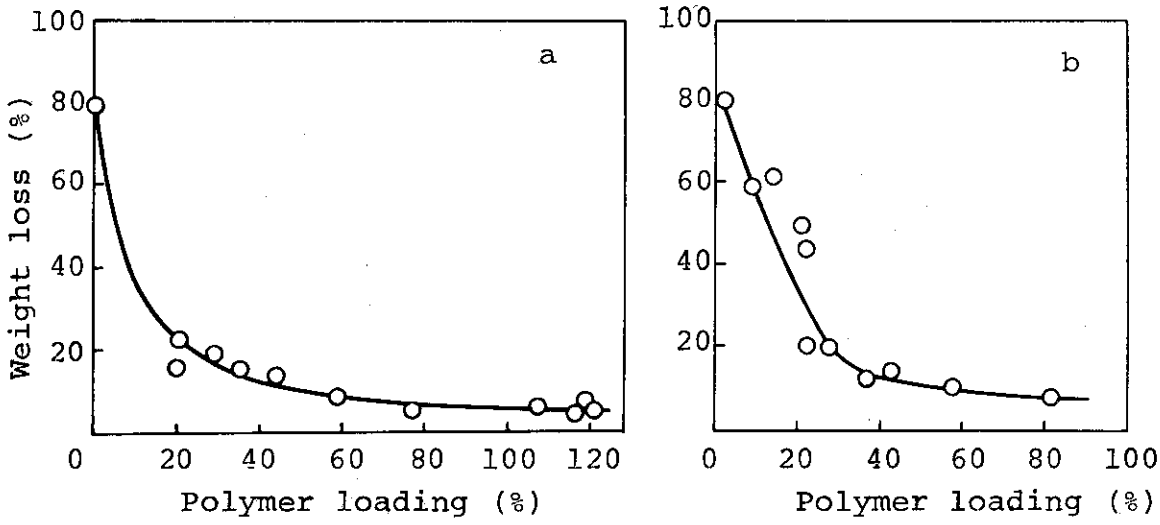

Fig. 2. Decrease of weight loss with increasing polymer loading. a, BCVP and b, BCVP/St (1 : 2).

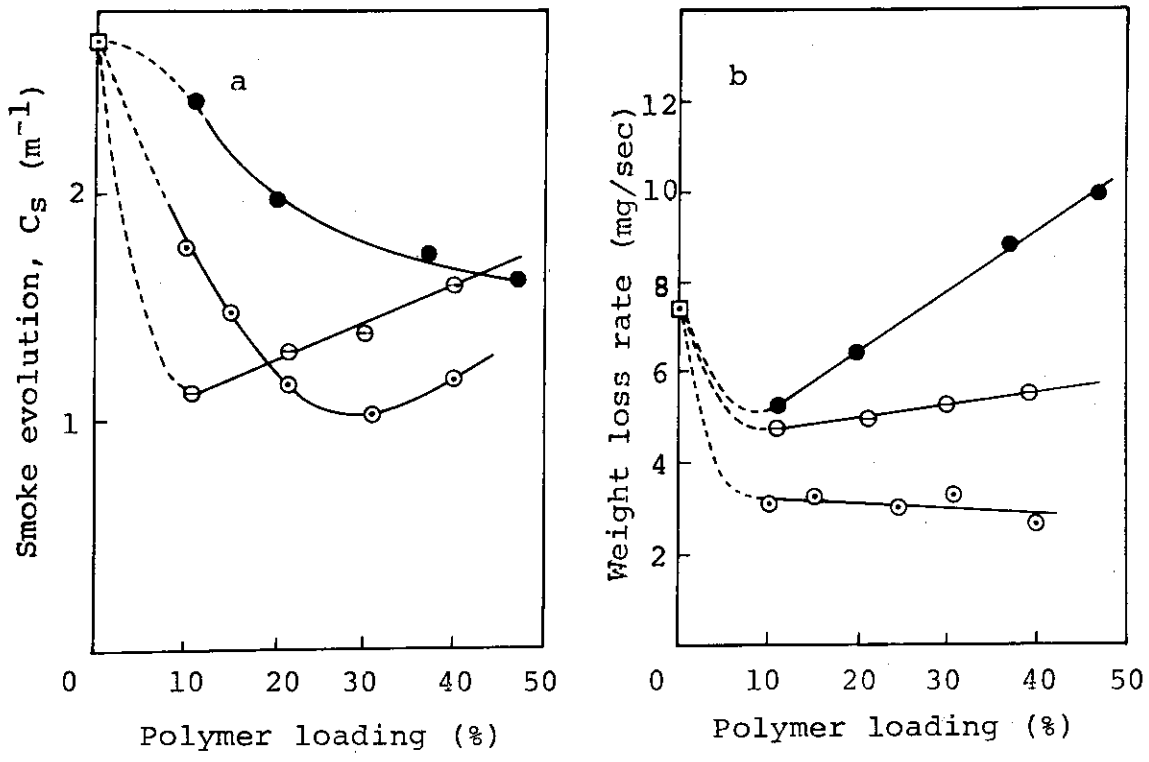

Fig. 3. Smoke evolution (a) and weight loss rate (b) vs. polymer loading at 350°C. (o) BCVP/St (1 : 2); (●) BCVP/AN (2 : 1); and (⊖) BCVP

in the case of BCVP (Fig. 2a) and of the mixture of BCVP with St (Fig. 2b).

Fig. 3a and 3b show the results of measurements of smoke evolution and weight loss rate carried out at 350°C on the specimens of type B loaded with three different monomers: BCVP, BCVP/St, and BCVP/AN. The smoke evolution of WPC loaded with BCVP is decreased to 1.1 m^{-1} by 10% polymer loading and then increases when the polymer loading increases further. The weight loss rate simultaneously measured is also decreased by the polymer loading up to 10% and then increased slowly. When BCVP/St is loaded, the smoke evolution is decreased until 30% polymer loading and then increased, while the weight-loss rate is steeply decreased until 10% polymer loading and then is gradually decreased by further increase of polymer loading. When BCVP/AN is used, the smoke evolution decreases with increasing polymer loading, but the weight loss rate has a minimum at 10% polymer loading.

As far as the results of the smoke evolution and weight loss rate measurements are concerned, it can be concluded that suitable amounts of polymer loading for the present purpose are 10% for BCVP, 30% for BCVP/St, and 10% for BCVP/AN.
(M. Gotoda, T. Yagi, Y. Horiuchi)

1) A. U. Ahmed, N. Takeshita, and M. Gotoda, JAERI, 5027, 82 (1971).
2) Handa, et al., Bull. of Fire Prevention Soc. of Japan, 22, 9 (1973).

[9] Electron Beam Curing

1. Electron Beam Curing of PVC Plastisol Based on PVC/Vinyl Monomer Mixtures

Plastisol of polyvinyl chloride (PVC) is used for coating steel panels, for instance, for pre-coat steel panels, but the hardness of the coating is rather low. In order to cover this point, thick coating is generally used. On the other hand, the insulating cable manufacturer developed technique to improve hardness and thermal properties of insulating materials by applying radiation-induced cross-linking of PVC containing multifunctional monomers. This technique is now widely used for industrial purposes.

Studies are carried out to examine whether this technique is applicable for improving properties of steel coating such as hardness. The studies are concerned with radiation-induced cross-linking of PVC plastisol which contains reactive monomer as plasticizer.

Commercially available PVC's (Kaneka Co., $\overline{DP} = 950$ and 1700) are used. Dioctylphthalate (DOP) and butyl acrylate (BA) are used as plasticizer. Cross-linking agents used are polyethylene glycol diacrylate (PEGDA-X) of various degrees of polymerization ($\overline{DP}$ increases with increasing X) and triallyl isocyanurate (TAIC). Stabilizer containing tin is also used.

An aluminum frame (10 X 50 mm, 1 mm thick) is filled with a mixture of PVC/DOP or BA/stabilizer (6/30/3), or that containing cross-linking agent (10% or 20% by weight of PVC) at room temperature. The aluminum frame containing monomer mixture is sandwitched with polyester film, and pressed at 50°C at 50 kg/cm^2 for 5 minutes to give a transparent specimen.

Irradiations are carried out using electron beams from a Van de Graaff (1.5 MeV, 50 μa, 0.35 Mrad/sec) on a conveyer. The dose absorbed by specimen on the conveyer is 1 Mrad/pass,

and the specimens travel on the conveyer to and fro under the irradiation window until required dose is irradiated.

Irradiated specimens are subjected to drying under vacuum at 50°C for 24 hr to remove unreacted monomer and then to Soxhlet extraction with tetrahydrofuran to determine sol and gel percent.

Gel percent is plotted against dose in Fig. 1a for the mixture of PVC ($\overline{DP}$ = 950 or 1700), DOP, and PEGDA-1 (10 or 20% by weight). The gel percent at 3 Mrad irradiation is the highest for the mixture containing 20% PEGDA-1 and PVC having $\overline{DP}$ of 1700. This situation is similar for the case when TAIC is used instead of PEGDA-1, but the gel percent at 3 Mrad irradiation is lower (Fig. 1b). Since the use of PVC of higher molecular weight with PEGDA at higher concentration gives good result, the experiment is carried out using mixtures of PVC ($\overline{DP}$ = 1700)/plasticizer/PEGDA-X (20%).

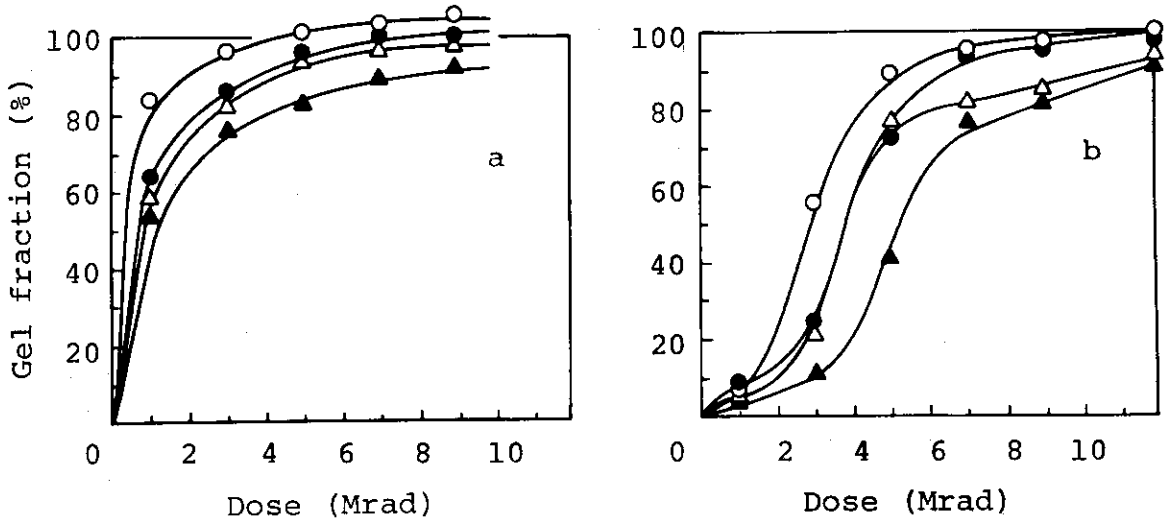

Fig. 1. Dose-conversion curves for PVC/DOP/cross-linking agent/stabilizer. a, PEGDA-1 as a cross-linking agent; b, TAIC as a cross-linking agent; circles, $\overline{DP}$ of PVC = 1700; triangles, 950; open symbols, content of cross-linking agent = 20%; filled symbols, 10%. Gel fractions of highly cross-linked specimens are overestimated because of residual solvent which is difficult to be removed by evacuation.

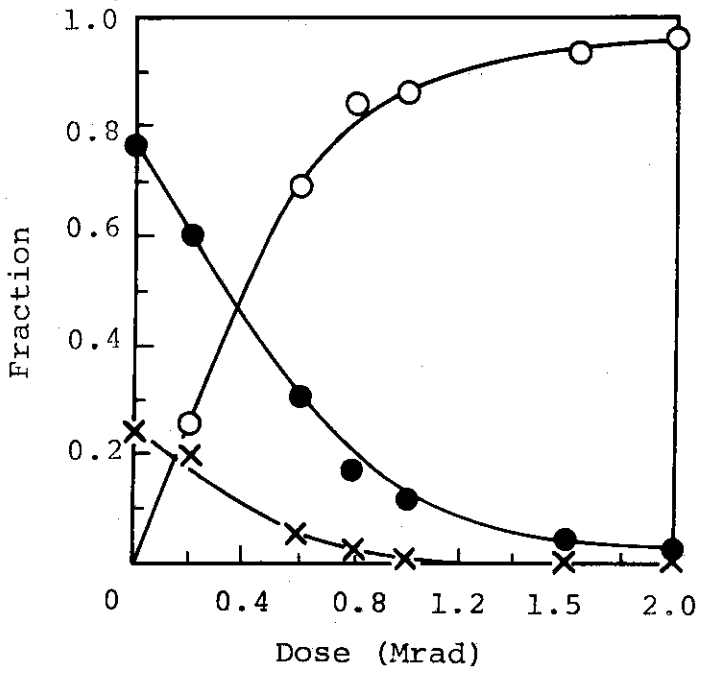

Fig. 2. Electron beam curing of PVC ($\overline{DP}$ = 1700)/BA/PEGDA-4/ stabilizer as a function of dose. (○) gel fraction; (●) sol fraction; (×) fraction of unreacted monomer.

Table 1. **Performances of the Electron Beam Cured Coatings of PVC/BA/PEGDA-4/stabilizer (60/30/15/3) Mixture on Chromate Treated Steel Panel**

Coating thickness: 0.2 mm
Preparation of coating: heated at 150°C for 5 min. at 50 kg/cm^2
Irradiation: 1.5 Mrad (0.35 Mrad/sec)

Test items		Performance
Flexibility and adhesion	Erichsen test	Little peeling
	Bending test	Perfect
	Cold crack test	No cracks, with little peeling
Adhesion by cross cut test		Perfect
Resistance to boiling water		No change, with reduced transparency
Self-extinguishability		Below 5 sec
Scratch hardness		Much improved

Nearly complete gelation is obtained when BA is used instead of DOP for the purpose of internal plasticizer (Fig. 2); without PEGDA, however, gel fraction does not exceed 80% even by the irradiation above 5 Mrad.

The dose required for complete gelation depends upon the $\overline{DP}$ of the PEGDA used, and the best result is obtained when PEGDA-4 is used, giving the lowest necessary dose for the practically complete gelation (Fig. 2).

Performance test is carried out on a steel panel coated with the mixture of the composition given in Fig. 2, which is found to be cured under the most convenient conditions. The results are proved to be satisfactory for most testing items as shown in the table. There is one disadvantage, however, that the pot life of the mixture is short. This is a problem which is to be solved before the mixture is used for industrial purpose. (M. Gotoda, T. Yagi)

2. Radiation Curing of Chlorinated Polymer/Vinyl Monomer Mixtures by High Dose Rate Electron Beams

Radiation curing by high dose rate electron beams (EB) is carried out of three kinds of chlorinated polymeric hydrocarbons (Cl-polymers) such as chlorinated polyethylene (Cl-PE), polypropylene (Cl-PP), and natural rubber (CR-X), instead of polyvinyl chloride. The Cl-polymers are taken up because they are fairly soluble in various vinyl monomers to give homogeneous liquid mixtures which are suitable for use in processing like coating. Another reason is that halogenated organic compounds are known to be very sensitive to radiation to form radicals in high yields. The Cl-polymers form polymer radicals which may lead to cross-linking in the presence of vinyl monomers.

Cl-polymers used are Superchlon LT as a Cl-PE and Superchlon 306 as a Cl-PP supplied by Sanyo-Kokusaku Pulp Co., and CR-5, 10, 20, 40, 90, and 150 (the molecular weight increases in this order) as CR-X's supplied by Asahi Denka Co. Butyl acrylate (BA) is used as a vinyl monomer, and

tetraethyleneglycol diacrylate (TEGDA) as a cross-linking agent. Cl-polymer/BA mixture in a rectangular aluminum vessel with a cover of polyester film (0.1 mm thick) is irradiated by a high dose rate electron accelerator (HDRA) (800 keV, 25 ma) with scanning width of 32 cm, on a conveyer with a travelling speed of 50 m/min. Dose rate used is 13.3 Mrad/sec which corresponds to 0.5 Mrad/pass. The extent of curing is followed by unreacted monomer %, and sol and gel %, which are calculated from the weight loss of the irradiated specimen by vacuum drying at 50°C for 24 hr, and the weights of extracted and unextracted parts of the dried specimen by Soxhlet extraction with acetone, respectively.

The results of the EB curing of the Cl-polymer/BA (50/50) mixtures are shown in Fig. 1a, b, and c, for the Cl-PE, Cl-PP, and CR-5, respectively. It may be seen from the figure that the unreacted monomer disappears at the same curing dose of ca. 8 Mrad for these three mixtures, indicating that the curability of the mixtures is almost independent of the kind of Cl-polymers. It is observed that sol % increases rapidly with simultaneous rapid decrease of the monomer in the initial stage of the reaction, and then decreases slowly, while the gelation begins at the point of the maximum sol %. This tendency is quite different from that of other popular prepolymer/vinyl monomer mixtures, e.g. polyester/styrene mixtures. The reason for this may be that the Cl-polymers are unexpectedly stable to radiation so that homopolymerization of BA predominates over graft polymerization of BA to the Cl-polymers.

It is found that by adding TEGDA to the Cl-polymer/BA mixtures the curing dosage is lowered to ca. 4 Mrad and gel fraction of the cured products is increased to ca. 60-90%. These results are shown in Fig. 1d, e, and f. The effect of molecular weight of the Cl-polymer on the curability of the Cl-polymer/BA (50/50) and Cl-polymer/BA/TEGDA (50/40/10) mixtures is examined using CR-X's. Dosages required for the perfect conversion of BA do not depend on the number of X and are ca. 8 and 4 Mrad for CR-X/BA and CR-X/BA/TEGDA,

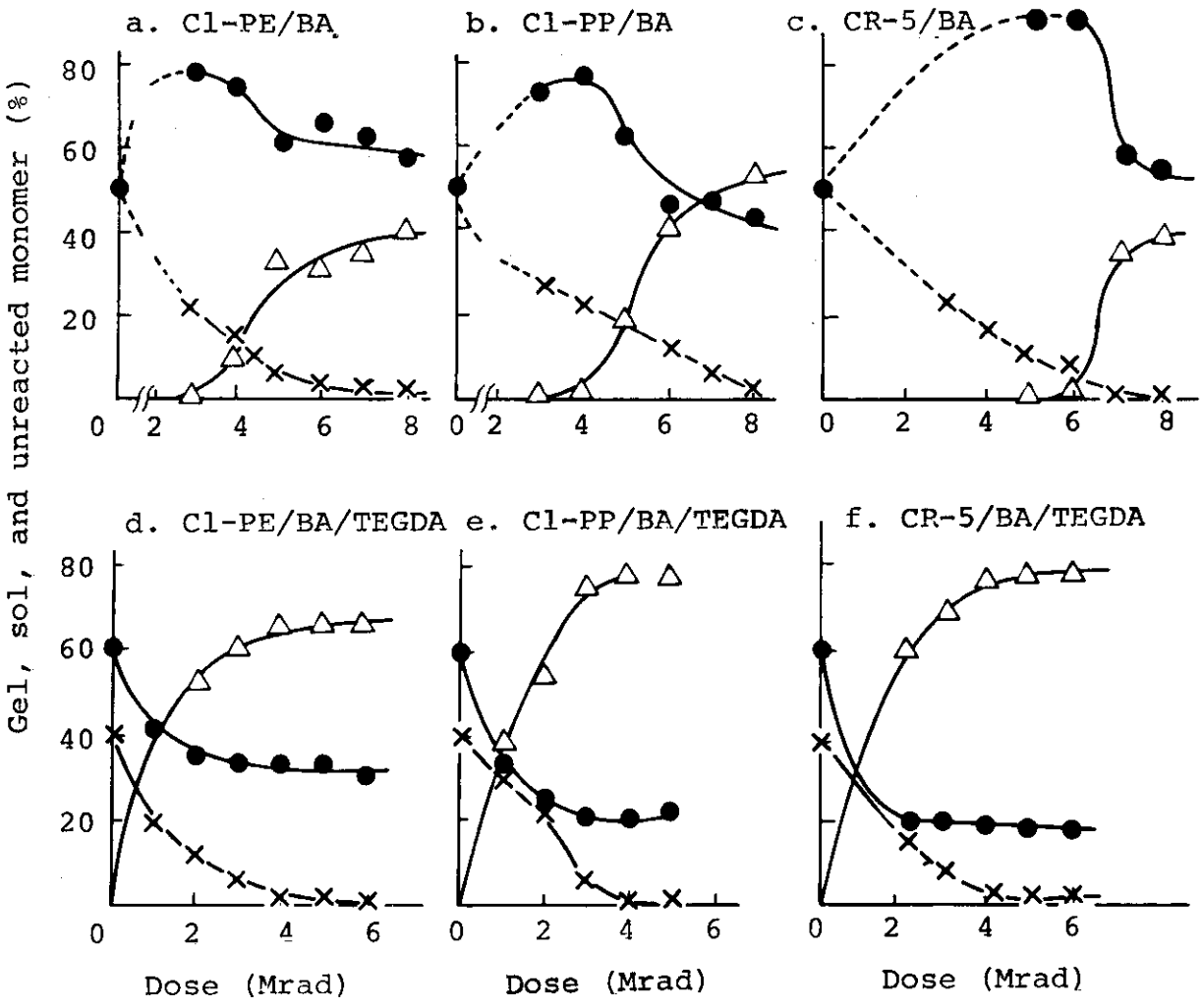

Fig. 1. EB curing of Cl-polymer/vinyl monomer mixtures.
(Δ) gel fraction; (●) sol fraction;
(x) fraction of unreacted monomer.

respectively. Gel %, on the other hand, becomes higher as the molecular weight of CR-X increases for CR-X/BA while in the presence of TEGDA the maximum gel % attained by the EB curing is nearly independent of the molecular weight of CR-X for X = 10-150. Therefore, the use of the CR-X of low X together with TEGDA is recommended for coating application.

In the course of these experiments, it is found that the cured resins often color brown after irradiation and the coloration proceeds for several days in the case where CR-X is used. In order to prevent the coloration and improve the

stability of the cured resins, phenyl glycidyl ether (PGE) is added to the mixtures before irradiation. The addition of 3% PGE prevents effectively the coloration without inhibiting appreciably the EB curing reaction.

For comparison, the EB curing is carried out of PVC/BA/TEGDA with a stabilizer containing tin, which shows better curability than that of the corresponding mixtures of the Cl-polymers.

Finally, performance tests of the cured Cl-polymer/BA/TEGDA mixtures on steel panels give satisfactory results, indicating that the mixtures are suitable for use in anti-corrosive paints. (M. Gotoda, T. Yagi)

3. Effect of Dose Rate on Electron Beam Curing of Epoxy Diacrylate

Electron beam curing of epoxyacrylates with or without vinyl monomers[1] has been carried out and it was found that the dose rate dependences of the highest gel yield are

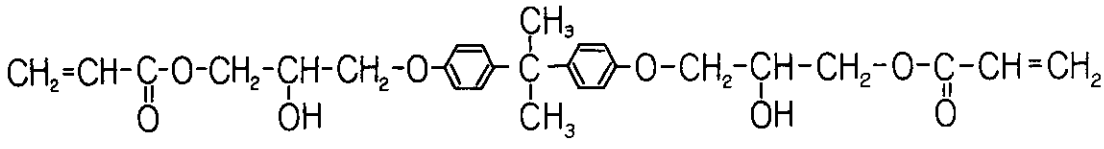

(monomer I)

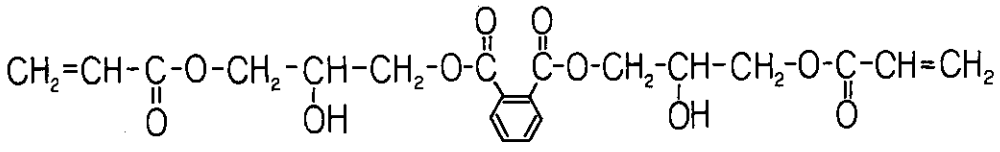

(monomer II)

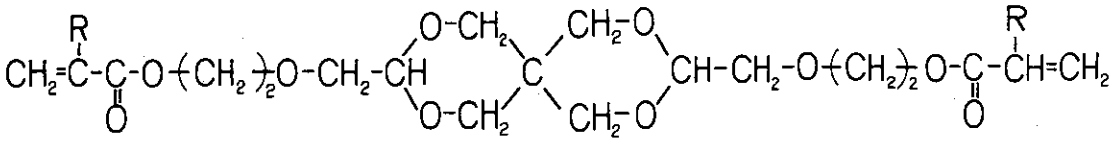

(monomer III : R = H)

(monomer IV : R = CH_3)

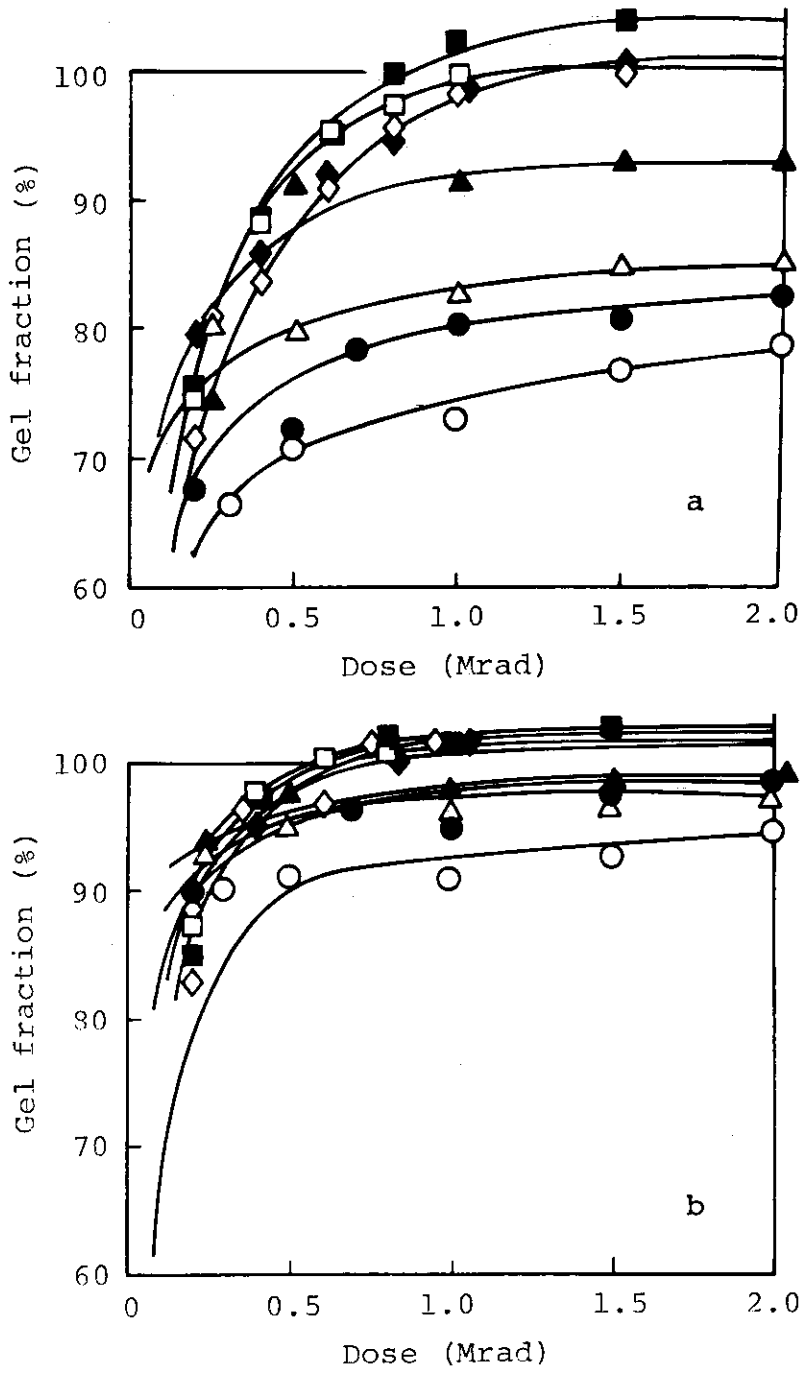

Fig. 1. Electron beam curing of (a) acrylic acid ester of bisphenol-A (monomer I) and (b) acrylic acid ester of phthalic acid (monomer II). Dose rate: (○) 0.09; (●) 0.18; (△) 0.35; (▲) 0.70; (□) 1.00; (■) 5.00; (◇) 10.00; (◆) 13.25 Mrad/sec. No corrections are made for residual solvent for extraction.

somewhat different from those of other commercial resin compositions which were developed for electron beam curing. The dose rate dependence study is extended up to a dose rate of 13.3 Mrad/sec using our new accelerator.

Monomers used are acrylic acid esters of bisphenol-A (I) and phthalic acid (II), spiroacetal acrylate (III), and methacrylate (IV). Samples of 1 mm thickness covered with polyester film are irradiated with 800 keV electron beams. Dose rate is changed by changing the beam current and the speed of the conveyer which carries the samples under scanner window in a single way.

With monomer I, it is found that complete gel formation is achieved at high dose rates as shown in Fig. 1 a. At low dose rate, for instance 0.2 Mrad/sec, highest gel fraction is less than 80% while at higher dose rate than 1.0 Mrad/sec, it reaches to 100%. Monomer II also behaves similarly as shown in Fig. 1b.

On the other hand in spiroacetal systems, the dosage required to obtain full gelation increases with the dose

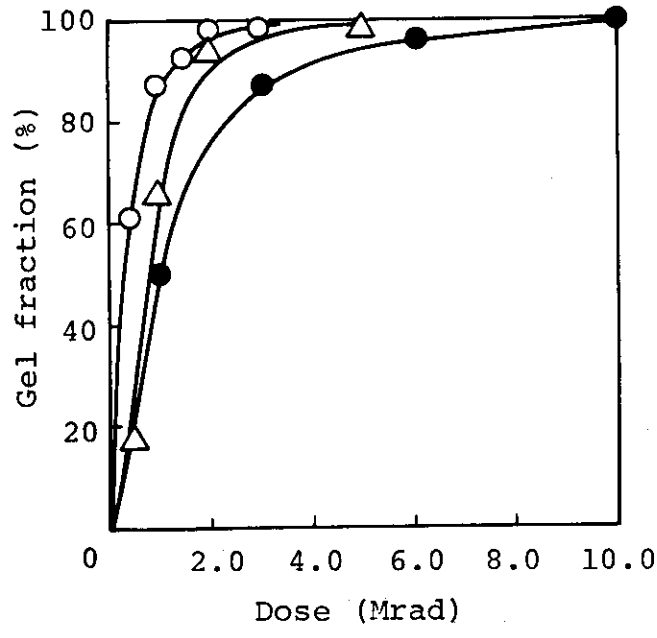

Fig. 2.' Electron beam curing of spiroacetal acrylate (monomer III). Dose rate: (o) 0.09; (Δ) 5.00; (●) 13.25 Mrad/sec.

rate; at 0.1 Mrad/sec, 1-2 Mrad, and at 13.3 Mrad/sec, 5-8 Mrad in monomer IV and 10 Mrad in monomer III (Fig. 2). Such an increase of necessary curing dosage with increasing dose rate is common for conventional resins.

Curing of 30% vinyl monomer mixtures of monomer I and II II is also studied. With high dose rate irradiation as 13.3 Mrad/sec, the mixtures containing acrylic esters (ethyl, butyl, and 2-hydroxyethyl) show complete gelation. In the case of mixtures, however, containing methacrylates (methyl and 2-hydroxyethyl), vinyl acetate, styrene, and acrylonitrile, no complete gelation is observed by the irradiation at this dose rate, and irradiation at lower dose rate is better to increase gel fraction. For the mixtures of I or II with vinyl monomers, unlike pure monomer I or II, it can be concluded that greater curing dosage is required when vinyl monomers are added and that the curing dosage becomes greater with the increase of the dose rate. (M. Gotoda, T. Yagi)

1) JAERI-M, 6260, 67 (1975).

4. Comparative Studies on the Curing by Electron Beam and Ultraviolet Irradiation of Epoxyacrylate. Evaluation of Degree of Cross-Linking by DSC Measurement

In the last annual report[1] it was described that the major difference between electron beam curing (EB) and ultraviolet (UV) curing was attributed to their curing temperatures. It was found that the difference of specific heat before and after transition, ΔC_p, increased with curing temperature up to 80°C. Since the ΔC_p is closely related to number of cross-links, this finding indicates that the number of cross-links increases with increasing curing temperature. Further studies on this topic are continued in some detail.

In Fig. 1, weight swelling ratio, i.e. the weight increase of polymer by swelling divided by its dry weight,

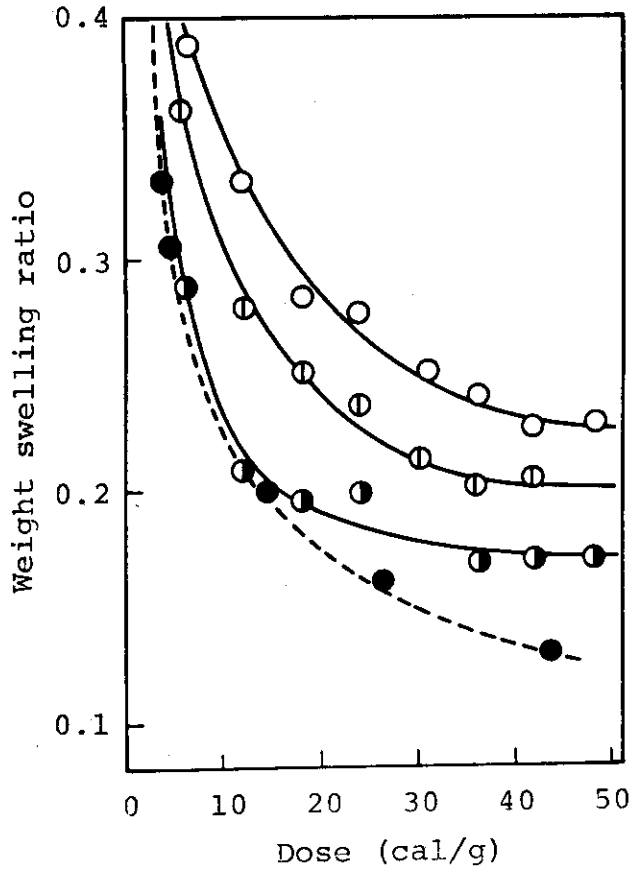

Fig. 1. Weight swelling ratio as a function of dose.
(○) UV (57°C); (◐) UV (70°C); (◑) UV (75°C)
at 0.05 cal/g·sec; (●) EB at 1.7 cal/g·sec.

is plotted as a function of radiation dose for EB and UV curing of acrylic acid ester of bisphenol-A glycidyl ether. At the initial stage of irradiation, the swelling ratios decrease greatly and then level down to the fixed values which depend on curing temperature. These variations of swelling ratio are very similar to those in double bond disappearance shown in the last annual report[1]. With the progress of the reaction, the viscosity of the system increases greatly resulting in harder diffusion of the reacting points for the cross-linking. This is why levelling-down value of the swelling ratio becomes lower with higher curing temperature, in other words, lower viscosity. The swelling ratio as a function of curing temperature is given in Fig. 2. This

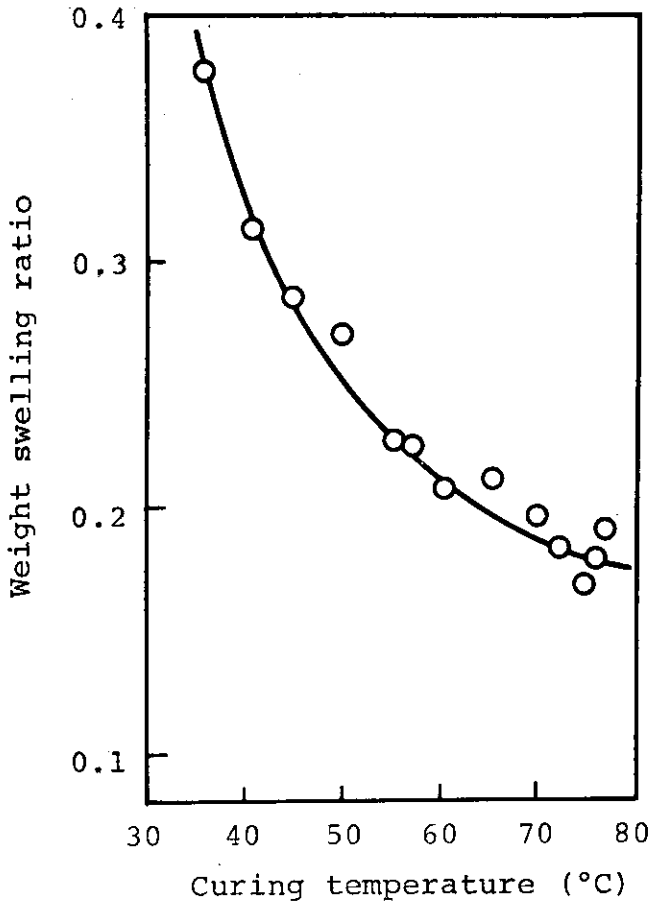

Fig. 2. Effect of curing temperature on weight swelling ratio.

shows a good correlation with ΔC_p change in Fig. 4 of the last annual report[1] indicating ΔC_p as a good measure of the degree of cross-linking.

Results with solvent extraction show a good correspondence with the above results. The relationship between dose and sol fraction is quite similar to that between dose and swelling ratio in all of the four series of treatments in Fig. 1. The sol fraction decreases with temperature, and is only 2 - 3% at 80°C.

Glass transition process of the cured samples is studied by a differential scanning calorimeter (DSC). Among four characteristic temperatures shown in a schematic diagram in Fig. 3, only temperature of E rises in an early stage of the curing. In Fig. 4, we can see further that only the

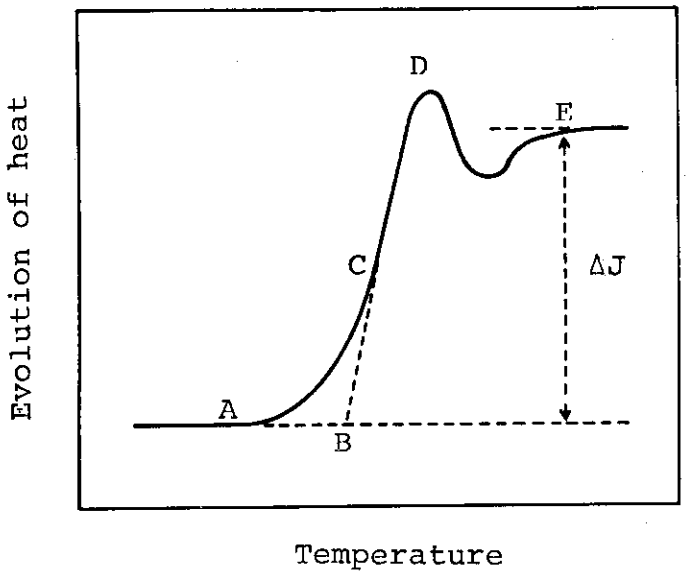

Fig. 3. Schematic diagram of glass transition by DSC.

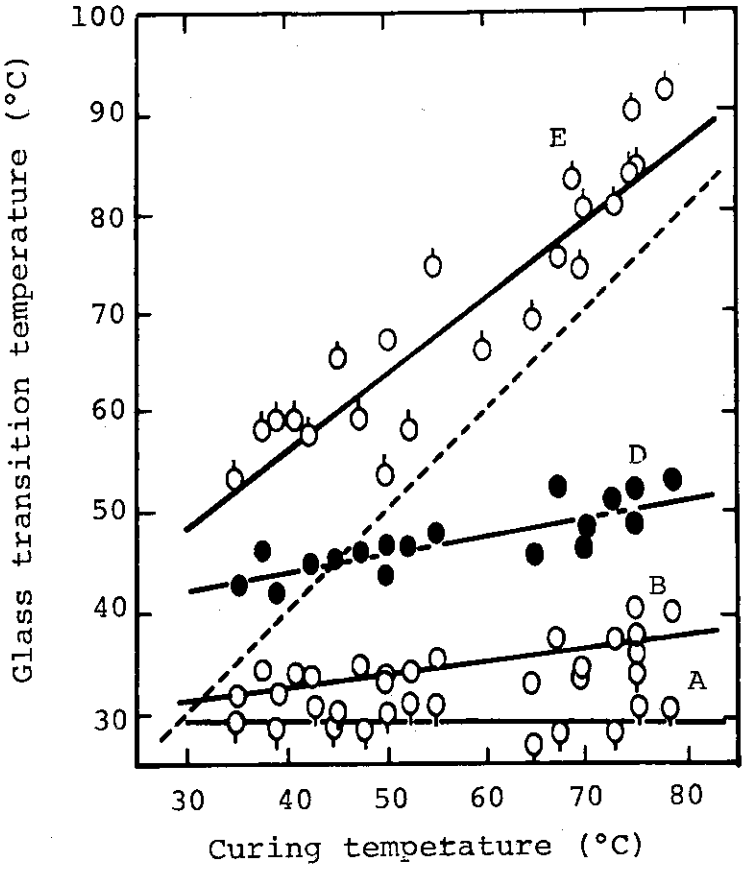

Fig. 4. Effect of UV curing temperature on glass transition temperature. Dose, 48 cal/g; dose rate, 4.8 X 10^{-2} cal/g·sec; heating rate, 32°C/min.

temperature at E changes markedly with the curing temperature and it is relatively close to the curing temperature which is shown with a dotted line in the figure. Since the glass transition process is conveniently measured by DSC, the temperature E is a good indication of the degree of cross-linking. (J. Kumanotani, T. Koshio, M. Gotoda, T. Yagi)

1) JAERI-M, 6260, 67 (1975).

[Appendix 1] Dosimetry of Electron Beams from the High Dose Rate Electron Accelerator

In addition to the Van de Graaff accelerator (VdG) which has been used since 1958, our laboratory is now equipped with an accelerator (HDRA) of rectified transformer type[1] which delivers electron beams of higher dose rate than those of the VdG. The HDRA is in full operation under busy schedule for study on radiation chemistry at high dose rate since May 1975. In order to perform satisfactory irradiations for research programs in Osaka Laboratory, several important technical data should be provided; the calibrated electron energy; the depth dose curves for materials of atomic number, Z, which is close to average Z of organic materials to be irradiated; dose distribution of the irradiation zone; and dose absorbed by samples travelling under the irradiation window at various speeds.

These data obtained using CTA film dosimeter[2] which has been developed by a joint research between CEA France and JAERI are described below.

1) JAERI-M, 6260, 73 (1975).
2) Y. Nakai, K. Matsuda, and T. Takagaki, JAERI 5029, 153 (1974).

1. Calibration of Electron Energy

Electron energy of the HDRA is calibrated by comparing the energy dissipation distribution curve with that obtained by the VdG, energy of which was calibrated by the threshold of Be (γ, n) reaction at 1.66 MeV. The direct calibration through Be (γ, n) reaction can not be made on the HDRA because the highest accelerating voltage available is 0.8 MeV which is lower than the threshold energy of the reaction. The energy dissipation distribution curves (Fig. 1) are obtained using CTA films at the electron energy of 0.8 MeV which is available commonly on the two accelerators. The

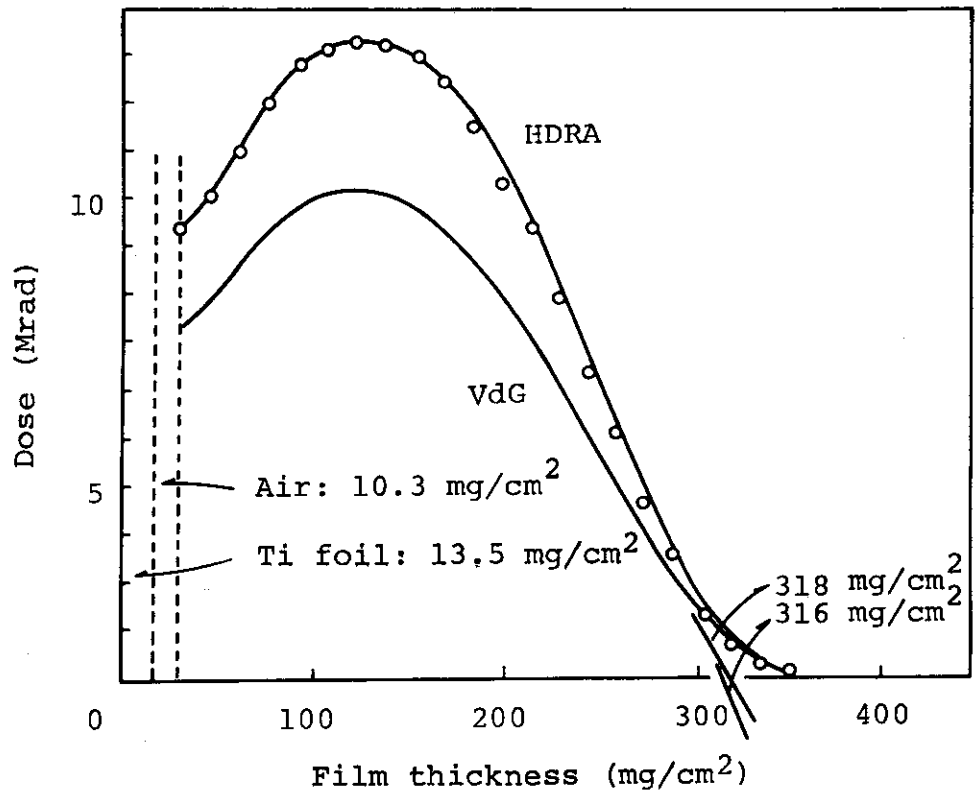

Fig. 1. Energy dissipation distribution in CTA film. Accelerating voltage, 800 keV; beam current, 30 μa; distance between cell and irradiation window, 8 cm.

range of electrons estimated by extrapolation of the linear part of the energy dissipation curve obtained for the HDRA is 316 mg/cm^2, while that for the VdG is 318 mg/cm^2, confirming that the accelerating voltages of the two accelerators agree well within 1%. (Y. Nakai, K. Matsuda, T. Takagaki)

2. Measurements of Energy Dissipation Curves in CTA Films

Energy dissipation distribution curves in CTA films are obtained for electrons delivered from the HDRA ranging from 300 keV through 800 keV at 100 keV intervals. The CTA films (thickness of each film is 15.4 mg/cm^2) are piled up to a required number of layers depending on the accelerating voltage and sandwitched by PMMA blocks for complete electronic equilibrium. The sample is held so that its upper

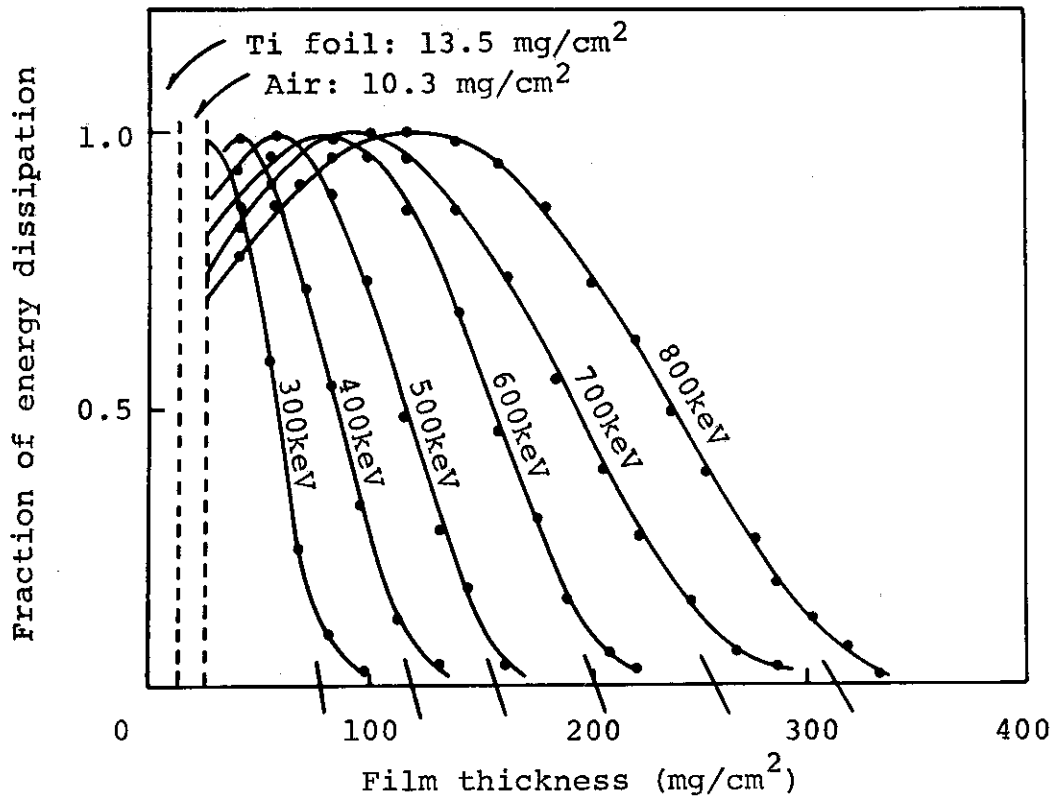

Fig. 1. Energy dissipation distribution in CTA film.

surface comes 8 cm below the titanium irradiation window. The results are given in Fig. 1, where the ordinate is normalized so that the maximum of each distribution curve comes to unity. As obvious from the figure, no initial increase of the energy dissipation is observed at lower electron energy, possibly because of energy dissipation in the titanium window and in air. The dissipation curves obtained for CTA films may be applicable for any organic substances consisting of C, H, and O atoms. (Y. Nakai, K. Matsuda, T. Takagaki)

3. Dose Distribution in the Irradiation Zone

The scanning of electron beams delivered from the HDRA is adjusted to provide uniform dose distribution along the direction of electron beam scanning on the surface of an irradiation sample placed under the irradiation window.

The dose distribution along the electron beam scanning below the sample surfaces, however, may be different from that on the surface. In order to study this point the depth dose distribution curves are measured at the center and at 20 cm away to either side from the center. The curves given in Fig. 1 are obtained for CTA films on a conveyor 12 cm below the irradiation window by 800 keV electrons with 45 cm scanning width. The curves show that the doses at the center and at both sides are the same on the surface as expected, but the dose at either side slightly exceeds that at the center up to 100 mg/cm^2 depth. The dose at the center, however, becomes higher by 20% than that at either side when the depth exceeds 120 mg/cm^2. The extrapolated range of electrons is 305 mg/cm^2 at the center, while it is 293 mg/cm^2

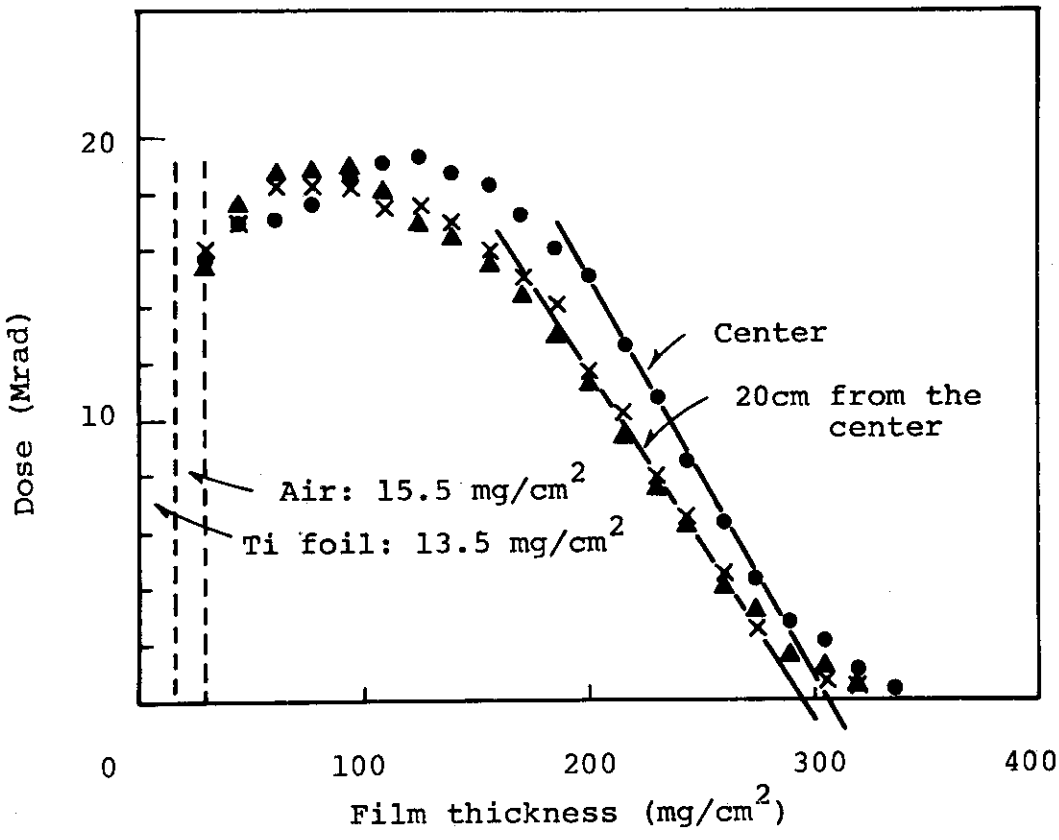

Fig. 1. Average measured depth dose distribution in CTA film. Accelerating voltage, 800 keV; beam current, 10 ma; conveyer speed, 50 m/min; number of passes, 20.

at either side. The possible reason for these results is that incident angle of electron beams with respect to the perpendicular direction to the sample surface is 30° at either side resulting in greater energy dissipation at short depth and shorter range due to scattering in longer air path.

Further experiments at lower electron energy are necessary for accurate estimation of dose absorbed by samples of large dimensions. (Y. Nakai, K. Matsuda, T. Takagaki)

4. Dosimetry of a Sample Travelling on a Conveyer

Dosimetry of a sample travelling on a conveyer through irradiation zone of the HDRA is carried out using a CTA film dosimeter to determine the relation between the absorbed dose and travelling speed as well as distance from the window to the sample.

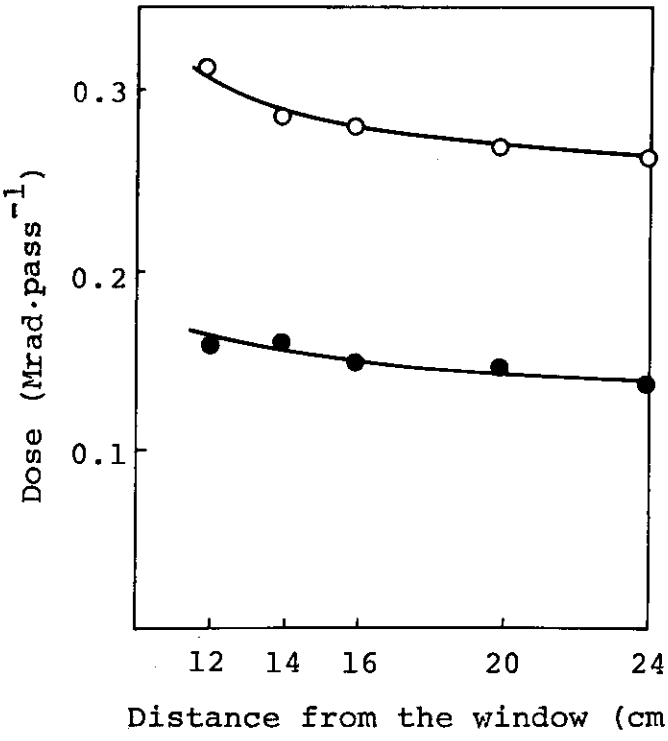

Fig. 1. Dose vs. distance from the window. Accelerating voltage, 800 keV; beam current, 25 ma; scanning width, 45 cm; conveyer speed, (o) 10 m/min, (●) 20 m/min. Dose is given as a value per unit beam current (ma).

CTA films to be irradiated are placed on a wood backing held on a tray which is carried under the scanner in the direction perpendicular to electron beam scanning, scanning width of which is kept constant at 45 cm throughout the experiment. The speed of the conveyer can be varied continuously from 2 m/min to 120 m/min, but the measurements are done at several conveyer speeds. Dose is accumulated up to a desired dose by repeating irradiation to allow precise optical density measurement.

Fig. 1 shows the plots of the dose as a function of distance from the window to the CTA film at travelling speeds of 10 m/min and 20 m/min. As shown in Fig. 2, plots of logarithm of dose against that of conveyer speed lie on a straight line which indicates that the dose is inversely proportional to the conveyer speed.

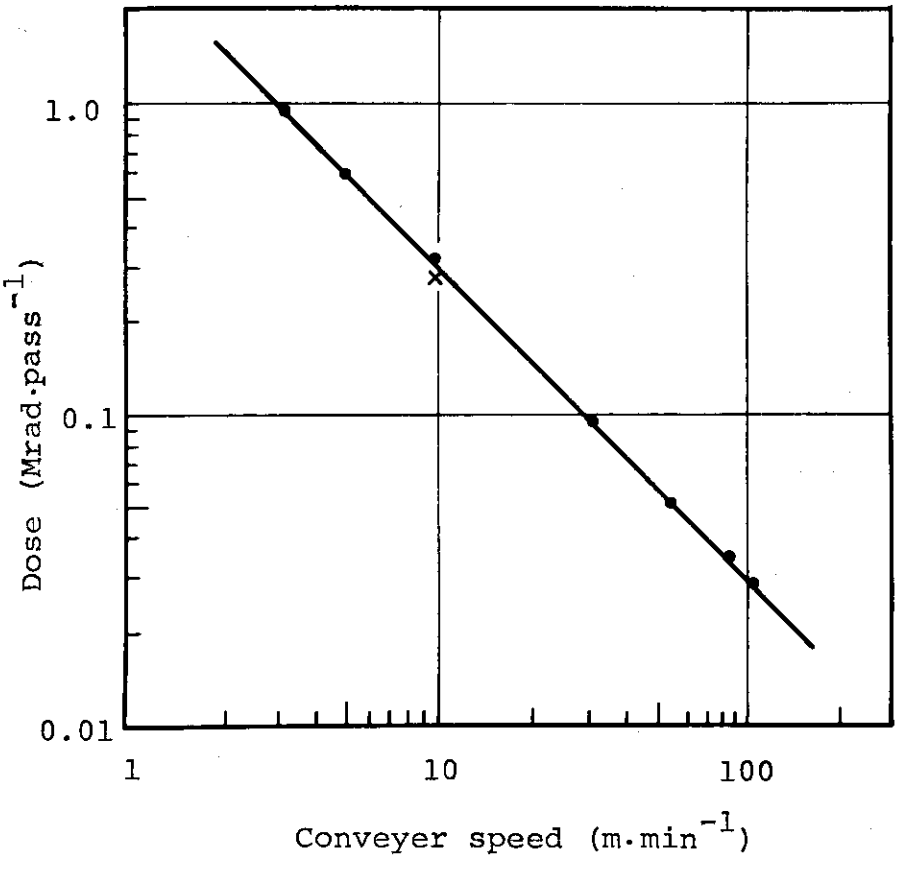

Fig. 2. Dose vs. conveyer speed. Accelerating voltage, 800 keV; scanning width, 45 cm; distance from the window, 12 cm; beam current, (●) 25 ma, (x) 2.5 ma.

From the results described above, one can select irradiation conditions such as conveyer speed and distance from the window depending on dose required. (Y. Nakai, K. Matsuda, T. Takagaki)

[Appendix 2] Measurement of Dose Rate Distribution and Temperature Rise in a Metal Cell Used for the Polymerization of Vinyl Monomers by Electron Beams

In the kinetic study of polymerization by electron beam irradiation at higher dose rates, we meet two big problems which offer no significant trouble in the study in γ-ray region. The first one is the dosimetry of electron beams in the reaction vessel. This includes evaluation of geometrical distribution of the dose rate in the vessel and of its average. The second problem is temperature rise due to energy dissipation of high energy electrons and heat from the reaction itself.

A new cell for the polymerization study is made as shown in Fig. 1. The main part is of brass block of 10 mm thickness.

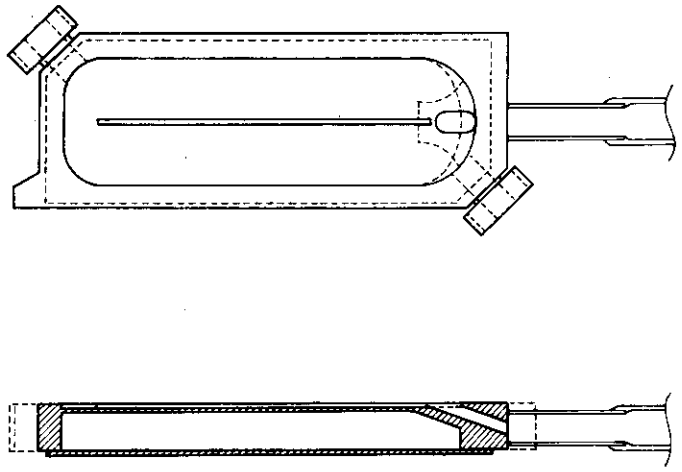

Fig. 1. A cell.

At the top of the block, there is a shallow space for monomer of 1 mm depth, 28 mm width and 88 mm length. At the center of the sample space, a ridge of 1 mm in height and width is left to prevent bending of 0.1 mm thick brass window, which is soldered to the main block. A coolant jacket is made back to back with the sample space in a distance of 1 mm thickness.

CTA film dosimeter (Numelec, France) of cellulose triacetate containing 15% triphenyl phosphate is employed. After the irradiation, optical density, OD at 280 mμ is measured through a slit of 1 X 5 mm by every 2 mm distance. Radiation dose is calculated with an equation[1], dose (Mrad) = 20.2 X $OD^{1.05}$.

First, three strips of CTA film placed on a horizontal plane which is 10 cm below the scanner window are irradiated with 800 kV electrons from our high dose rate accelerator (HDRA) to obtain a lateral distribution or a distribution right angle to the direction of the beam scanning. Three curves in Fig. 2 are the lateral distributions, measured at

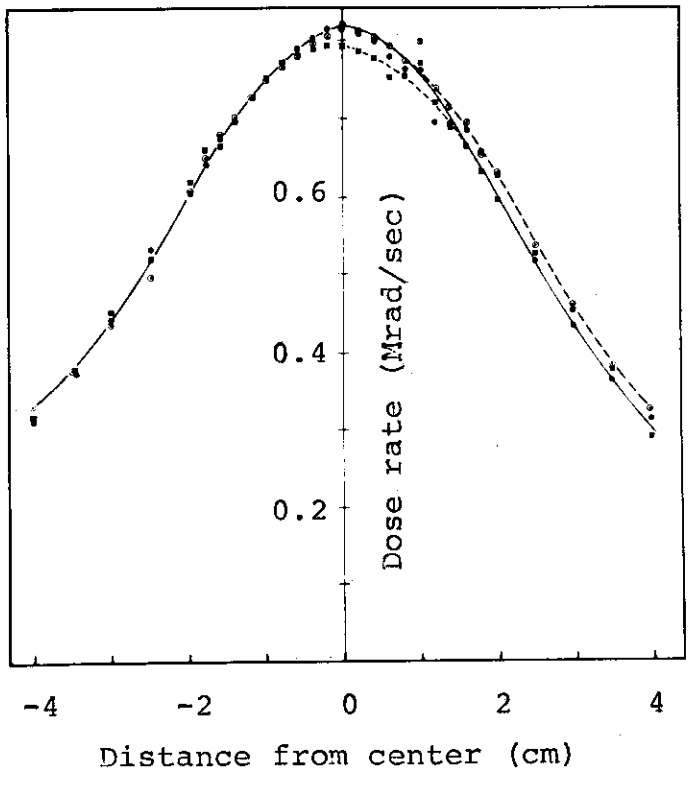

Fig. 2. Lateral dose rate distributions with the HDRA. (·····■·····) north side, (——●——) center and (----⌀----) south side.

the middle of the scanning width and 10 cm aside, north and south. We find they are almost identical and their symmetrical axes fall on a straight line, called 'scanning line' hereafter, on the plane.

Next, the cell packed with CTA films is placed on the plane to fit its center line or the ridge to the scanning line of the beams. Irradiation is made at the same conditions as in Fig. 2. The lateral distribution in the cell is given in Fig. 3. Within a limit of the cell width, the distribution

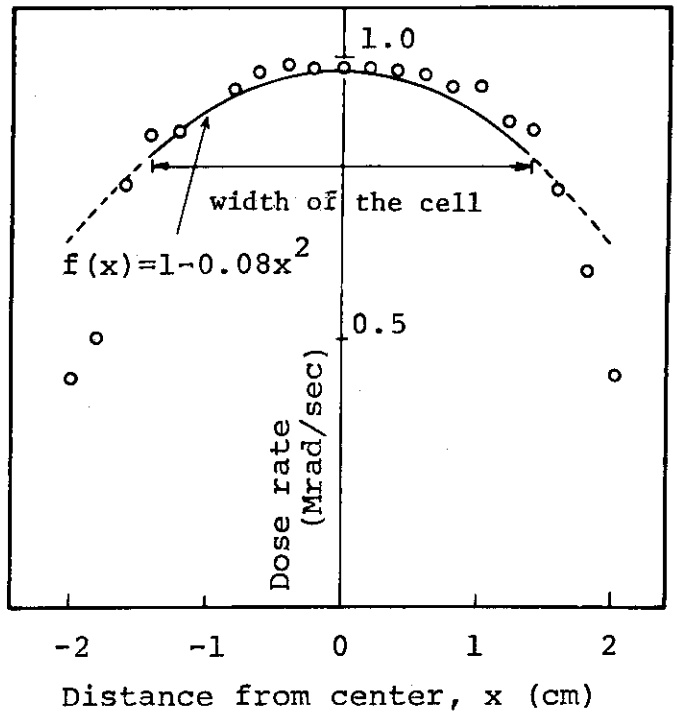

Fig. 3. Lateral dose rate distribution in the cell with the HDRA.

is well approximated with a function, $f(x) = 1 - 0.08x^2$ (x: distance from the center of the cell) when it is normalized with the peak value. In Fig. 4, a longitudinal distribution, i.e., a distribution parallel to the scanning line is shown. The distribution denoted as I is from the determination at the top film below which nine sheets of the film are placed for a depth dose study, while II is from a single sheet determination. The dose rate difference between I and II is accounted for by the back-scattering of electrons from the bottom. From this figure, we can see the dose rate is almost independent of the direction of the beam scanning. The depth dose curve is given in Fig. 5. This is well approximated with the equation, $h(z) = \exp(-5.13z)$ when normalized with

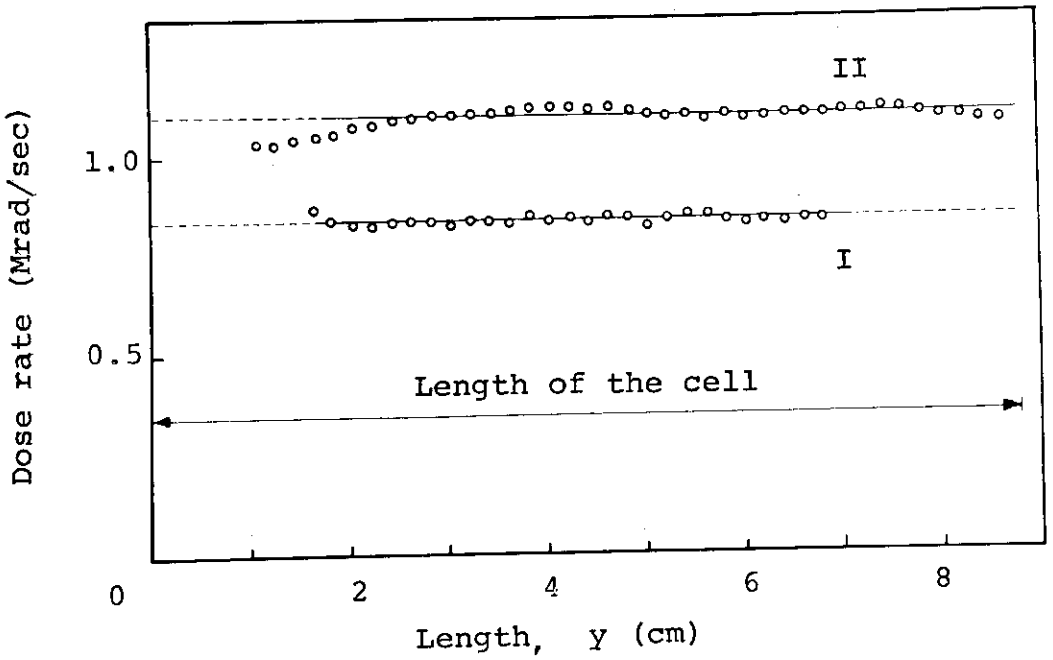

Fig. 4. Longitudinal dose rate distribution in the cell with the HDRA.

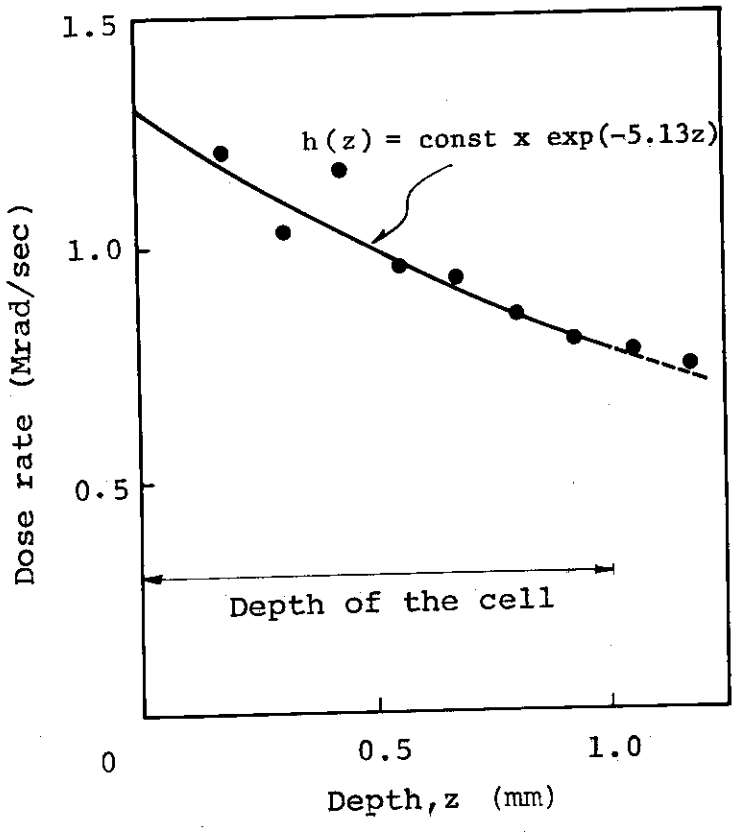

Fig. 5. Depth dose in the cell with the HDRA.

the dose rate of the top film.

Then the space-average dose rate in the cell is given by,

$$DR_{av} = DR_0 \times f_1 \times f_2 ,$$

$$f_2 = \int_x \int_z f(x) \cdot h(z) dxdz \times \frac{1}{2.8 \times 0.1} .$$

DR_0 is the highest dose rate in the sample space when back-scattering of electrons is excluded, i.e. 8.4×10^5 rad/sec which is read from the distribution I in Fig. 4. $f_1(1.03)$ is a correction of the depth dose effect to give the dose rate at the top surface of the space since DR_0 is regarded as a dose rate averaged over the thickness of the CTA film, 0.1 mm. As a result of the integration over the sample space, we find f_2 to be 0.740. Therefore DR_{av} is calculated to be 6.4×10^5 rad/sec in CTA.

Dosimetry of electrons from a Van de Graff accelerator (VdG) is also carried out by the same procedure. The lateral distributions at two ends of the cell are shown in Fig. 6. Both of these two curves are approximated with an equation, $f'(x) = 1 - 0.225x^2$ when normalized with their peak values though a little greater dose rate at the middle of the scanning width is found. In a longitudinal distribution shown in Fig. 7, curve III is a determination of the top film below which nine sheets of CTA film are placed. Curve IV is obtained for the same experiment except that doubly piled sheets are used instead of the ten-fold piled sheets. The reason that curve IV comes above curve III is that back-scattered radiation from the bottom of the cell contributes more to the dose absorbed by the upper sheet of the two and less to the dose absorbed by the top sheet of the ten, because absorption of the back scattered radiation increases with increasing number of the sheets between the top sheet and the bottom of the cell. Reflecting a small decline of the dose rate in curve III which is consistent with the peak dose rate difference of the two curves in Fig. 6, the normalized dose rate distribution is approximated with,

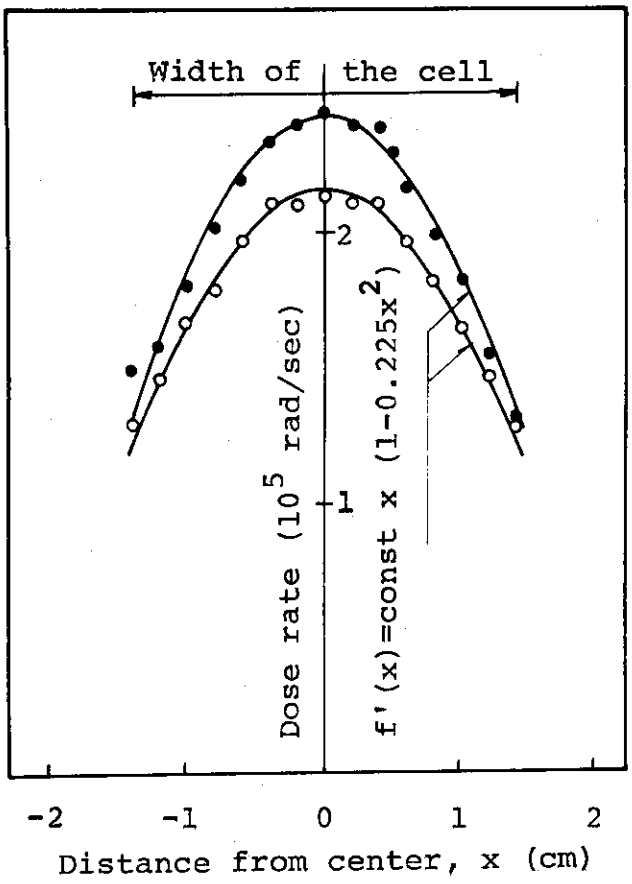

Fig. 6. Lateral dose rate distributions in the cell with the VdG.

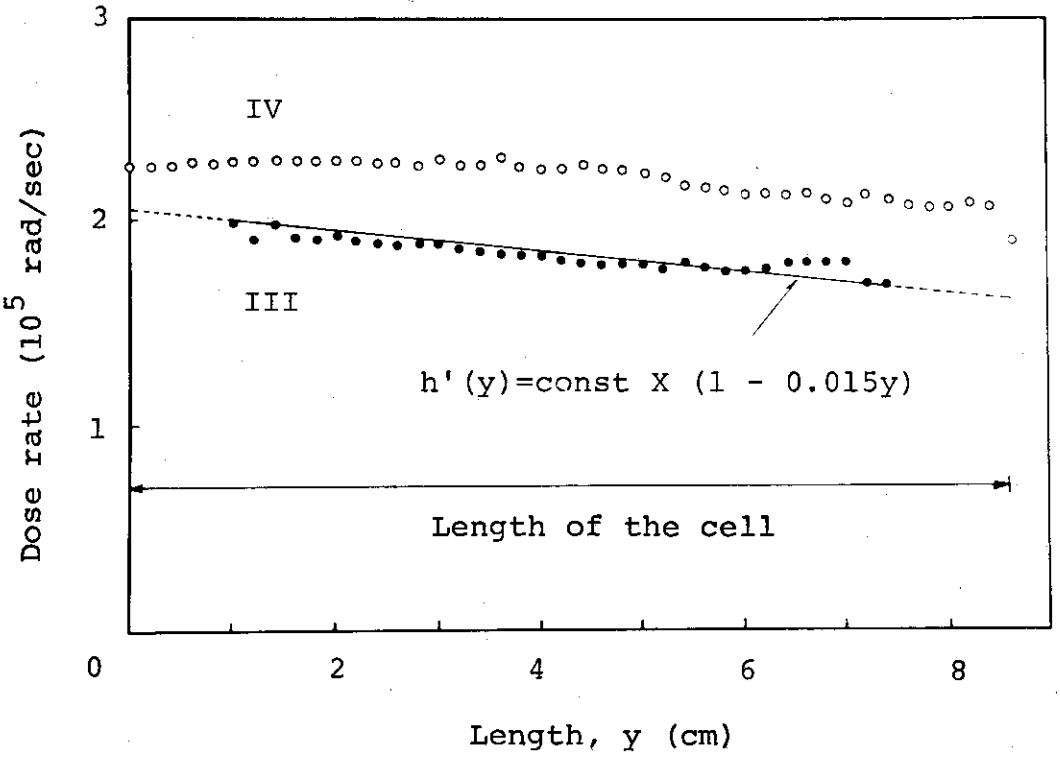

Fig. 7. Longitudinal dose rate distributions in the cell with the VdG.

h'(y) = 1 - 0.015y. The depth dose curves measured at three different points are given in Fig. 8. We can see the dose

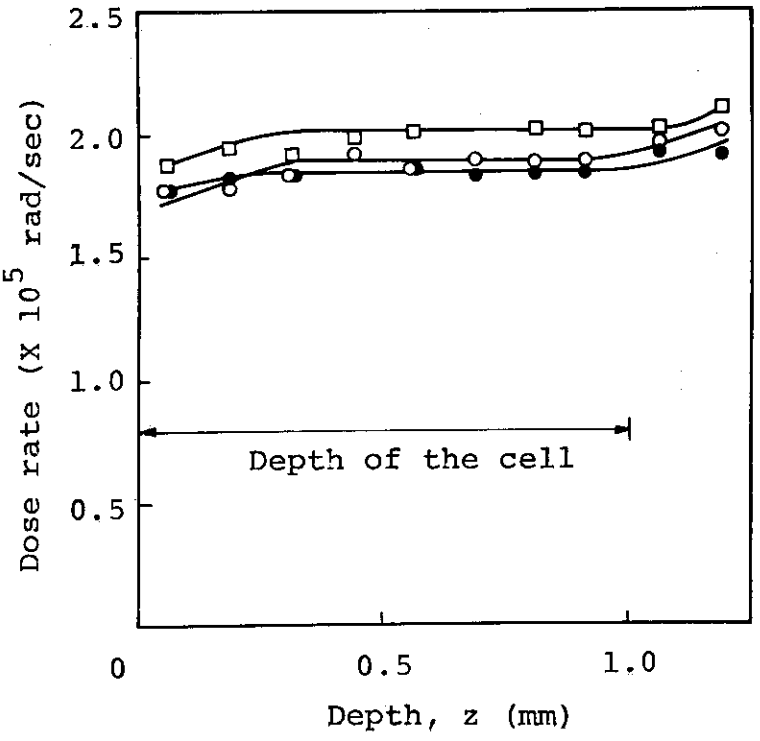

Fig. 8. Depth dose in the cell with the VdG.

rate is almost invariant in this direction if we can neglect a slight drop at top region and increase at bottom, which cancel each other.

For the calculation of DR_{av}, DR_0 is taken from the peak value of curve I in Fig. 6 to be 2.45 X 10^5 rad/sec. In this case it is not correct to use the value in Fig. 7 as DR_0 since the dose rate variation in the slit width of CTA film, 5 mm is still substantial as is noticed from Fig. 6. Using f_1 (1.06) and f_2 (0.804), we get DR_{av} to be 2.08 X 10^5 rad/sec in CTA.

As a summary of the dosimetry study, DR_{av} in water which is calculated by multiplying number ratio of electrons in gram water and CTA is given in Table 1 along with possible dose rate deviations from DR_{av}.

As the second problem, temperature rise in the cell under irradiation is studied. A thin thermocouple is inserted into the cell close to the central ridge. Temperature and

Table 1. Average Dose Rate and Inhomogeneity

	VDG	HDRA
Irradiation conditions		
Electron energy (keV)	1,500	800
Beam current (μa)	50	500
Scanning width (cm)	30	30
Distance from the scanner window (cm)	9	9
Average dose rate in water, DR_{av} (rad/sec)	2.2×10^5	6.76×10^5
Inhomogeneity		
DR_{max}/DR_{av}	1.35	1.29
DR_{min}/DR_{av}	0.68	0.65
DR_{min}/DR_{max}	0.51	0.50

flow rate of a coolant (water or methanol) are maintained at 25°C and 3.0 l/min, respectively. In Fig. 9, variations of temperature in four liquids are shown at the beam current of 50 and 100 μa from the VdG. Other irradiation conditions are the same as those of the dosimetry study. We can see greater temperature rise in organic liquids compared with water becaise of their low specific heats. The relative rates of the temperature rise, however, are found almost independent of the nature of liquids; at 50μa irradiation, more than 90% of the final temperature rise is achieved in the first 10 seconds in all of these liquids. In Fig. 10, the final temperature rise is given as a function of the beam current. Within the dose rate studied, the temperature rise is proportional to the beam current.

Therefore, as a practical way to make the polymerization at a fixed temperature, we easily realize that the coolant temperature must be reduced by some degree, which is a function of the beam current. Here a problem arises; what

does it mean the temperature rise we measured? If the thermal conduction in the sample goes extremely well, which is very

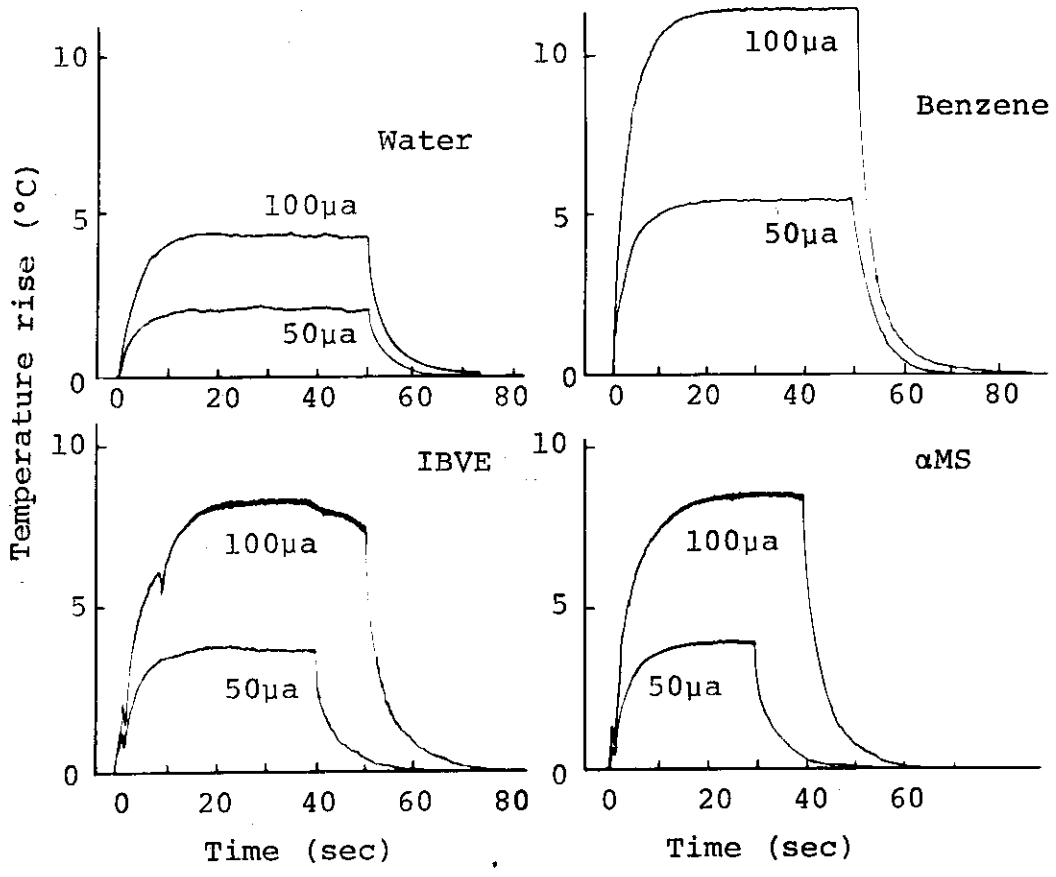

Fig. 9. Temperature rise in water, benzene, isobutyl vinyl ether (IBVE) and α-methylstyrene.

unlikely, our value measured is a temperature rise averaged all over the sample space. On the contrary, if it is only a local temperature rise in a small space where the thermocouple tip is situated, our value must be close to the maximum temperature rise in the cell. In this case we may assume the same degree of inhomogeneity of temperature rise as that of the dose rate from the consequence of Fig. 10.

Now we will take the observed temperature rise divided with 1.35 as an average temperature rise, ΔT_{av} in the sample space. Possible deviation of temperature is ±35% of ΔT_{av} in accordance with the dose rate deviations. For instance with IBVE at the beam current of 50 μa, ΔT_{av} is 4.0/1.35 =

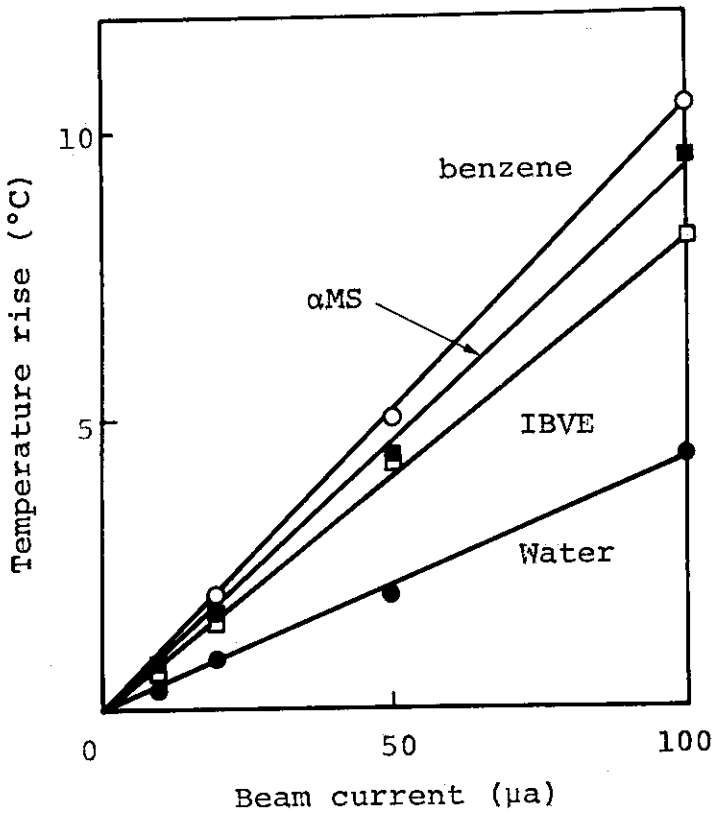

Fig. 10. Temperature rise against the beam current of the VdG.

3.0°C with the maximum deviation of ±1.0°C. Taking account of an accuracy of temperature adjustment of the coolant, ±0.2°C and possible error in ΔT_{av} estimation, 10%, the average temperature in the sample can be maintained with a precision of 0.2 + 0.3 X ($\underline{i}$/50)°C, where $\underline{i}$ is the beam current in μa. In a short period irradiation such as 10 seconds at high beam current, however, the influence of temperature change during irradiation is much more serious. (Ka. Hayashi)

1) Y. Nakai, K. Matsuda, and T. Takagaki, JAERI, 5029, 153 (1974).

III. LIST OF PUBLICATIONS

[1] Published Papers

1. T. Takagaki and T. Sugiura, "On the Treatment of Ozone by Active Carbons", J. Environmental Pollution Control, 12, 306 - 314 (1976).

2. S. Okabe, T. Tabata, and Y. Nakai, "Interaction of Electrons with Matter in the Energy Region from 10 eV to Several Tens MeV", Oyo Butsuri, 45, 2 - 17 (1976).

3. S. Nagai, "ESR Study on Radiation-Induced Radicals in Stearic Acid and Its Related Compounds Adsorbed on Interlamellar Surfaces of Montmorillonite", Chem. Phys. 8, 178 - 184 (1975).

4. F. Horii, Y. Ikada, and I. Sakurada, "Estimation of the Purity of Graft Copolymer by Thin-Layer Chromatography", J. Polymer Sci., Chem. Ed., 13, 755 (1975).

5. Y. Ikada, F. Horii, Y. Nishizaki, and T. Kawahara, "Radiation-Chemical Yield of Graft Copolymerization in Radiation Grafting", Macromolecules, 8, 276 (1975).

6. I. Sakurada, K. Kaji, T. Okada, and A. Tsuchiya, "Degradation of Cellulose by Gamma-Ray Irradiation", Cellulose Chemistry and Technology, 5, 347 (1975).

7. Ka. Hayashi and D. C. Pepper, "Ionic Polymerization of p-Methoxystyrene and Other Styrene Derivatives by Radiation", Polymer J., 8, 1 (1976).

* * * *

8. K. Hirota, M. Hatada, and T. Ogawa, "Low Energy Electron-Impact Emission from Gases", Int. J. Radiat. Phys. Chem., 8, 205 - 219 (1976).

9. S. Ohnishi and S. Nagai, "Magnetic Resonance of Polymers", Chap. 4, 393 - 432, Kyoritsu Publ. Co., Tokyo, (1975).

[2] Oral Presentations

1. S. Sugimoto, M. Nishii, and T. Sugiura, "Homogeneous Gas Reactions in the Binary Mixtures of CO and H_2 by Electron Irradiation (I) ----- Reaction Products in Low Conversion", The 32nd Annual Meeting of the Chemical Society of Japan, Apr. 4, 1975.

2. M. Kumakura, K. Arakawa, and T. Sugiura, "Ion-Molecule Reactions in Propyl Acetate (III)", The 23rd Annual Meeting of the Mass Spectroscopy Society of Japan, Jun. 14, 1975.

3. T. Sugiura, "Radiation-Induced Reactions in Binary Mixtures of Carbon Monoxide and Hydrogen". Meeting of Study Group "Radiation Effects and Its Dynamic Behavior on Matter" ---- under the Auspices of the Atomic Energy Society of Japan, Sept. 11, 1975.

4. S. Sugimoto, M. Nishii, and T. Sugiura, "Homogeneous Gas Reactions in the Binary Mixtures of CO and H_2 by Electron Irradiation (II) ----- Effect of Composition of Reactant Gases and Pressure Dependence", The 18th Discussion Meeting on Radiation Chemistry, Oct. 7, 1975.

5. T. Sugiura, "The Studies of Molecular Dynamic Processes", Autumn Symposium of "Applications of SOR to the Processes of Atoms and Molecules" ----- under the Auspices of the Physical Society of Japan, Oct. 12, 1975.

6. H. Kamiyama, "Aggregation State of Water Molecules Sorbed into the Cellulose Acetate Membrane", The 24th Annual Meeting of the Society of Polymer Science, Japan, May 25, 1975.

7. K. Kaji, T. Okada, and I. Sakurada, "Radiation-Induced Grafting of Acrylic Acid onto Polyvinyl Chloride Fiber", Annual Meeting of the Society of Fiber Science and Technology, Jun. 10, 1975.

8. Y. Mori and T. Okada, "Modification of Polyester Film by Radiation-Induced Chlorination", The 13th Annual Meeting of Adhesion Society of Japan, Jun. 17, 1974.

9. K. Kaji, T. Okada, and I. Sakurada, "Radiation-Induced Grafting of Acrylonitrile onto Polyvinylidene Chloride Fiber", The 21st Regional Meeting of the Society of Polymer Science (Kobe), Jul. 11, 1975.

10. T. Mita and Y. Ikada, "Cross-Linking Reaction of Polyvinyl Alcohol by Use of Dialdehyde Starch", The 21st Regional Meeting of The Society of Polymer Science (Kobe), Jul. 11, 1975.

11. T. Okada, K. Kaji, and I. Sakurada, "Radiation-Induced Chlorination of Polyester Fiber", The 33rd Annual Meeting of the Chemical Society of Japan, Oct. 18, 1975.

12. Y. Ikada, H. Iwata, and S. Nagaoka, "Thin-Layer Chromatography of Polymers Having Functional Groups at Chain Ends", The 33rd Meeting of the Research Institute for Chemical Fibers, Japan, Oct. 17, 1975.

13. Y. Ikada and F. Horii, "Tensile Properties of Polyvinyl Alcohol Membrane Swelled with Water", The 24th Discussion Meeting of the Society of Polymer Science, Japan, Nov. 6, 1975.

14. Y. Ikada, H. Iwata, S. Nagaoka, and M. Hatada, "Monomolecular Layers of Block- and Graft-Copolymer Consisted of Polyvinyl Alcohol and Polystyrene at Air-Water Interface", The 24th Discussion Meeting of the Society of Polymer Science, Japan, Nov. 6, 1975.

15. M. Nishii and M. Hatada, "Polymerization of Vinyl Stearate Multilayers Initiated by Electron Beam Irradiation", The 33rd Annual Meeting of the Chemical Society of Japan, Oct. 17, 1975.

16. M. Hatada, "Water Permeation through Monomolecular Films of Octadecyl Acrylate and Poly (Octadecyl Acrylate) at Air-Water Interface", The 21st Regional Meeting of the Society of Polymer Science (Kobe), Jul. 11, 1975.

17. Ka. Hayashi, "Polymerization of Methyl Methacrylate and Alkyl Acrylates by Electron Beams", The 33rd Annual Meeting of the Chemical Society of Japan, Oct. 17, 1975.

18. J. Takezaki, T. Okada, and I. Sakurada, "Studies on Polymerization of Styrene with Electron Beams by Gel Permeation Chromatography", The 24th Annual Meeting of the Society of Polymer Science, Japan, May 25, 1975.

19. J. Takezaki, T. Okada, and I. Sakurada, "Radiation-Induced Polymerization of Methyl Methacrylate by Electron Beams", The 18th Discussion Meeting on Radiation Chemistry, Oct. 8, 1975.

20. H. Iwata and Y. Ikada, "Coupling Reaction of Polyvinyl Alcohol with Polyvinyl Acetate Having Aldehyde Groups", The 24th Annual Meeting of the Society of Polymer Science, Japan, May 24, 1975.

21. S. Nagaoka, H. Iwata, and Y. Ikada, "Preparation of Poly (Methyl Methacrylate) Having Amino Groups at Chain Ends and Analysis of the Polymer by Thin-Layer Chromatography, The 24th Annual Meeting of the Society of Polymer Science, Japan, May 25, 1975.

22. Y. Ikada, T. Mita, F. Horii, I. Sakurada, and M. Hatada, "Preparation of Cross-Linked Polyvinyl Alcohol by Radiation Method", The 24th Annual Meeting of the Society of Polymer Science, Japan, May 25, 1975.

23. M. Gotoda, K. Mori, and T. Yagi, "Electron Beam Curing of Polyvinyl Chloride Plastisol", The 24th Annual Meeting of the Society of Polymer Science, Japan, May 22, 1975.

24. J. Kumanotani, T. Koshio, and M. Gotoda, "Curing of Resins by EB and UV Irradiations", The 24th Annual Meeting of the Society of Polymer Science, Japan, May 22, 1975.

25. M. Gotoda and T. Yagi, "Radiation Curing of Epoxy-acrylate by High Dose Rate Electron Beams", The 18th Discussion Meeting on Radiation Chemistry, Oct. 18, 1975.

26. M. Gotoda and T. Yagi, "Radiation Curing of Chlorinated Polymer/Vinyl Monomer Mixtures by High Dose Rate Electron Beams", The 25th Congress on Thermosetting Resins, Oct. 24, 1975.

IV. LIST OF SCIENTISTS

(Jun. 30, 1976)

[1] Staff Members

Masao GOTODA, Dr., polymer chemist, Head

Ichiro SAKURADA, Professor emeritus, Kyoto University, Former head

Toshio SUGIURA, Dr., physical chemist

Toshio OKADA, Dr., polymer chemist

Yohta NAKAI, Dr., physicist

Motoyoshi HATADA, Dr., physical chemist

Kanae HAYASHI, Dr., polymer chemist

Hideo KAMIYAMA, Physical chemist

Shun'ichi SUGIMOTO, Physical chemist

Koji MATSUDA, Physicist

Jun'ichi TAKEZAKI, Physical chemist

Masanobu NISHII, Dr., polymer chemist

Siro NAGAI, Dr., physical chemist

Torao TAKAGAKI, Physicist

Kanako KAJI, Polymer chemist

Toshiaki YAGI, Engineering chemist

[2] Advisors and Visiting Researchers

Isamu NITTA, Professor emeritus, Osaka University, Advisor

Kozo Hirota, Professor, Chiba Institute of Technology, Advisor

Koichiro HAYASHI, Professor, Osaka University, Advisor

Shun'ichi OHNISHI, Professor, Kyoto University, Advisor

Yoshito IKADA, Assoc. Professor, Kyoto University, Advisor

Chong Kwang LEE, Physical chemist, Korea Atomic Energy Research Institute (Mar. 1975 - Aug. 1975)

Akiko TSUCHIYA, Chemist, Research Institute for Chemical Fibers (Apr. 1973 - Mar. 1976)

Takao TAKEUCHI, Physical chemist, Unitika Co., Ltd. (Jul. 1975 - Dec. 1975)

Masao Kajimaki, Physicist, Duskin Co., Ltd. (May 1975 -)

Shuichi TANIGUCHI, Electrical engineer, Nissin-High Voltage Co., Ltd. (May 1976 -)